

GRAVITATIONAL LENSING

23 - SEARCHING AND USING STRONG LENSES

Massimo Meneghetti
AA 2018-2019



SERENDIPITOUS DISCOVERIES

Discovery of the first galaxy-QSO lens system (1979)

0957+561 A, B: twin quasistellar objects or gravitational lens?

D. Walsh

University of Manchester, Nuffield Radio Astronomy Laboratories, Jodrell Bank, Macclesfield, Cheshire, UK

R. F. Carswell

Institute of Astronomy, Cambridge, UK

R. J. Weymann

Steward Observatory, University of Arizona, Tucson, Arizona 85721

0957+561 A, B are two QSOs of mag 17 with 5.7 arc s separation at redshift 1.405. Their spectra leave little doubt that they are associated. Difficulties arise in describing them as two distinct objects and the possibility that they are two images of the same object formed by a gravitational lens is discussed.

SPECTROSCOPIC observations have been in progress for several years on QSO candidates using a survey of radio sources made at 966 MHz with the MkIA telescope at Jodrell Bank. Many of the identifications have been published by Cohen *et al.*¹ with interferometric positions accurate to ~2 arc s and a further list has been prepared by Porcas *et al.*². The latter list consists of sources that were either too extended or too confused for accurate interferometric positions to be measured, and these were observed with the pencil-beam of the 300 ft telescope at NRAO, Green Bank at λ 6 cm and λ 11 cm. This gave positions with typical accuracy 5–10 arc s and the identifications are estimated as ~80% reliable.

The list of Porcas *et al.* includes the source 0957+561 which has within its field a close pair of blue stellar objects, separated by ~6 arc s, which are suggested as candidate identifications. Their positions and red and blue magnitudes, m_R and m_B , estimated from the Palomar Observatory Sky Survey (POSS) are given in Table 1 and a finding chart is given in Fig. 1. Since the images on the POSS overlap, the magnitude estimates may

be of lower accuracy than normal, but they are very nearly equal and object A is definitely bluer than object B. The mean position of the two objects is 17 arc s from the radio position, so the identification is necessarily tentative.

Observations

The two objects 0957+561 A, B were observed on 29 March 1979 at the 2.1 m telescope of the Kitt Peak National Observatory (KPNO) using the intensified image dissector scanner (IIDS). Sky subtraction was used with circular apertures separated by 99.4 arc s. Some observational parameters are given in Table 2. The spectral range was divided into 1,024 data bins, each bin 3.5 Å wide, and the spectral resolution was 16 Å. After 20-min integration on each object it was clear that both were QSOs with almost identical spectra and redshifts of ~1.40 on the basis of strong emission lines identified as C IV λ 1549 and C III] λ 1909. Further observations were made on 29 March and on subsequent nights as detailed in Table 2. By offsetting to observe empty sky a few arc seconds from one object on both 29 and 30 March it was confirmed that any contamination of the spectrum of one object by light from the other was negligible.

Table 1 Positions and magnitudes of 0957+561 A, B

Object	RA	Dec (1950.0)	M_R	M_B
0957+561A	09 57 57.3	+56 08 22.9	17.0	16.7
0957+561B	09 57 57.4	+56 08 16.9	17.0	17.0

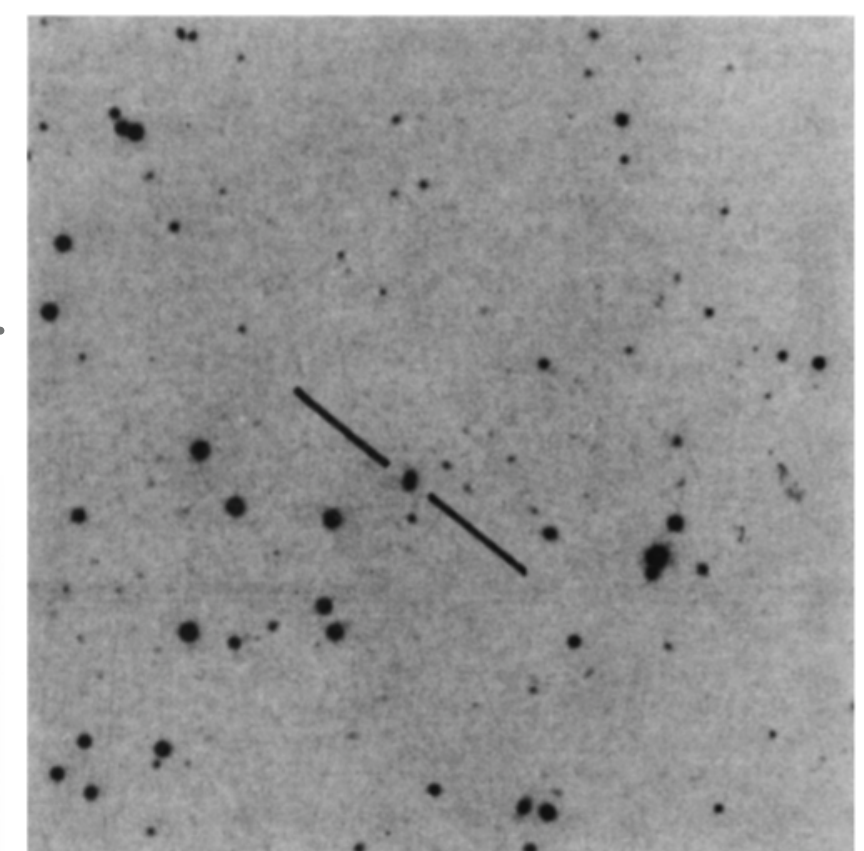


Fig. 1 Finding chart for the QSOs 0957+561 A and B. The chart is 8.5 arc min square with the top right hand corner north preceding and is from the E print of the POSS.

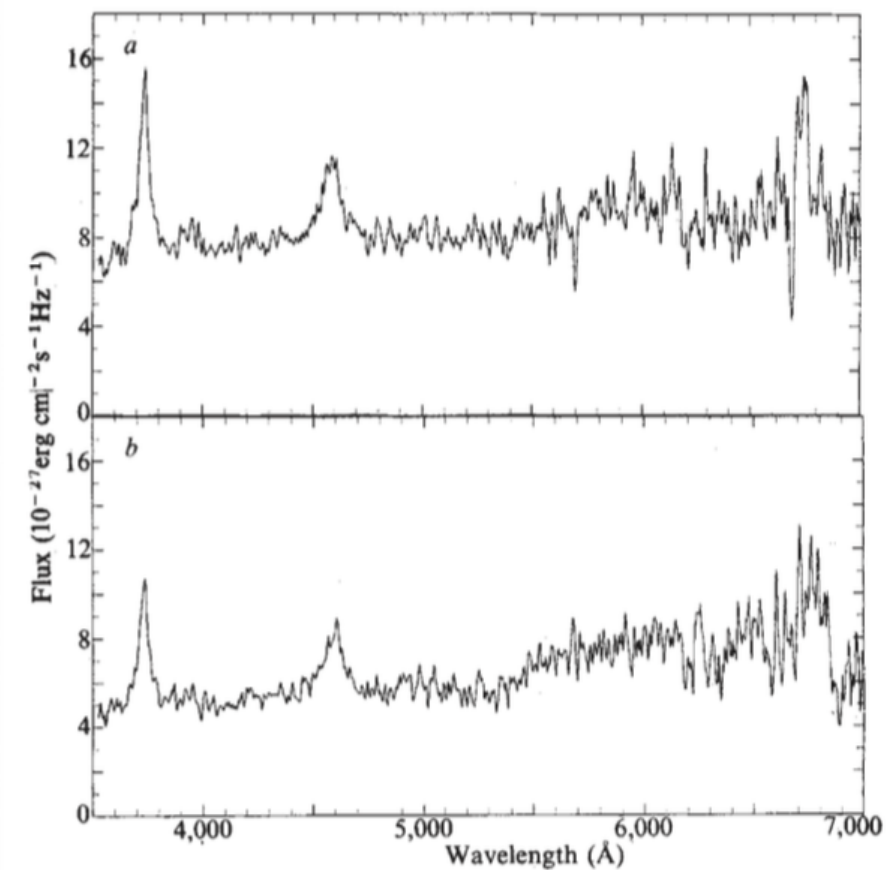


Fig. 2 IIDS scans of 0957+561 A(a) and B(b). The data are smoothed over 10 Å and the spectral resolution is 16 Å.

SE

Disc

095
obje

D. Wal

University o

R. F. C

Institute of

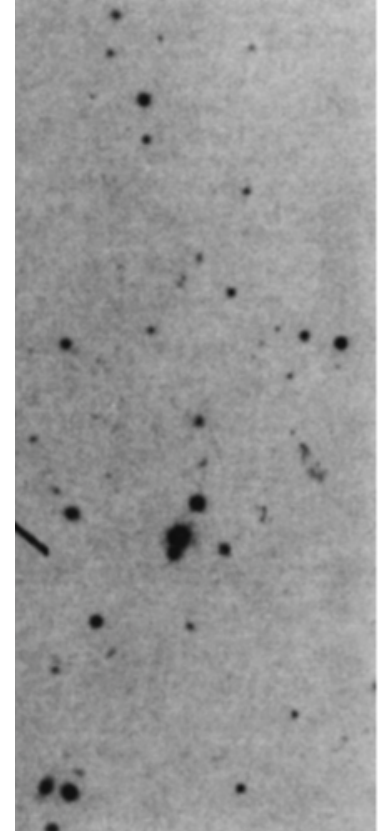
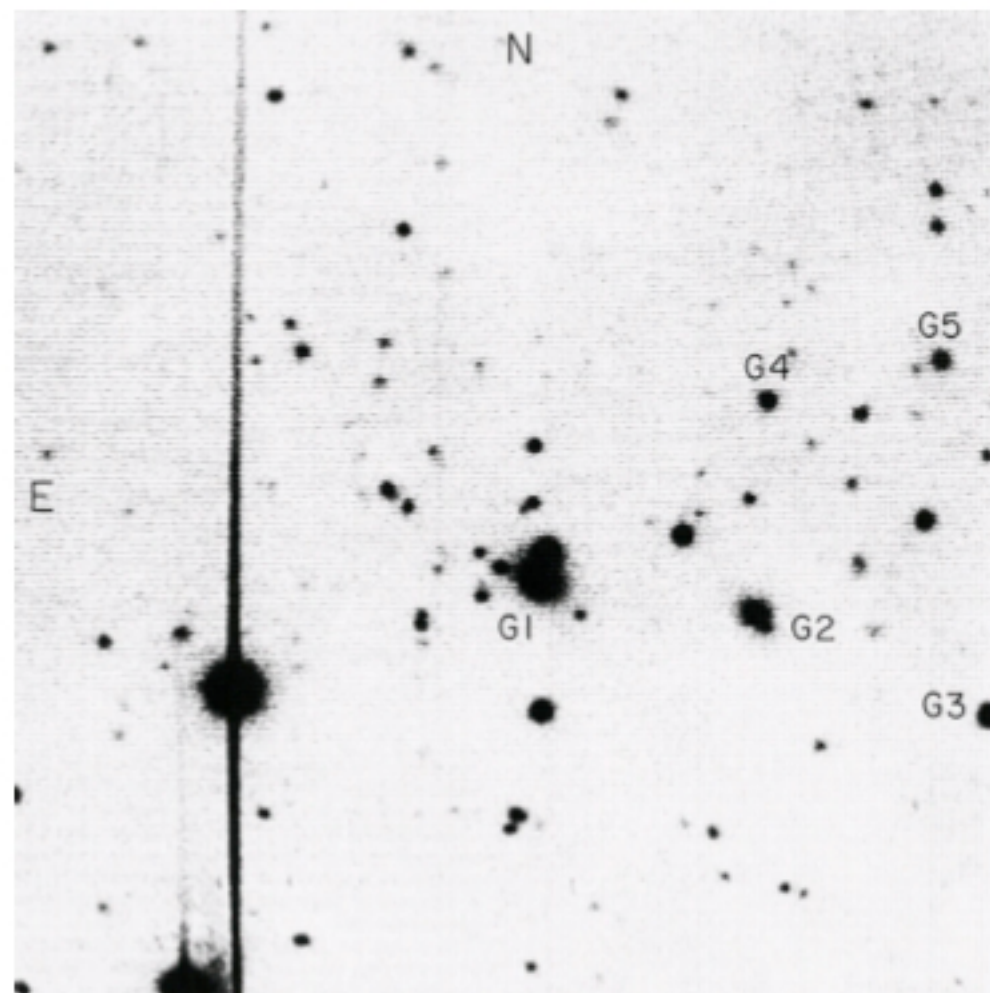
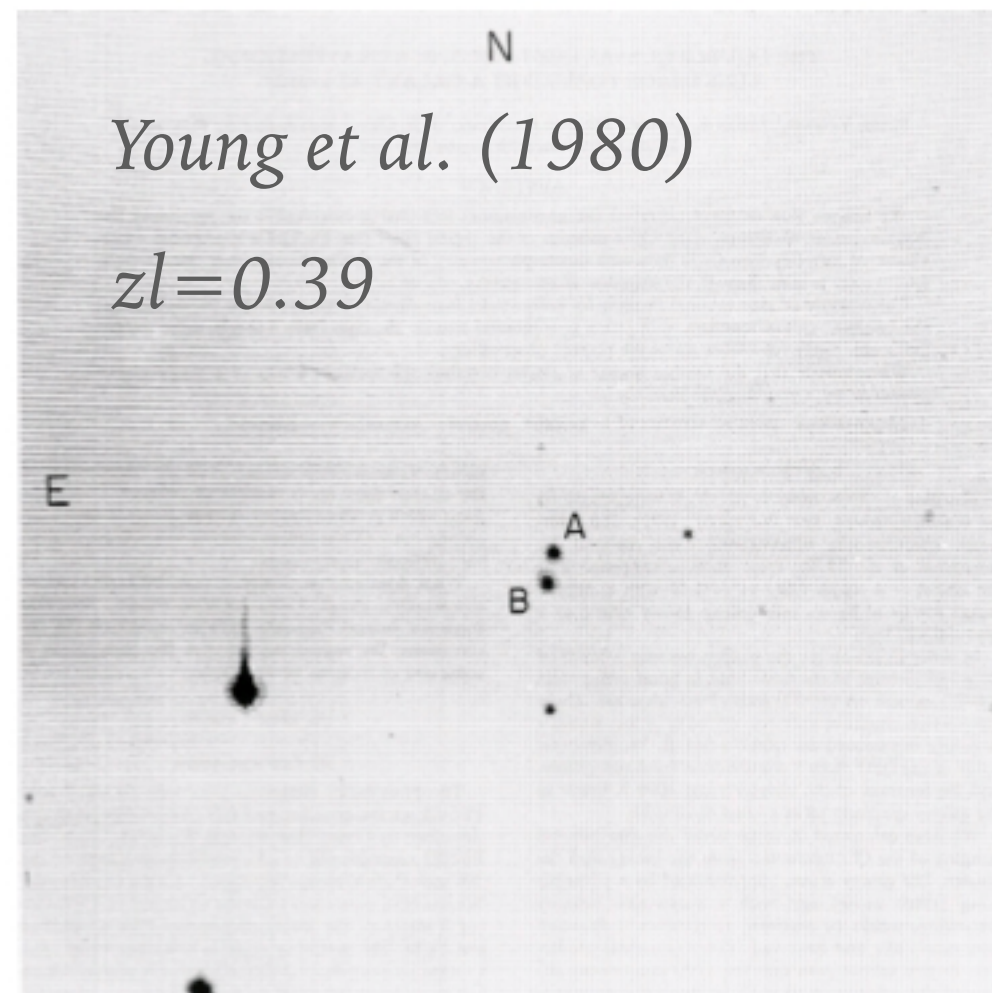
R. J. V

Steward Ob

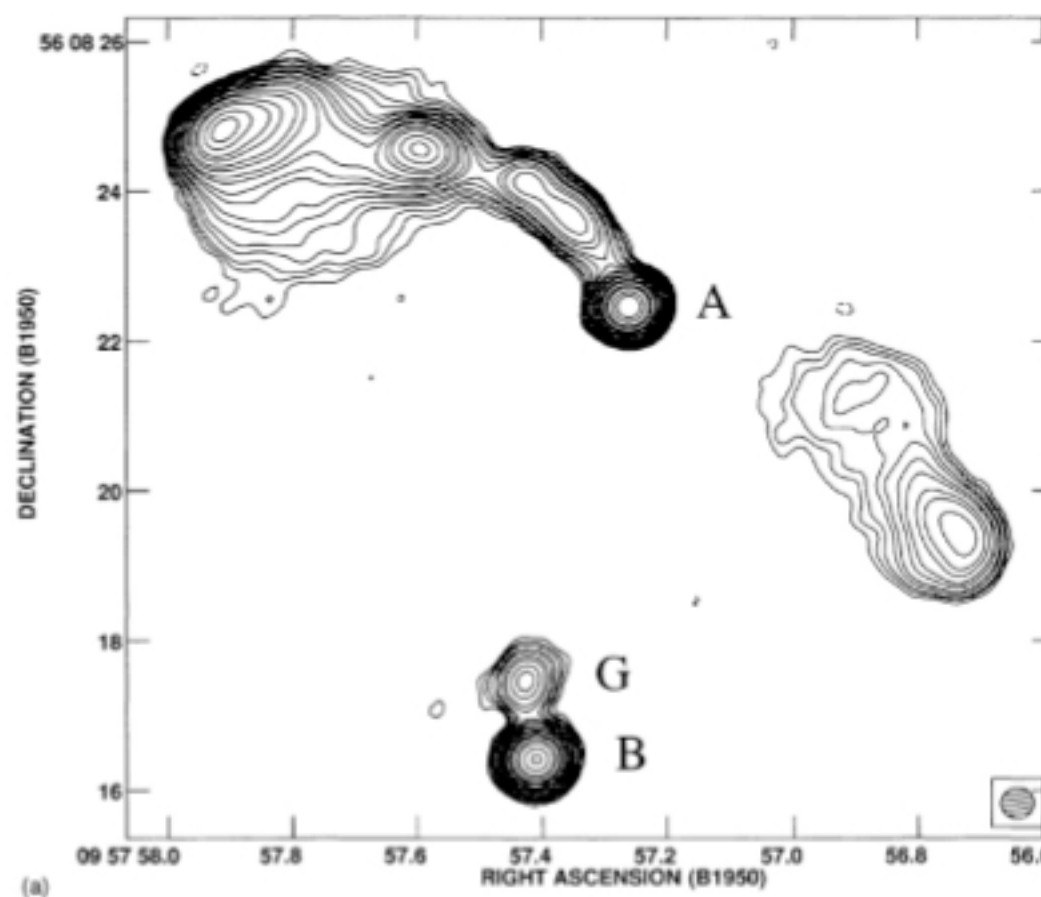
0957+56
separation
that they
them as tw
two image
lens is dis

SPECTROS
several year
made at 96
Many of the
with interfe
list has bee
sources tha
accurate in
were obser
NRAO, Gr
with typica
estimated a

The list c
has within i
by ~6 arc s
Their posit
estimated f
are given in
the images



957+561 A and B. The chart at hand corner north preceding it of the POSS.



Gorenstein et al. (1984)

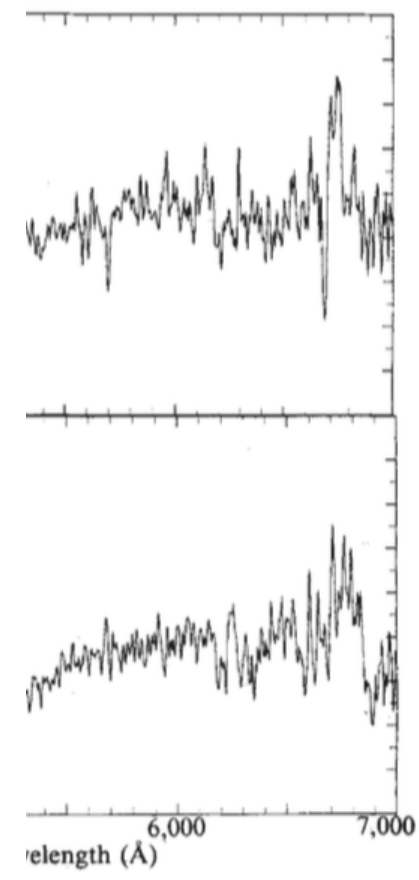
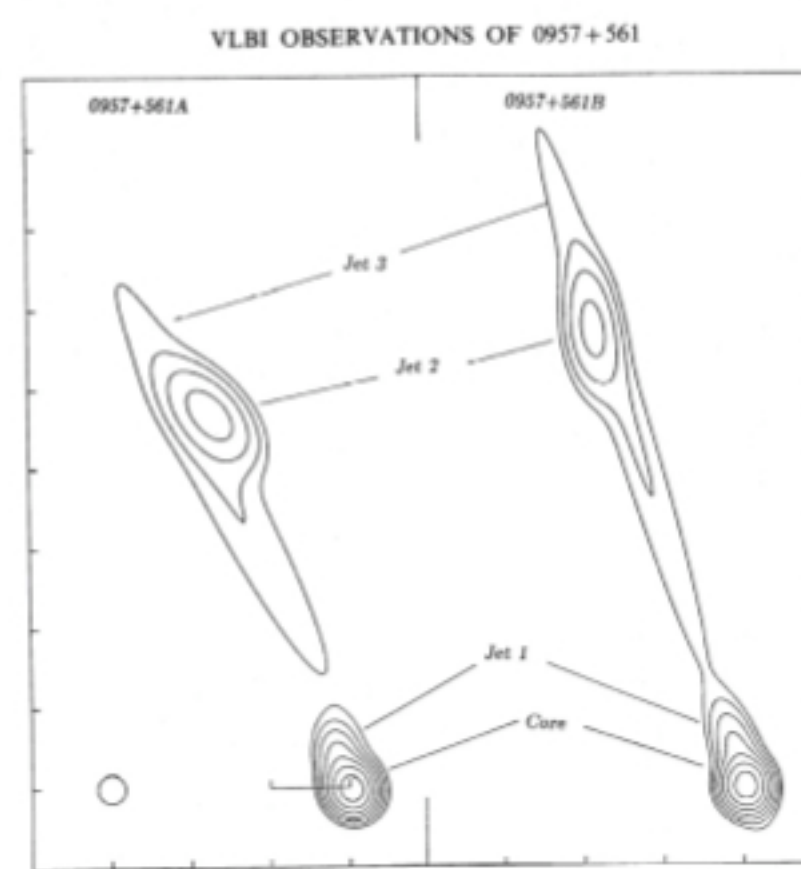
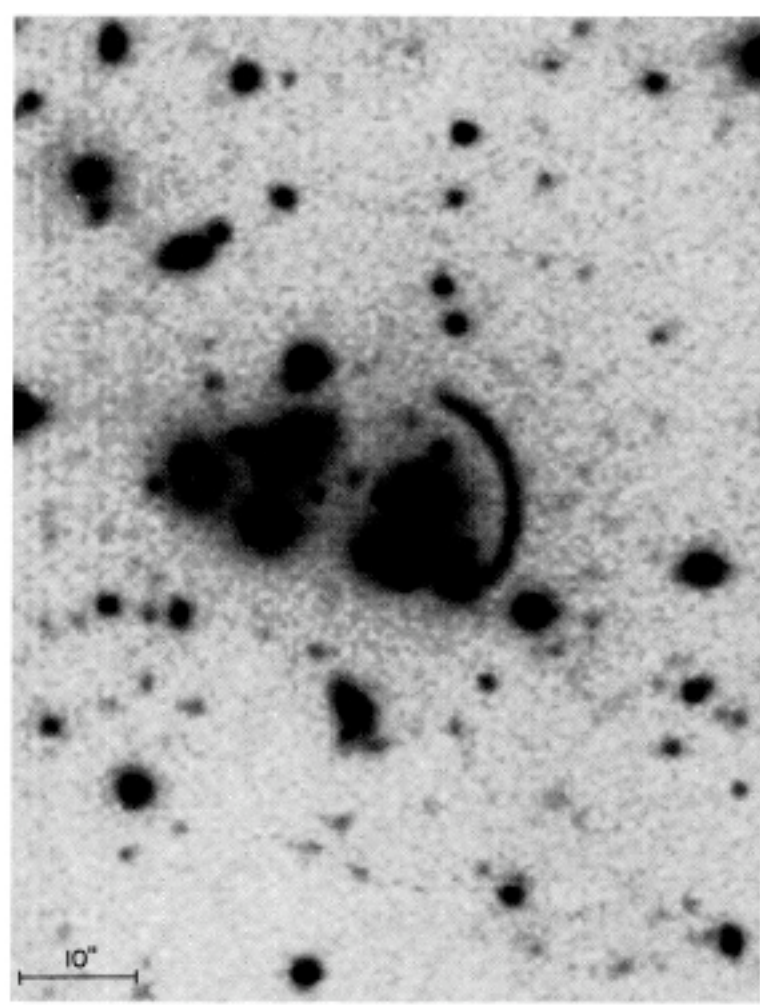
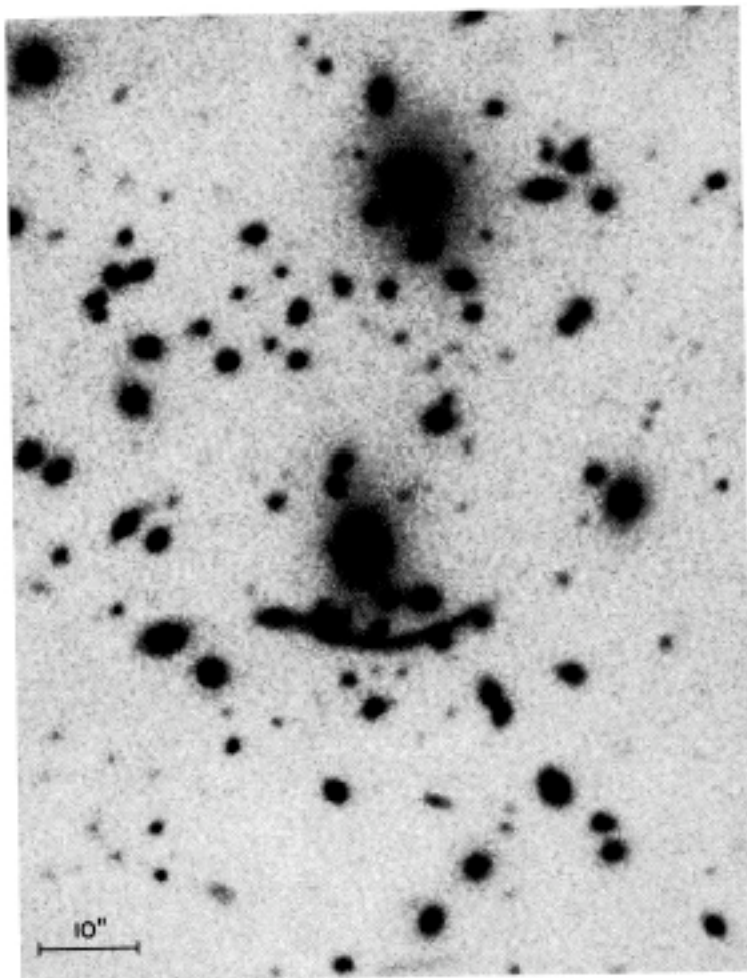


Fig. 2 IIDS scans of 0957+561 A(a) and B(b). The data are smoothed over 10 Å and the spectral resolution is 16 Å.

Historical remark: The first gravitational arcs

The first detection of gravitational arcs in galaxy clusters is dated 1986. In this year, two groups independently discovered strongly elongated, curved features around two clusters of galaxies (Soucail et al., 1987; Lynds & Petrosian, 1989): A370 (left panel below) and CL2244-02 (right panel).



They were seen displaced from the cluster center and curving around it. Several hypothesis were put forward about the nature of these features, all proven wrong. The correct interpretation of these observations as gravitational lensing effects was made by Paczynski (1987), when the redshift of the arc in A370 was measured and discovered to be much larger than the redshift on the cluster. In particular, A370 is at redshift $z_d = 0.374$, while the arc is at redshift $z_s = 0.724$. The arc in CL2244-02 ($z_d = 0.3$) is at redshift $z_s = 2.24$. The figures below show color higher quality images of the same clusters observed with HST and with ISAAC@VLT.

HOW TO FIND STRONG LENSES

- Then the search became more systematic
- Strong lens searches followed two approaches so far:
 - Find strong lensing features around the most probable lenses
 - Find probable strongly lensed sources and find their lenses

EXAMPLE 1: THE CLASS SURVEY (SOURCE ORIENTED)

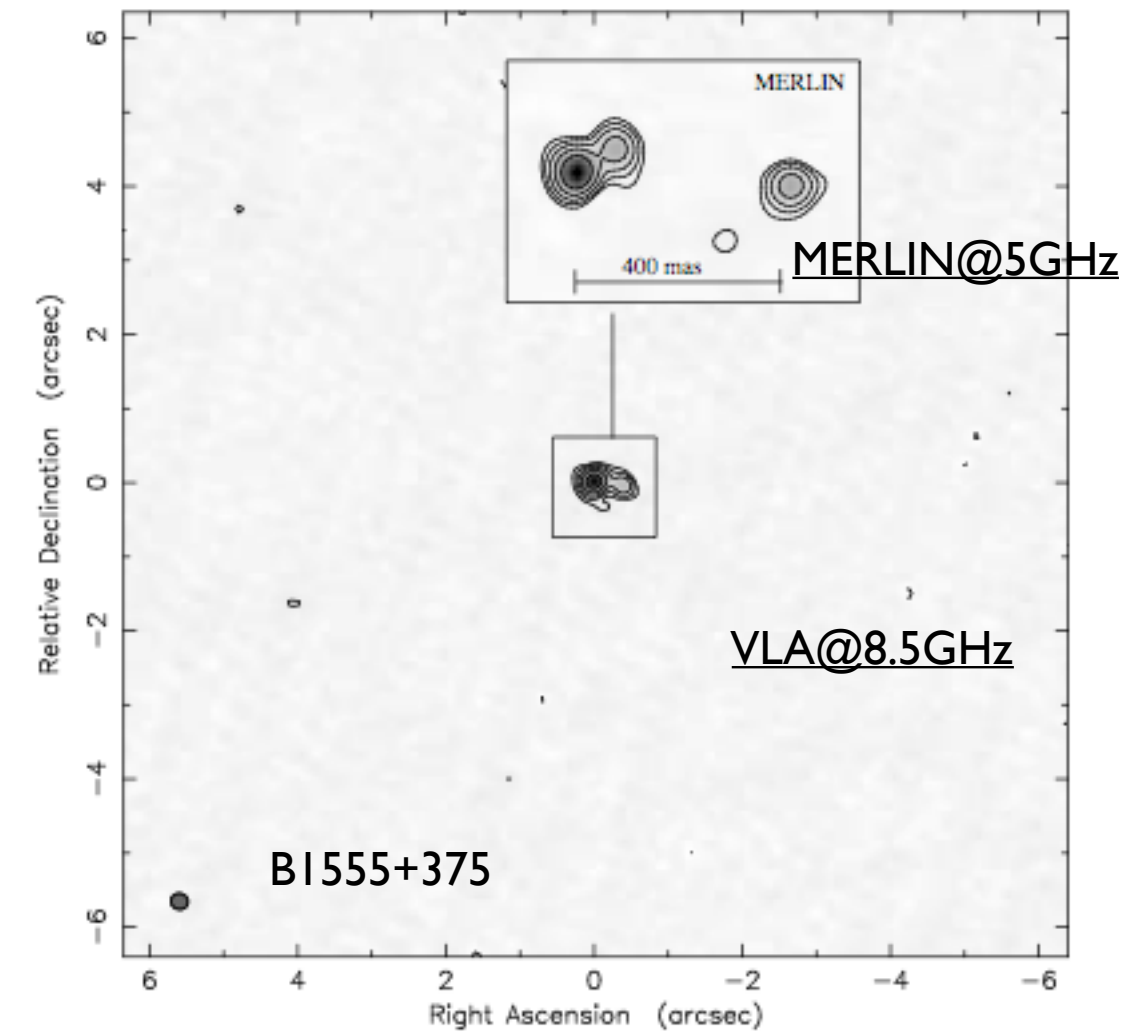
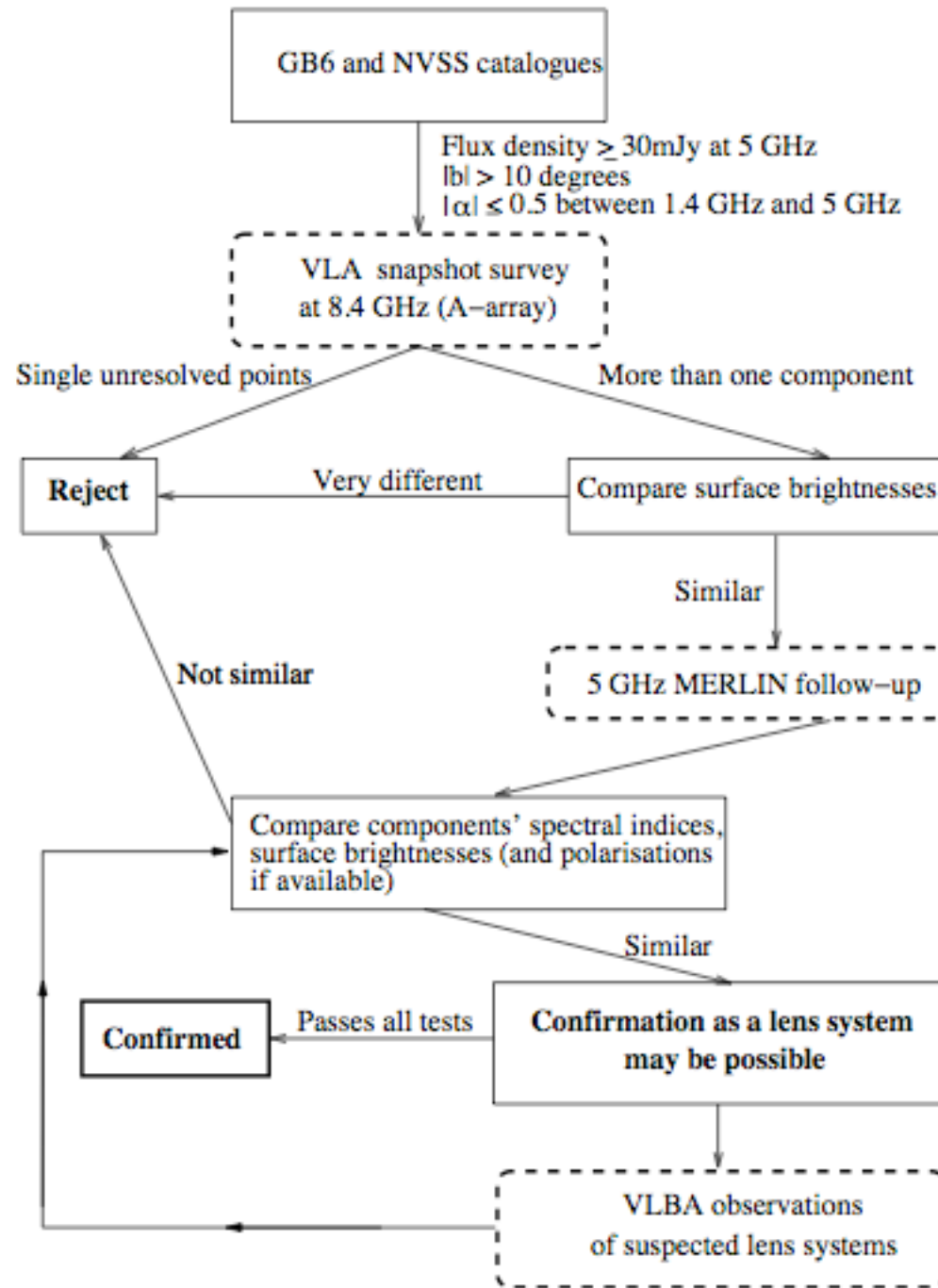
The CLASS (Cosmic Lens All-Sky Survey) was an international project (UK, USA, Netherlands) whose goal was searching for gravitational lenses in the radio domain.

The survey was conducted between 1990 and 1999. During the survey 16503 flat-spectrum radio sources were monitored. Such objects are usually **quasars** and have very **simple radio structures**; they are typically point sources, and occasionally weak extended emission is visible. The point-like radio emission is thought to originate from the base of a relativistic radio jet in an active galaxy, which points more or less at the observer.

The simplicity of these sources is useful for gravitational lensing searches. This is because any flat-spectrum radio source which has extended structure is a possible gravitational lens, as the **extended structure** could represent **multiple images** of a point-like radio source, produced by the gravitational field of an intervening galaxy.

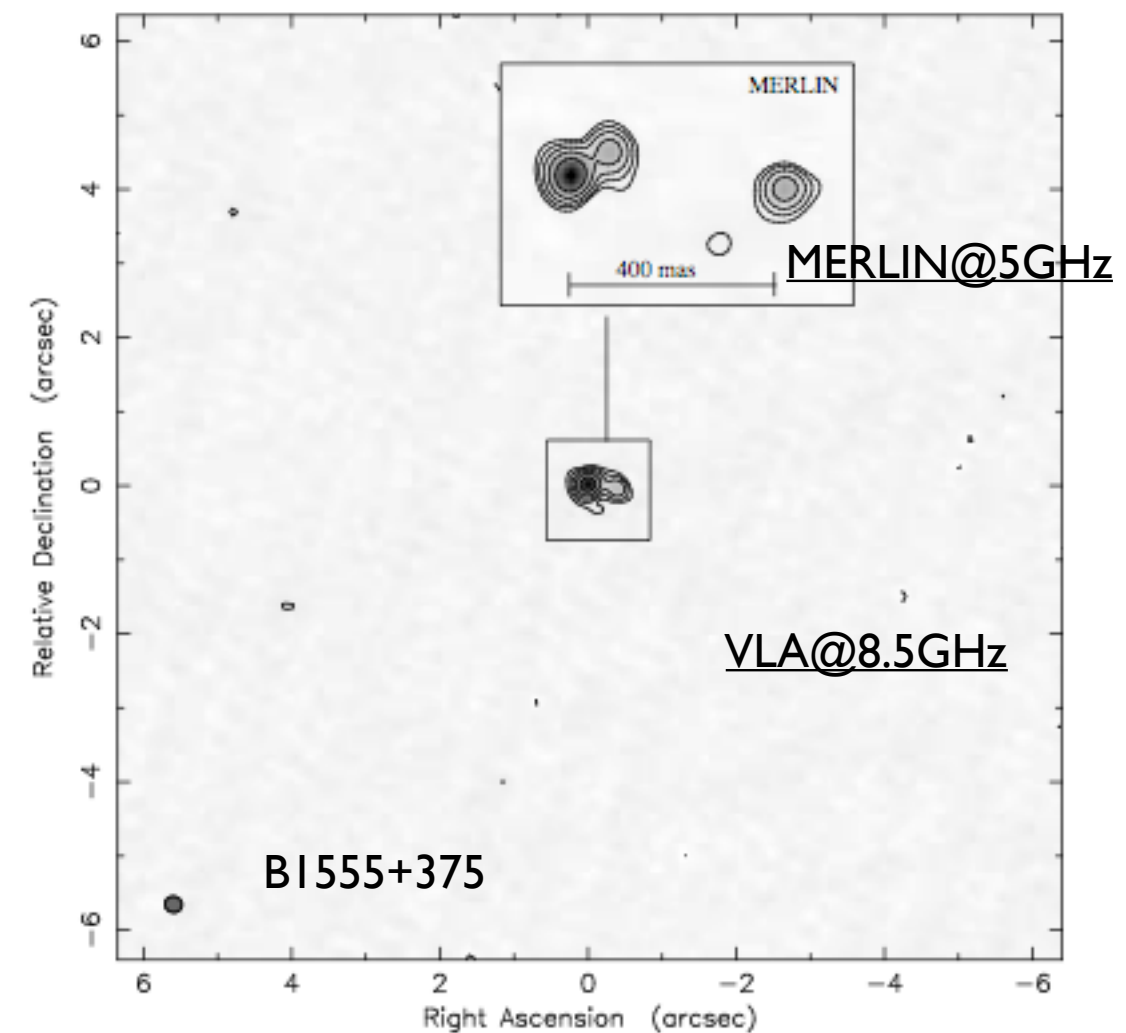
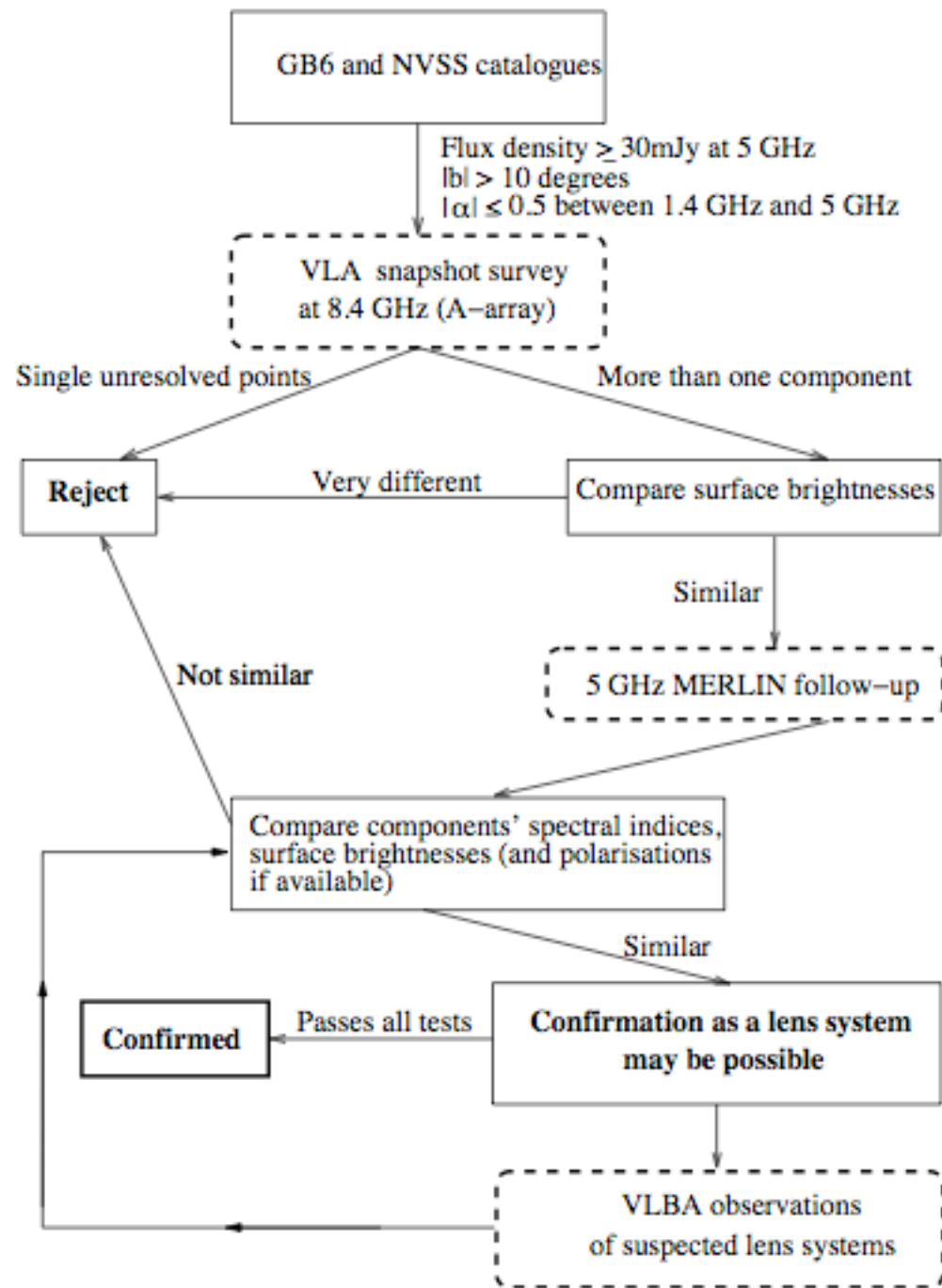
Instruments: VLA (radio maps at 0.2" res.) + follow-up with MERLIN (0.05" res.) and VLBA (0.003" res).

CLASS STRATEGY

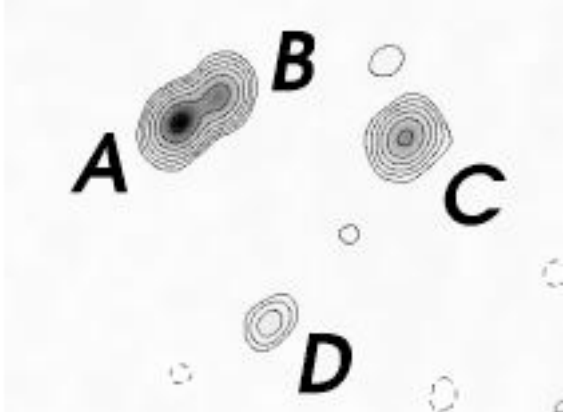


Browne et al. 2002

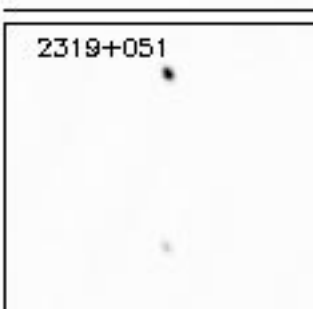
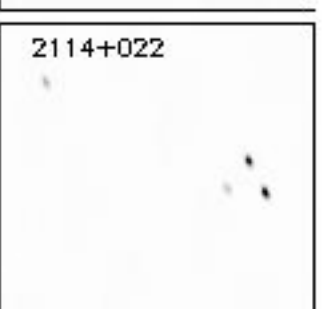
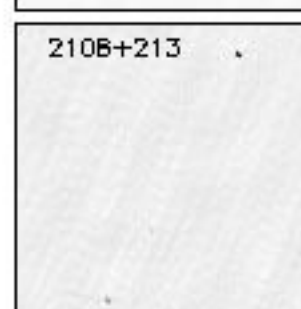
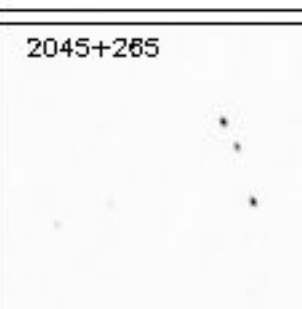
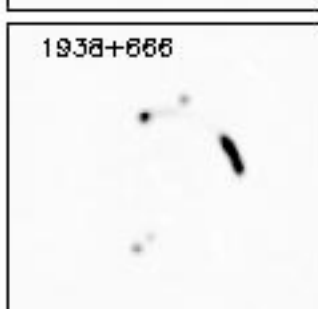
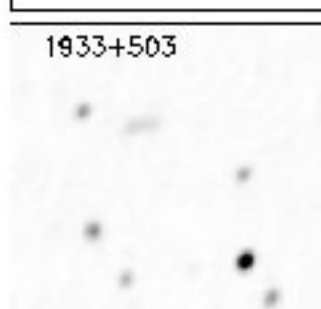
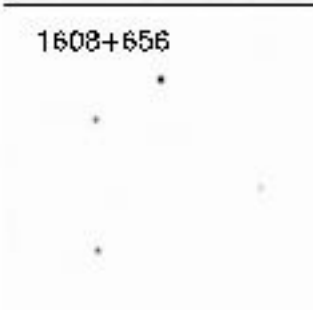
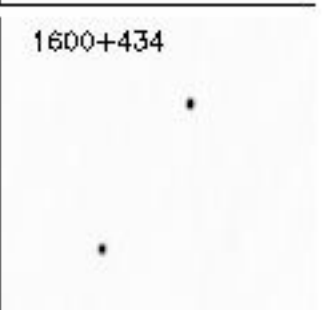
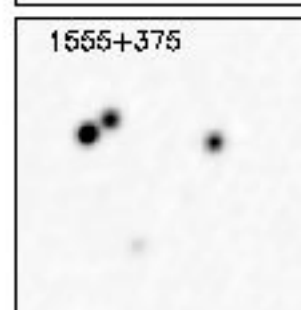
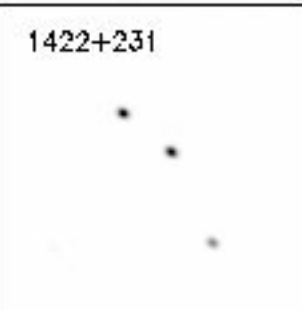
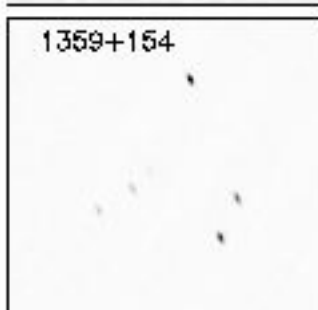
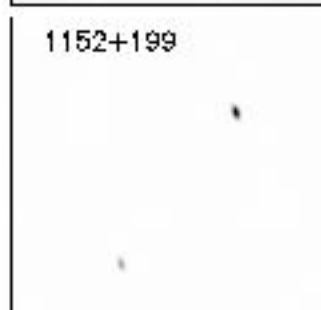
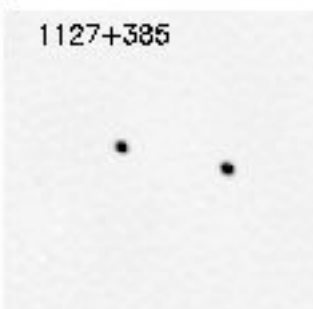
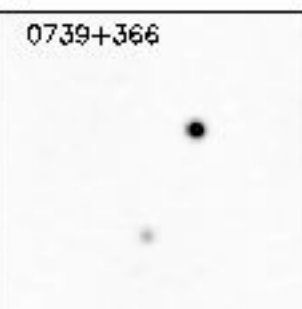
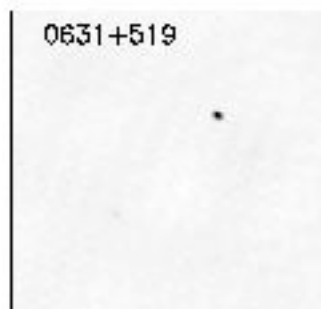
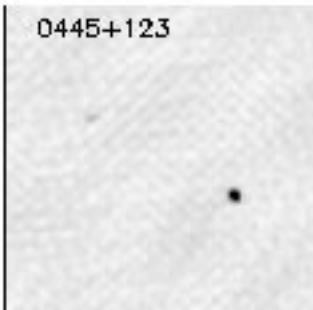
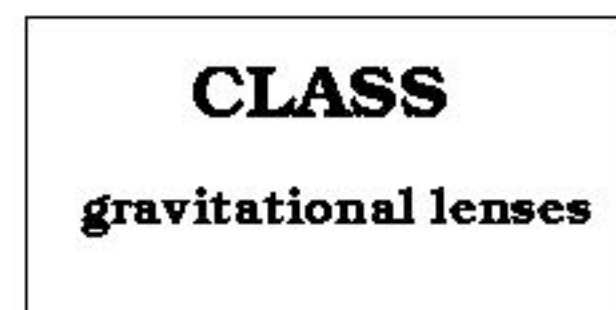
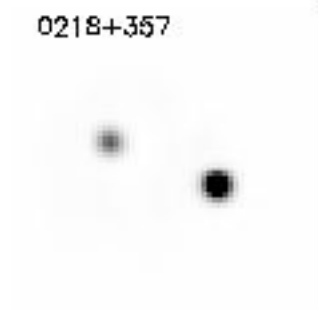
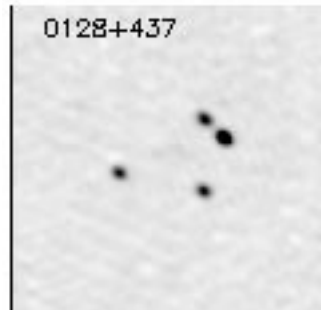
CLASS STRATEGY



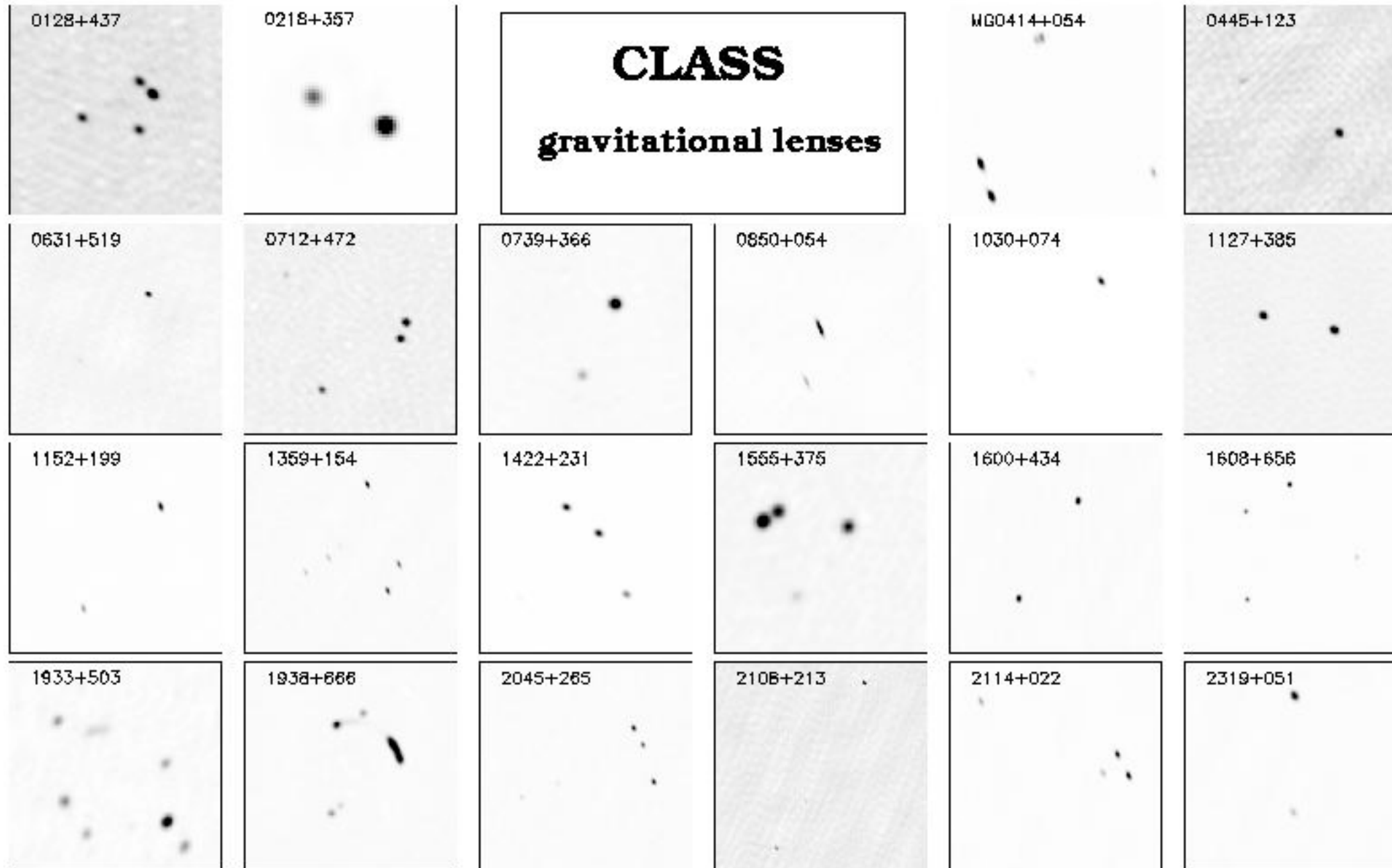
Browne et al. 2002



CLASS LENSES

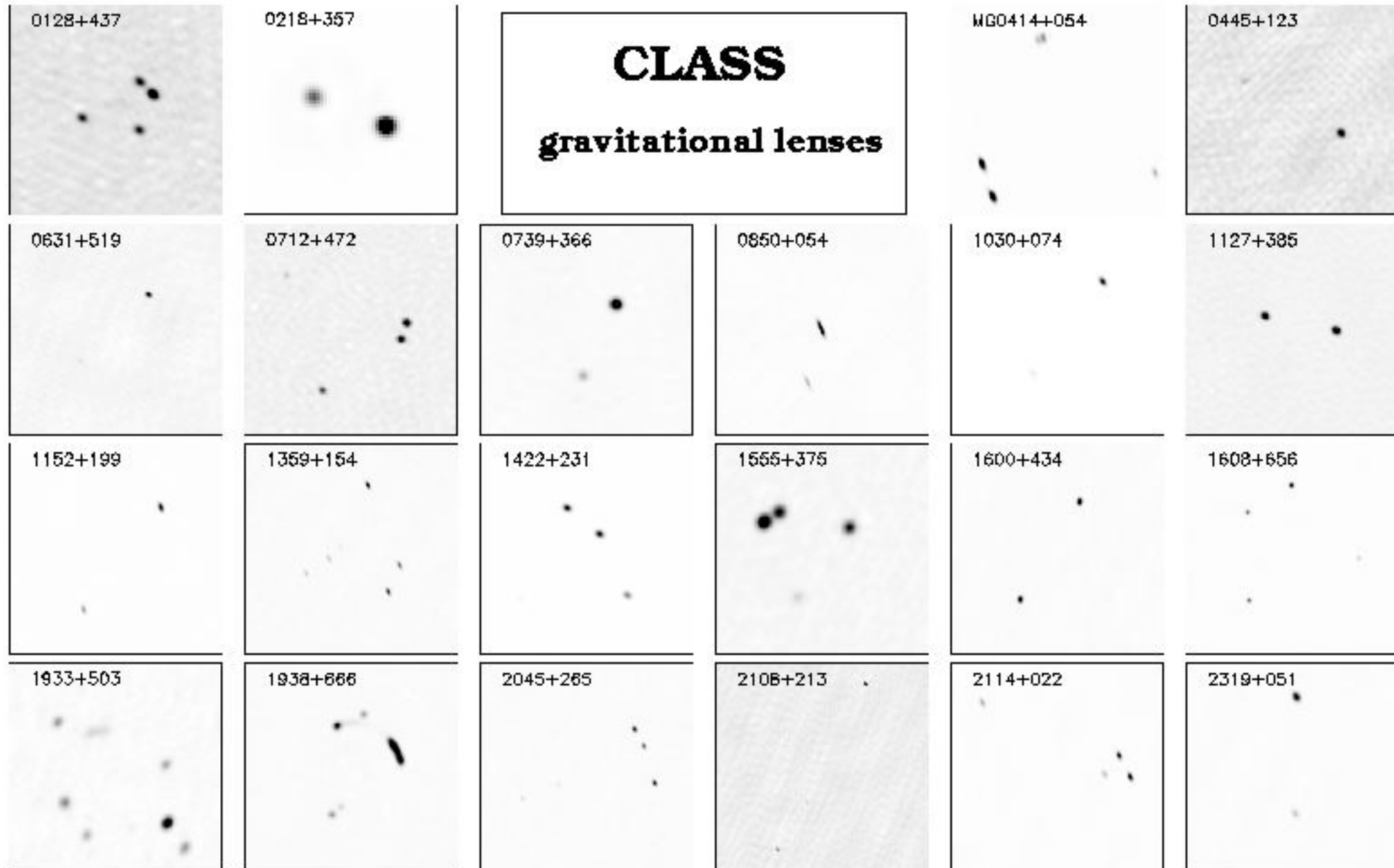


CLASS LENSES



12 double

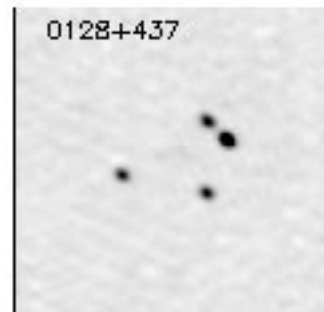
CLASS LENSES



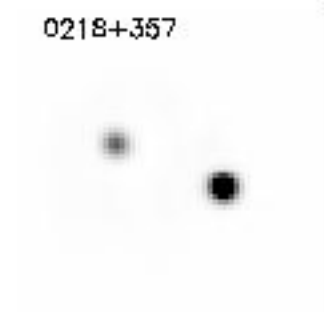
12 double

9 quadruple

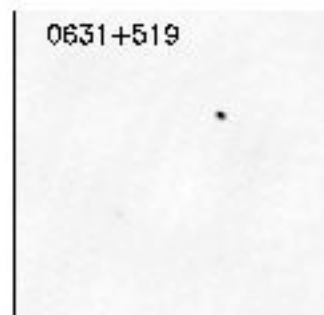
CLASS LENSES



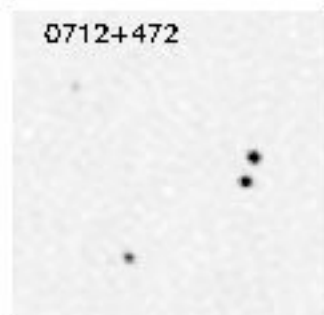
0128+437



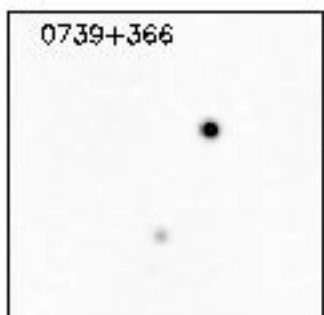
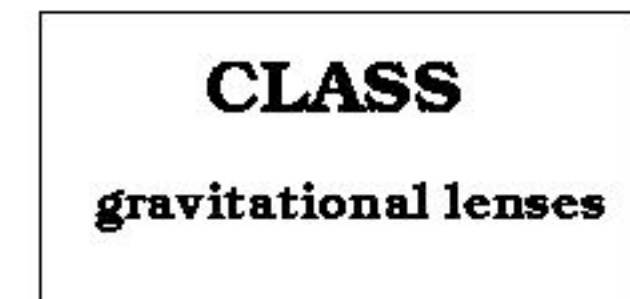
0218+357



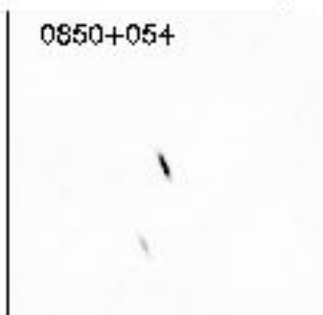
0631+519



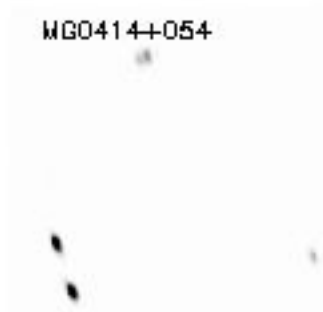
0712+472



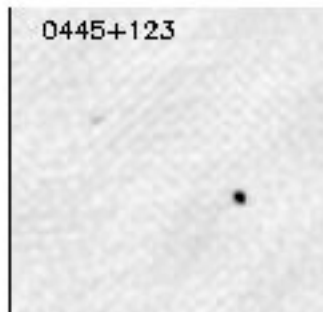
0739+366



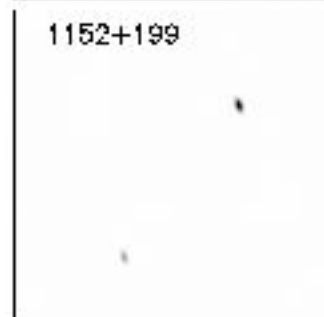
0850+054



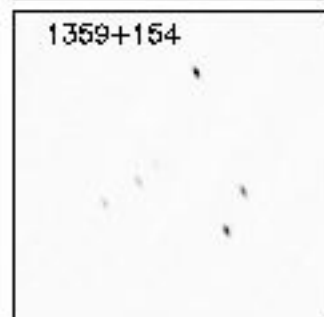
MG0414+054



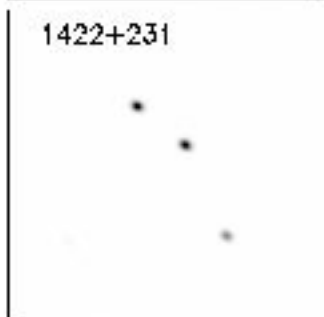
0445+123



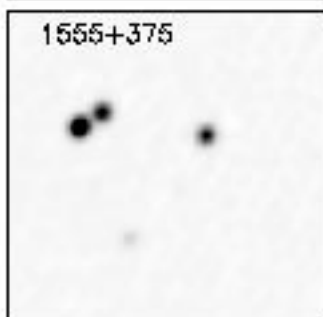
1152+199



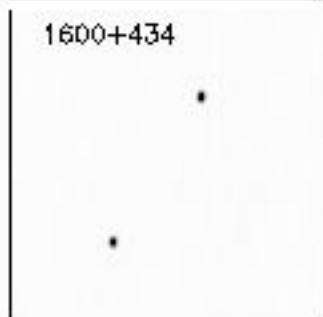
1359+154



1422+231



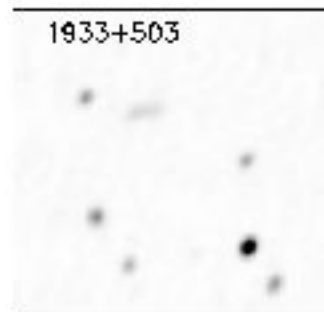
1555+375



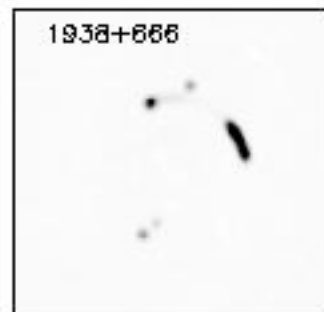
1600+434



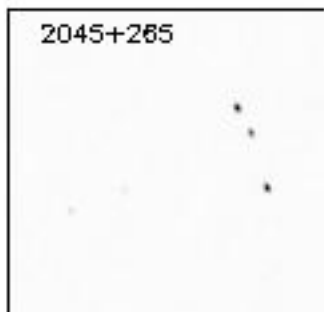
1608+656



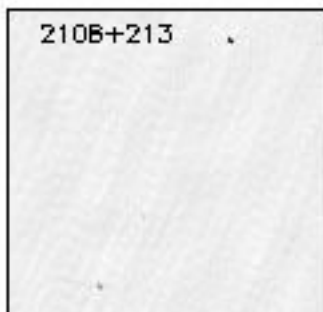
1933+503



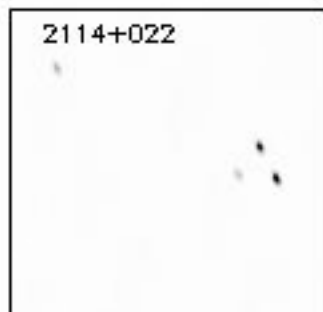
1938+666



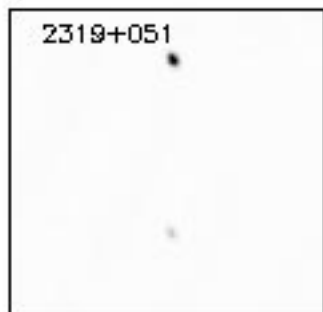
2045+265



2108+213



2114+022



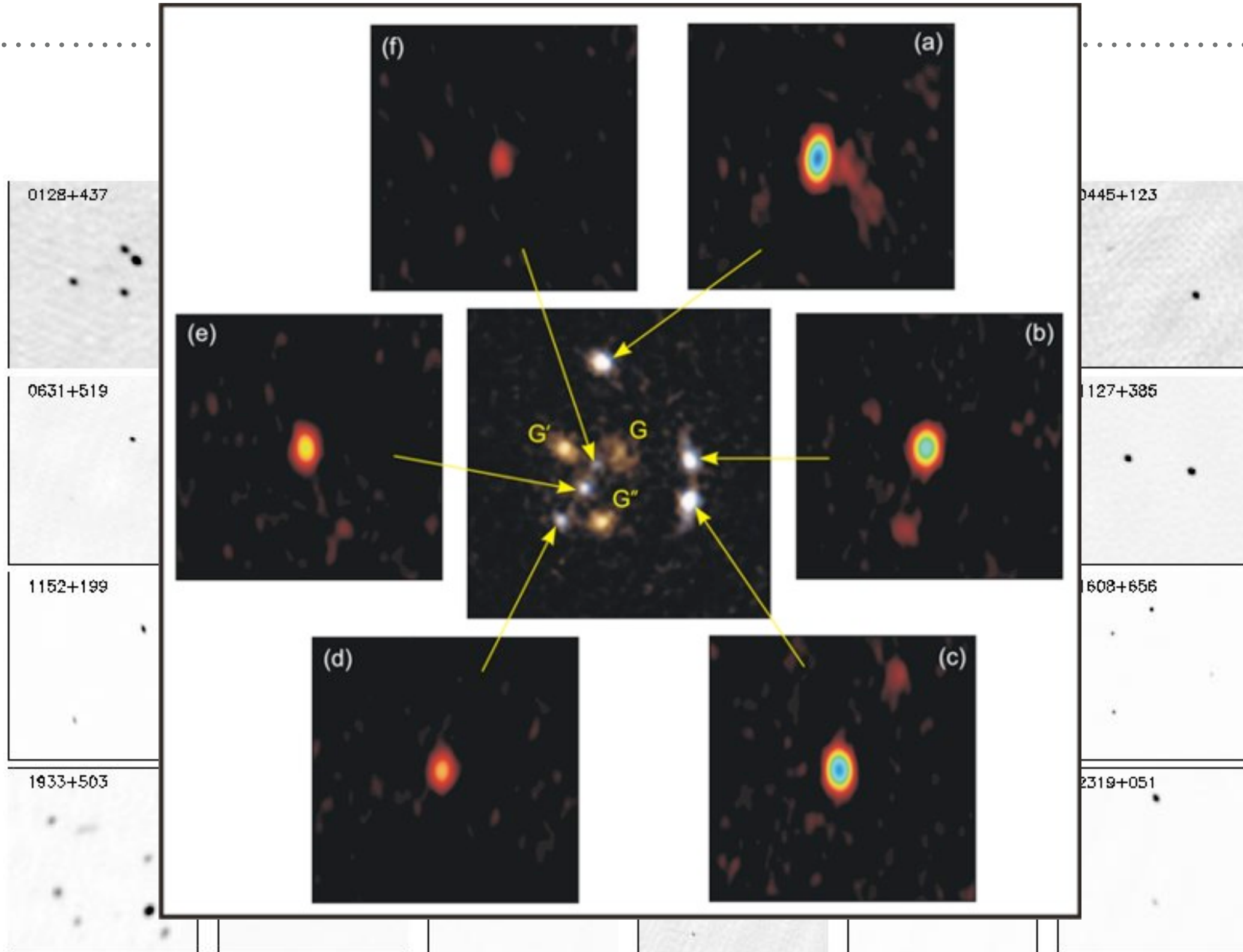
2319+051

12 double

9 quadrupole

1 sextuple

CLASS LENSES

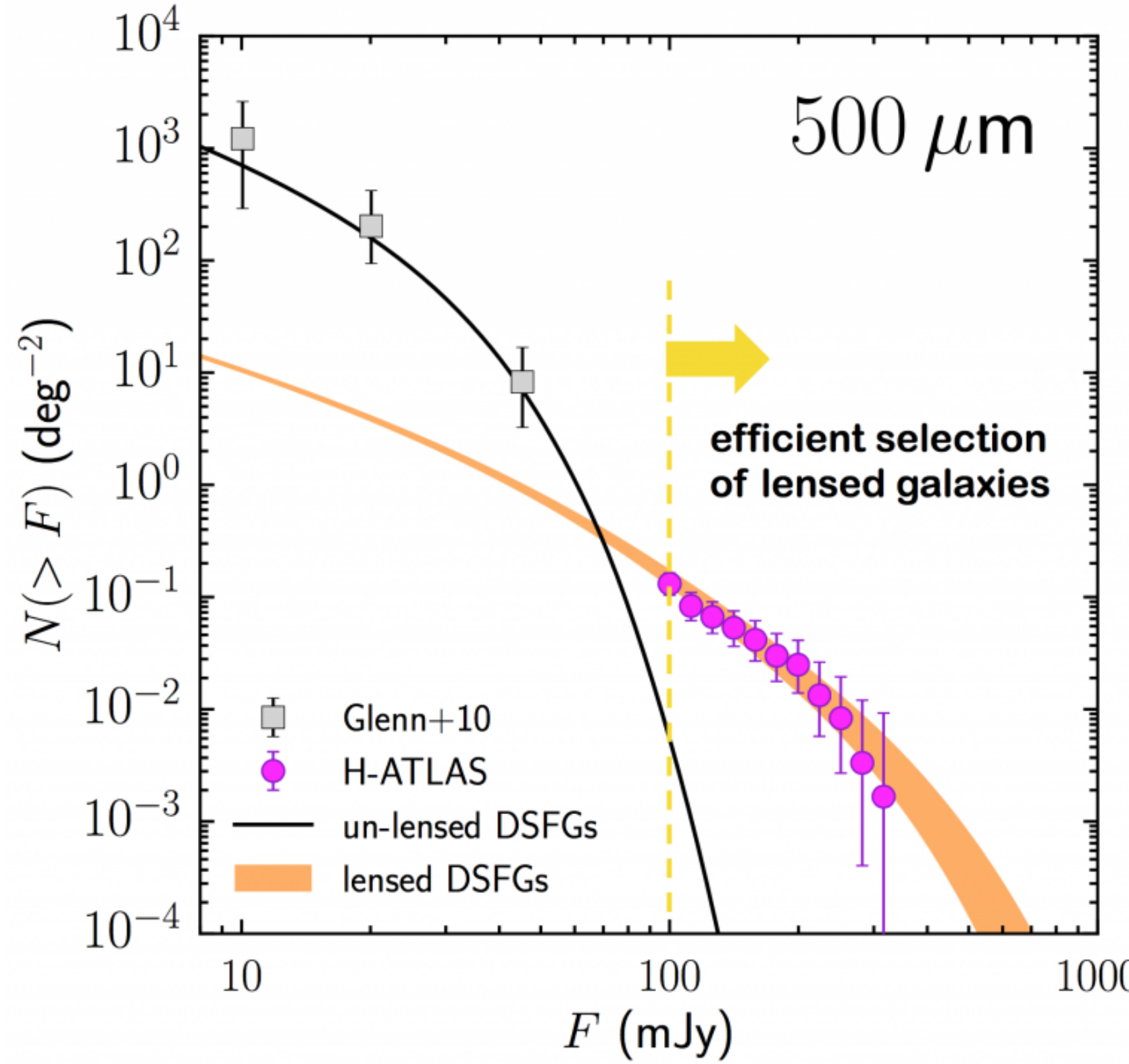


12 double

9 quadrupole

1 sextuple

SEARCHES AT THE SUB-MM WAVELENGTHS: MAGNIFICATION BIAS



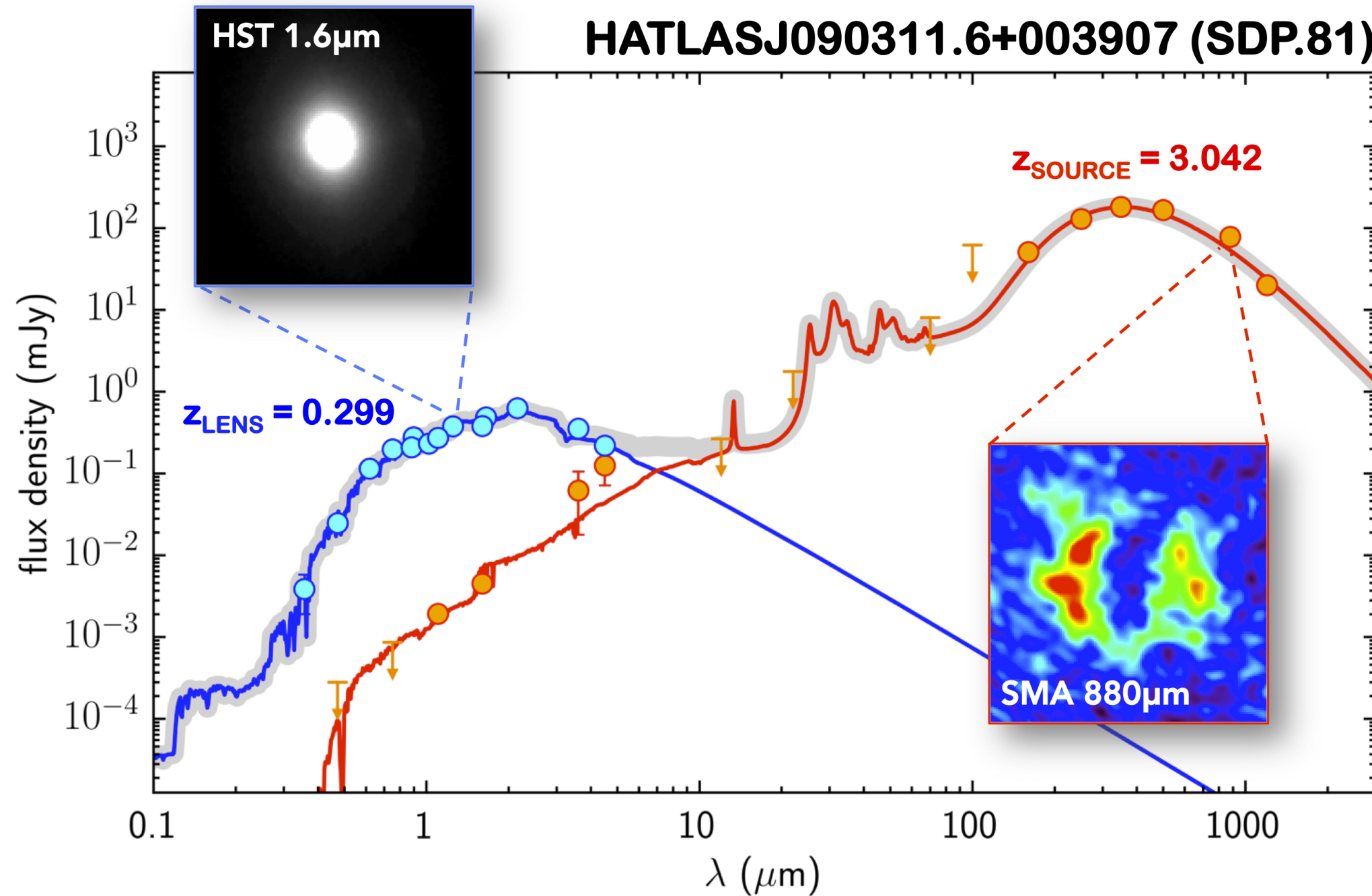
$$N_0(> F) = Q F^{-\alpha}$$

$$N_{obs}(> F') = \frac{N_0(> F/\mu)}{\mu}$$

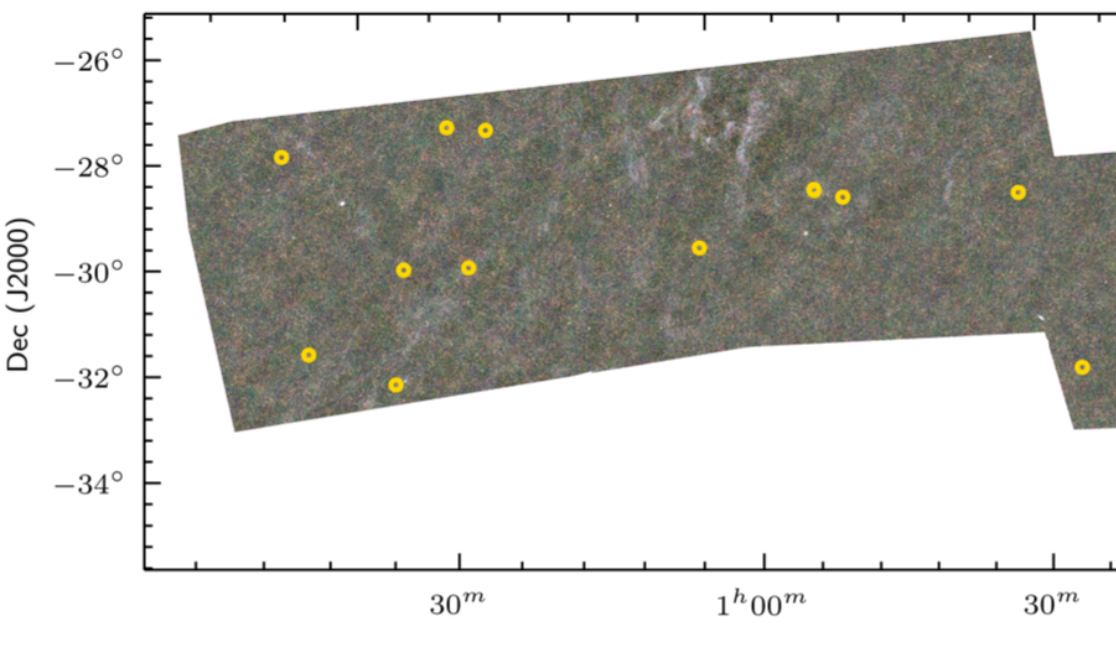
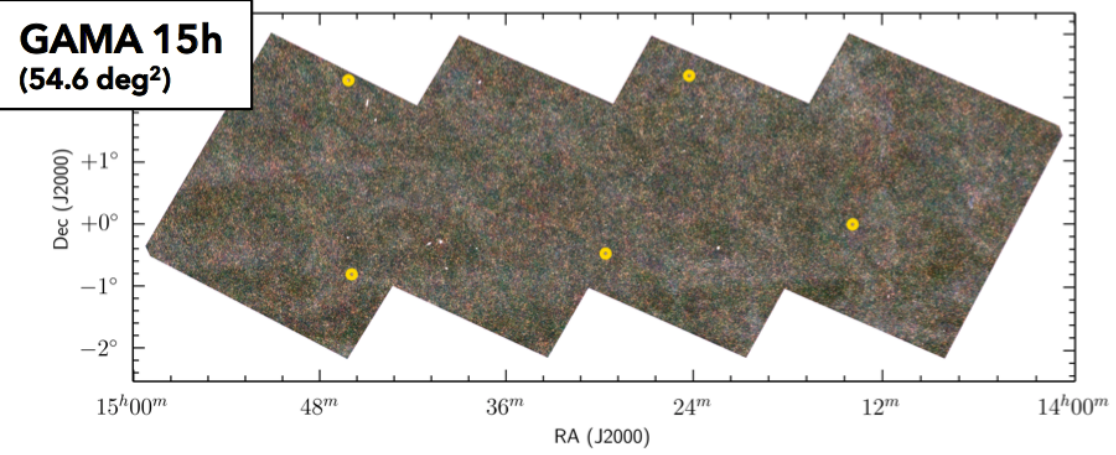
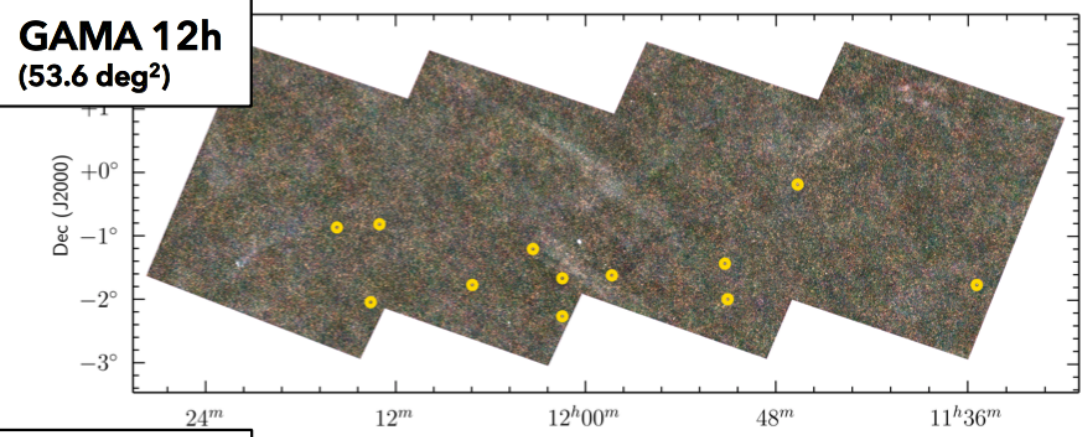
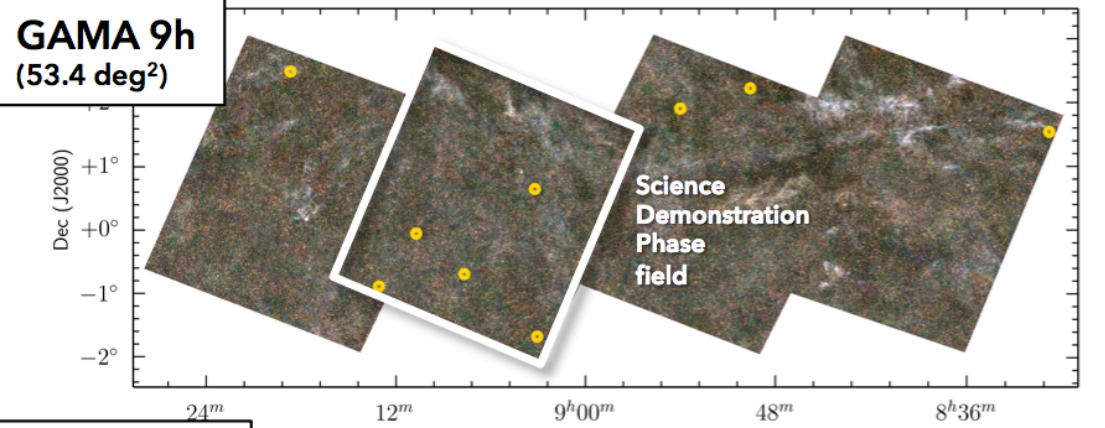
$$\begin{aligned} N_{obs}(> F') &= Q \frac{(F/\mu)^{-\alpha}}{\mu} \\ &= Q \frac{F^{-\alpha}}{\mu^{1-\alpha}} \\ &= N_0(> F) \mu^{\alpha-1} \end{aligned}$$

Negrello et al. 2010

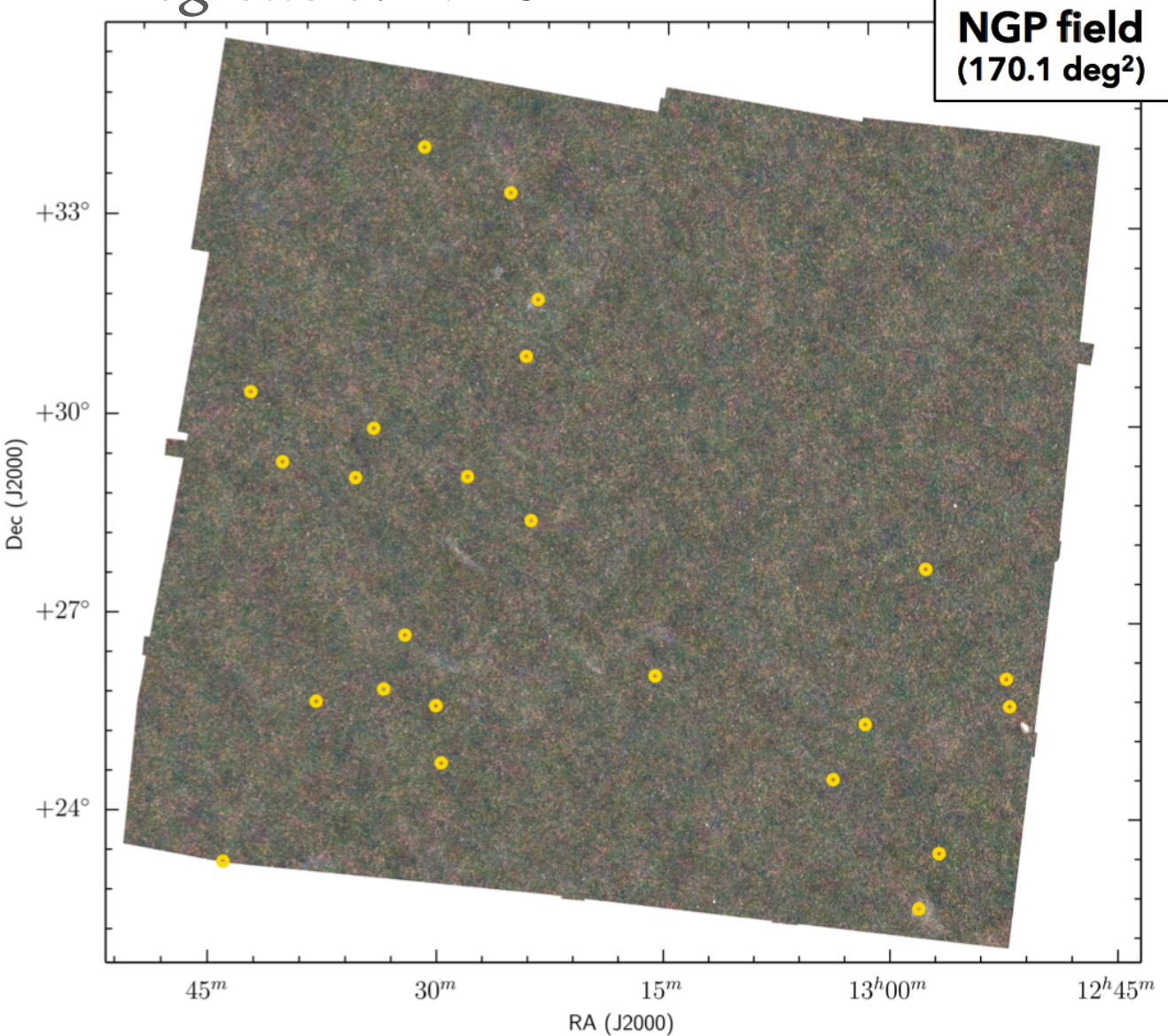
SEARCHES AT THE SUB-MM WAVELENGTHS



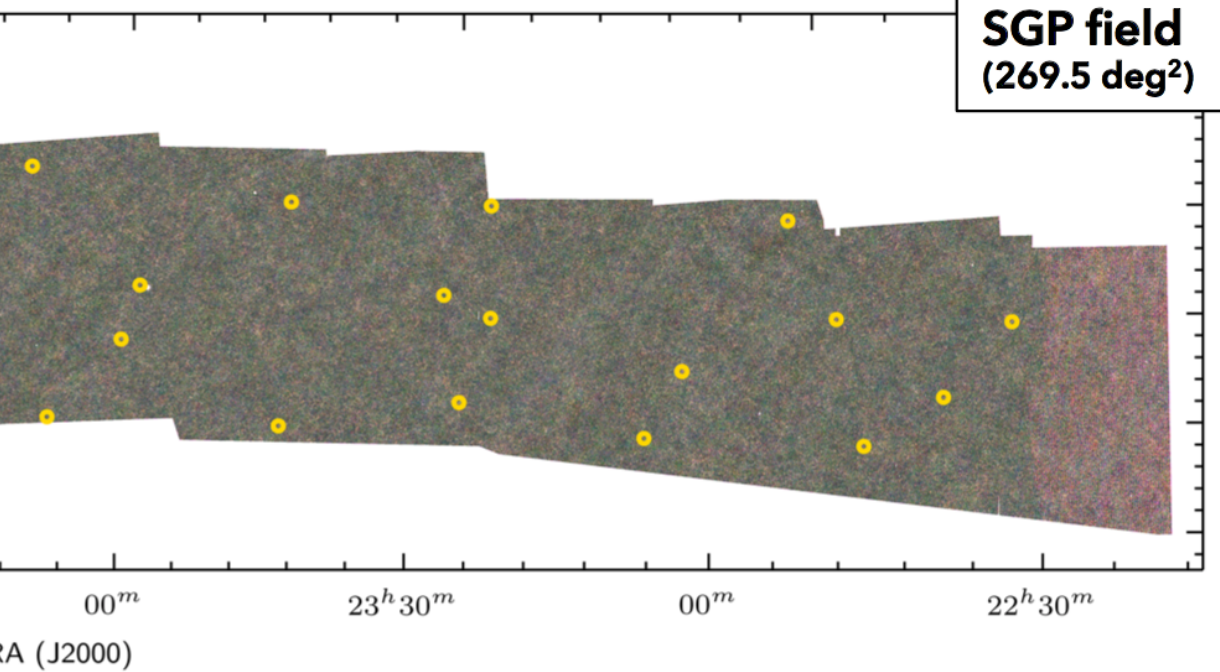
Negrello et al. 2010



Negrello et al 2017



SGP field
(269.5 deg²)



SLACS (OPTICAL)

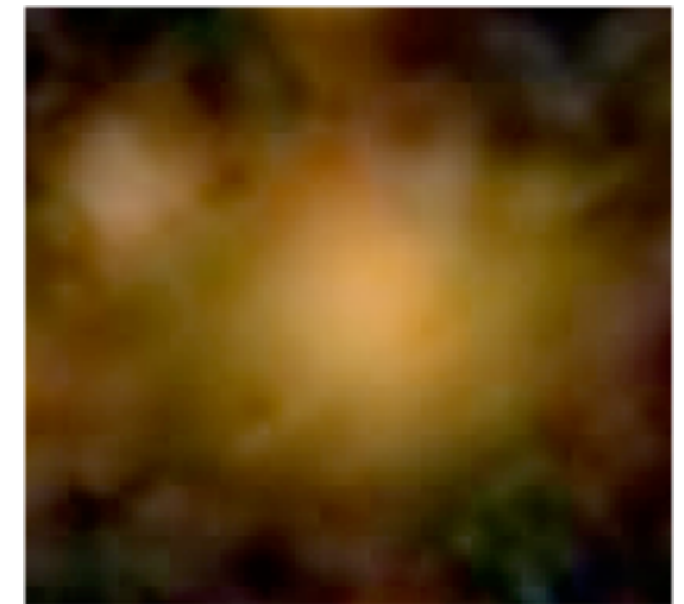
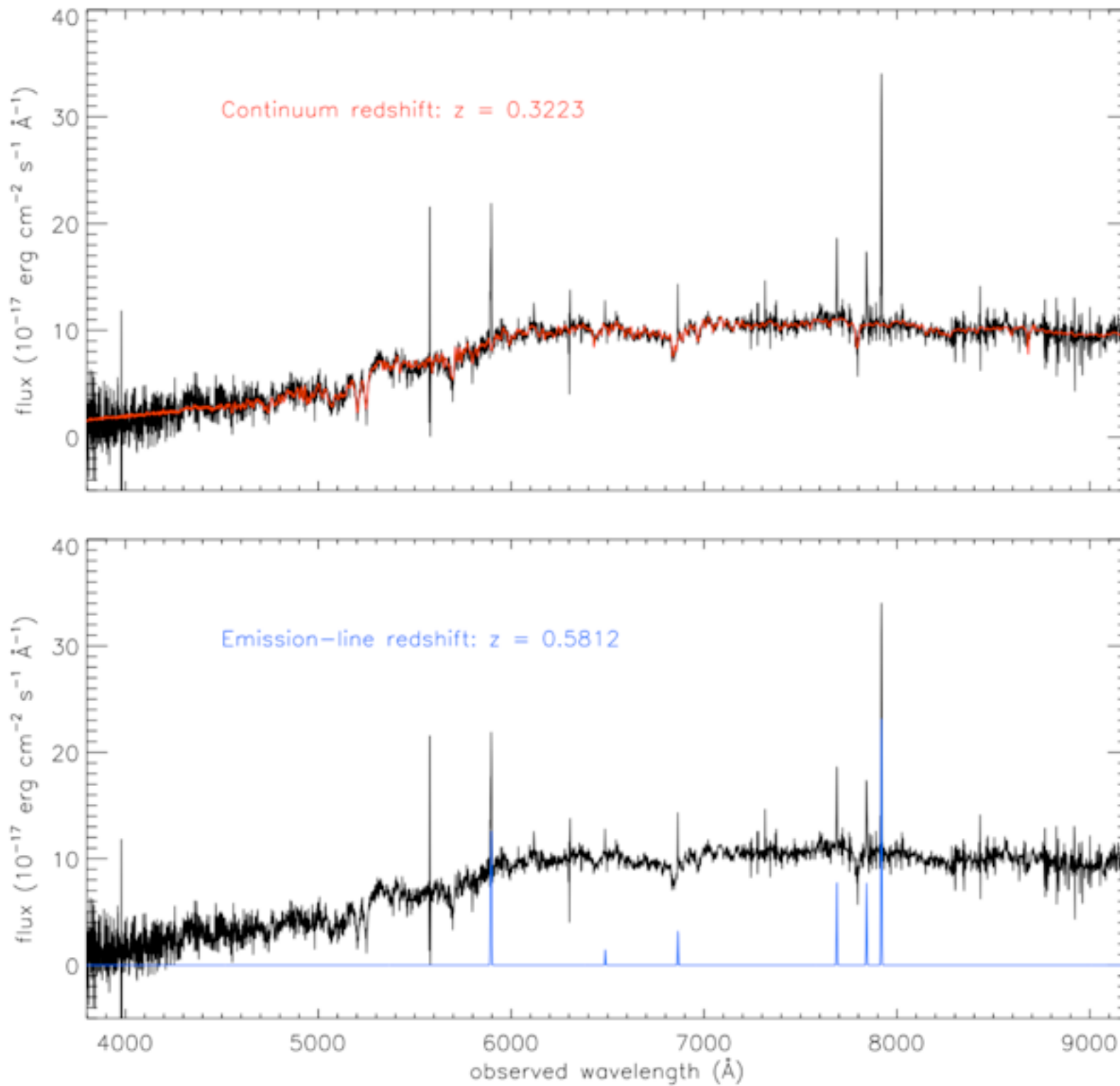
The SLACS (Sloan Lens ACS survey, Bolton et al. 2006) is a very successful project whose goal was finding strongly lensed galaxies behind SLOAN selected galaxies.

The candidate lenses are selected from the spectroscopic database of the Sloan Digital Sky Survey. This survey has produced imaging and spectra for galaxies on a huge portion of the sky (8400 sq. degree). The observations were conducted between 2000-2005 (SDSS-I) and 2005-2009 (SDSS-II) using a dedicated 2.5m-telescope at Apache Point (New Mexico).

The candidate lenses are galaxies whose spectra can hardly be fitted with a single spectrum. This is an indication of superposition of two different galaxies along the line of sight. This technique follows the discovery of a lens system by Warren et al. (1996)

The selected candidates are observed at high-resolution with the ACS onboard HST.

SLACS STRATEGY

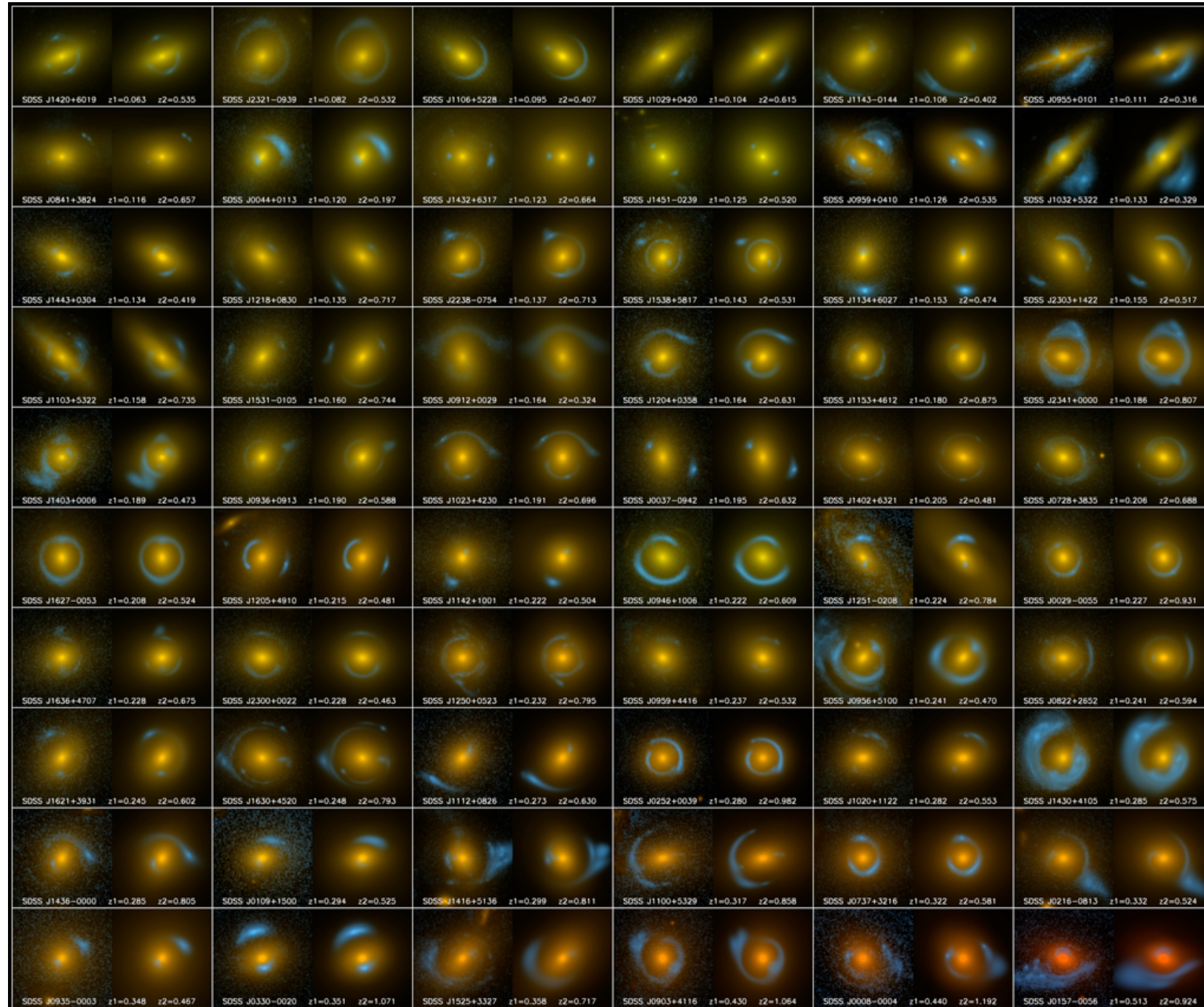


SLOAN image



HST follow-up

SLACS LENSES



- 85 galaxy lenses
- 13 probable lenses
- redshifts for all systems
- 80% ellipticals
- 10% lenticular
- 10% spirals (mostly bulge dominated)
- big galaxies with v. disp.
~200-300 km/s (average:
248 km/s)

SLACS: The Sloan Lens ACS Survey

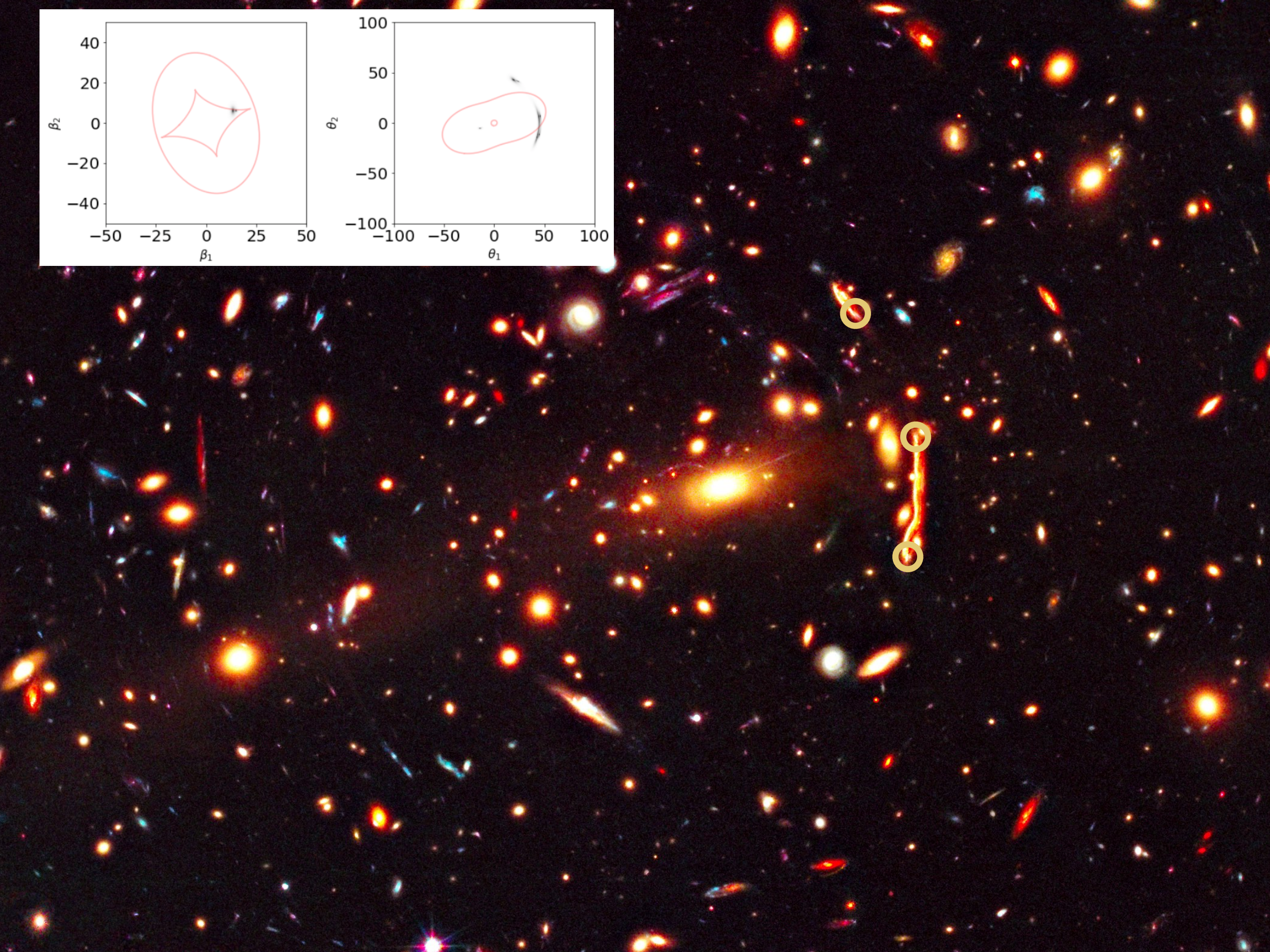
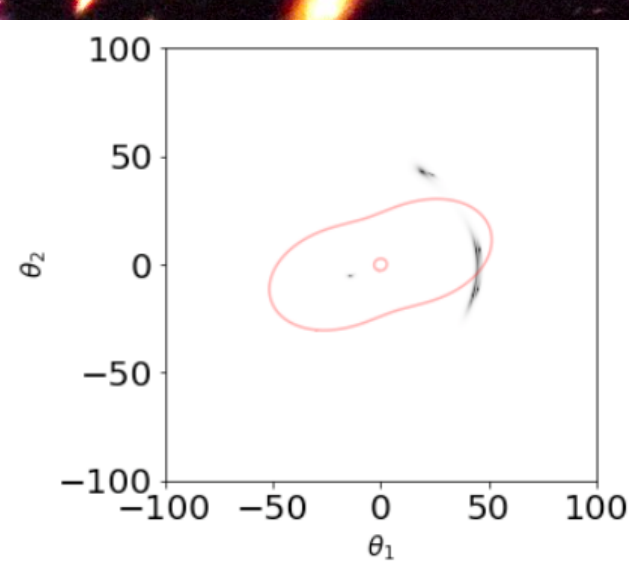
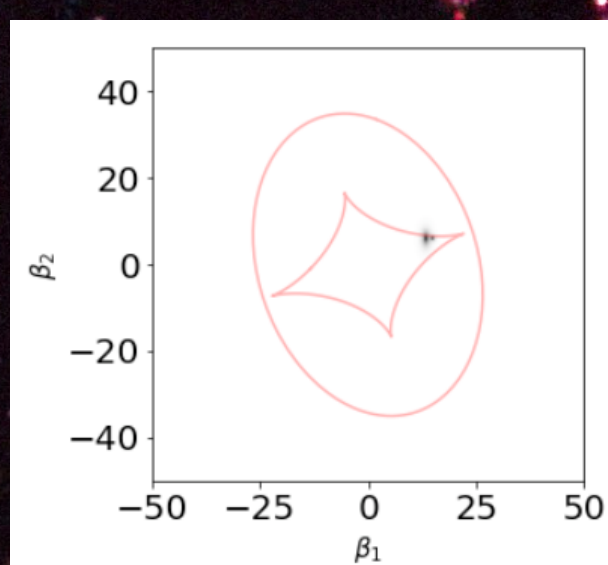
A. Bolton (U. Hawai'i IfA), L. Koopmans (Kapteyn), T. Treu (UCSB), R. Gavazzi (IAP Paris), L. Moustakas (JPL/Caltech), S. Burles (MIT)

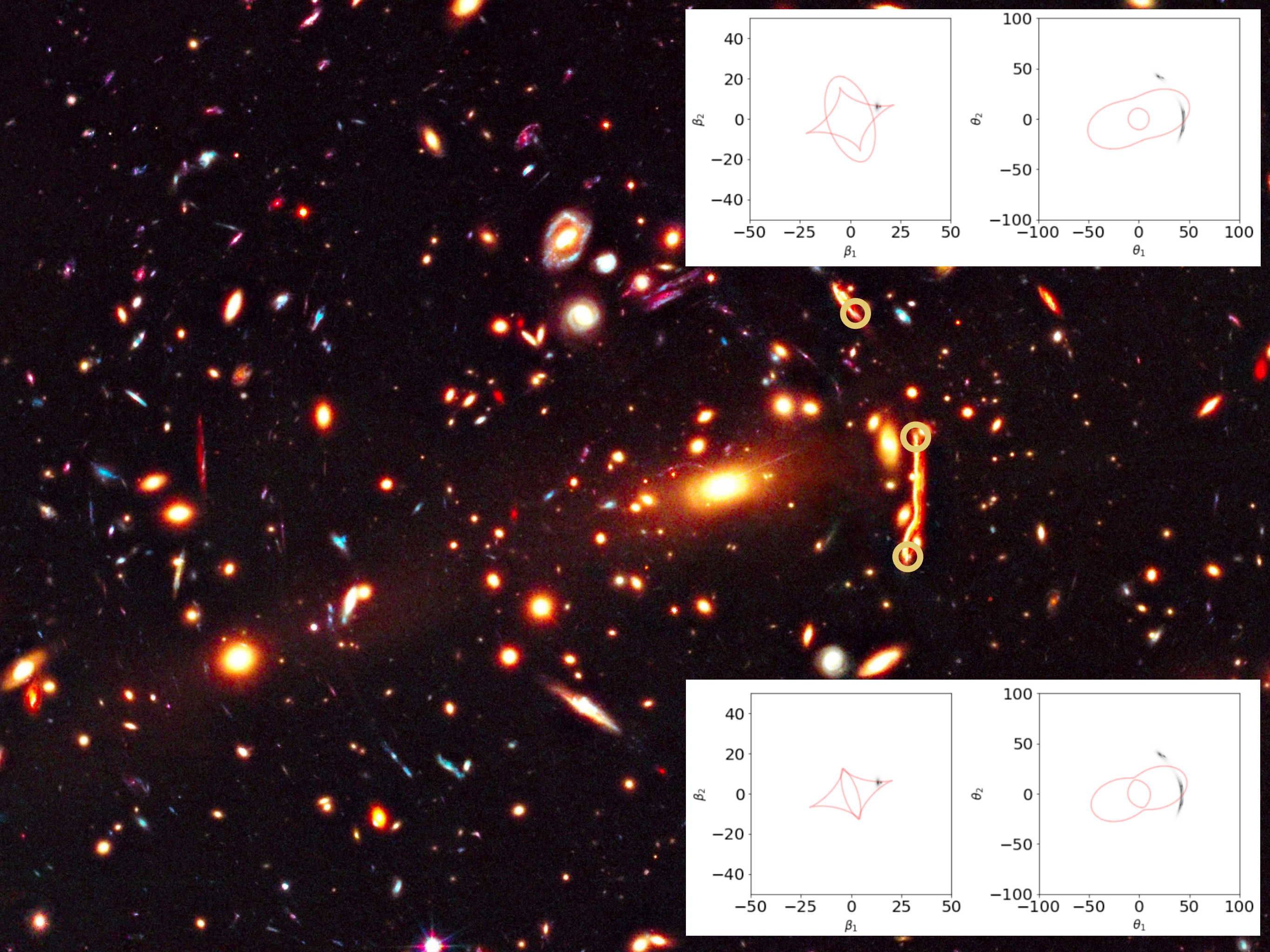
www.SLACS.org

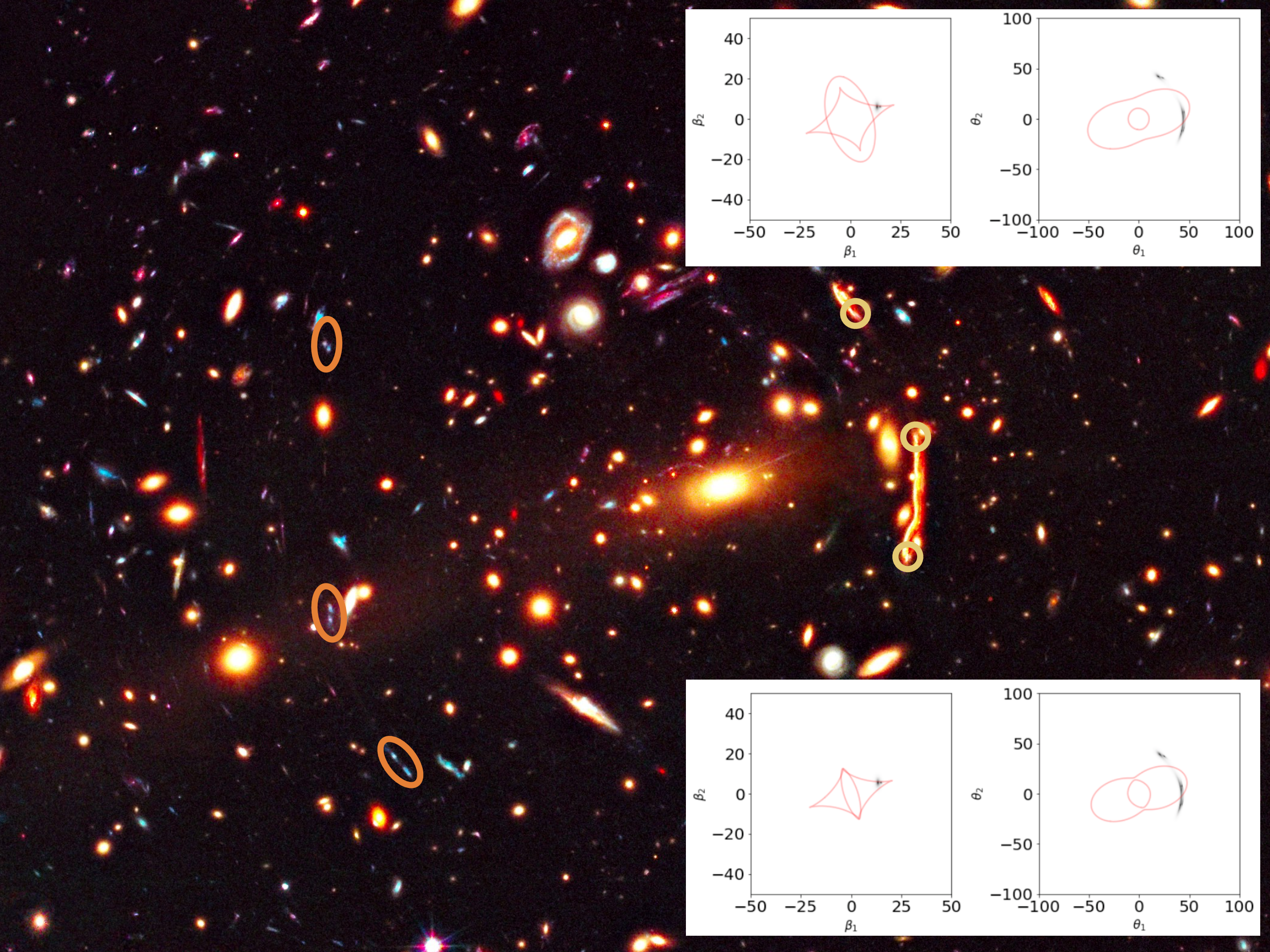
Image credit: A. Bolton, for the SLACS team and NASA/ESA

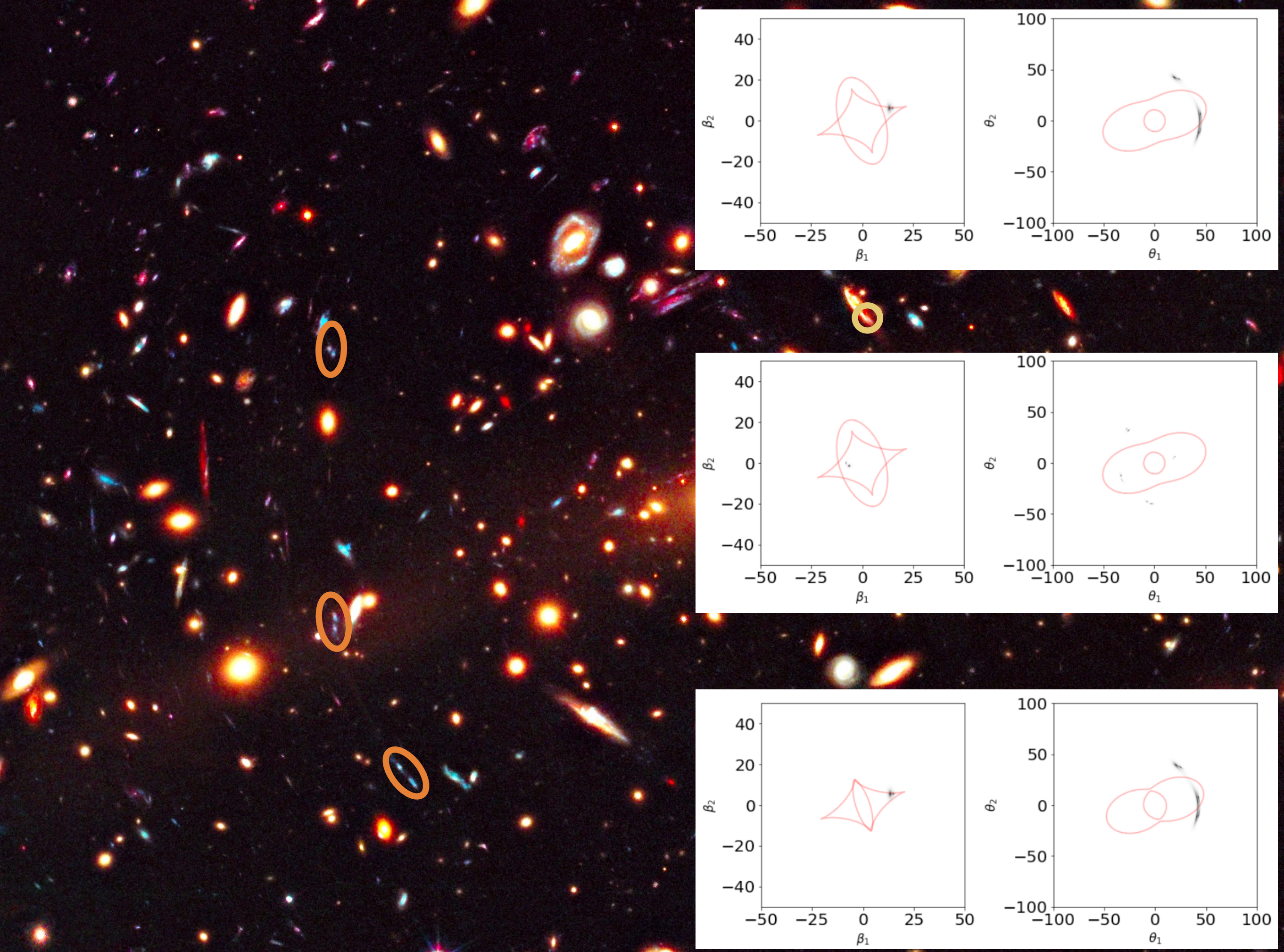


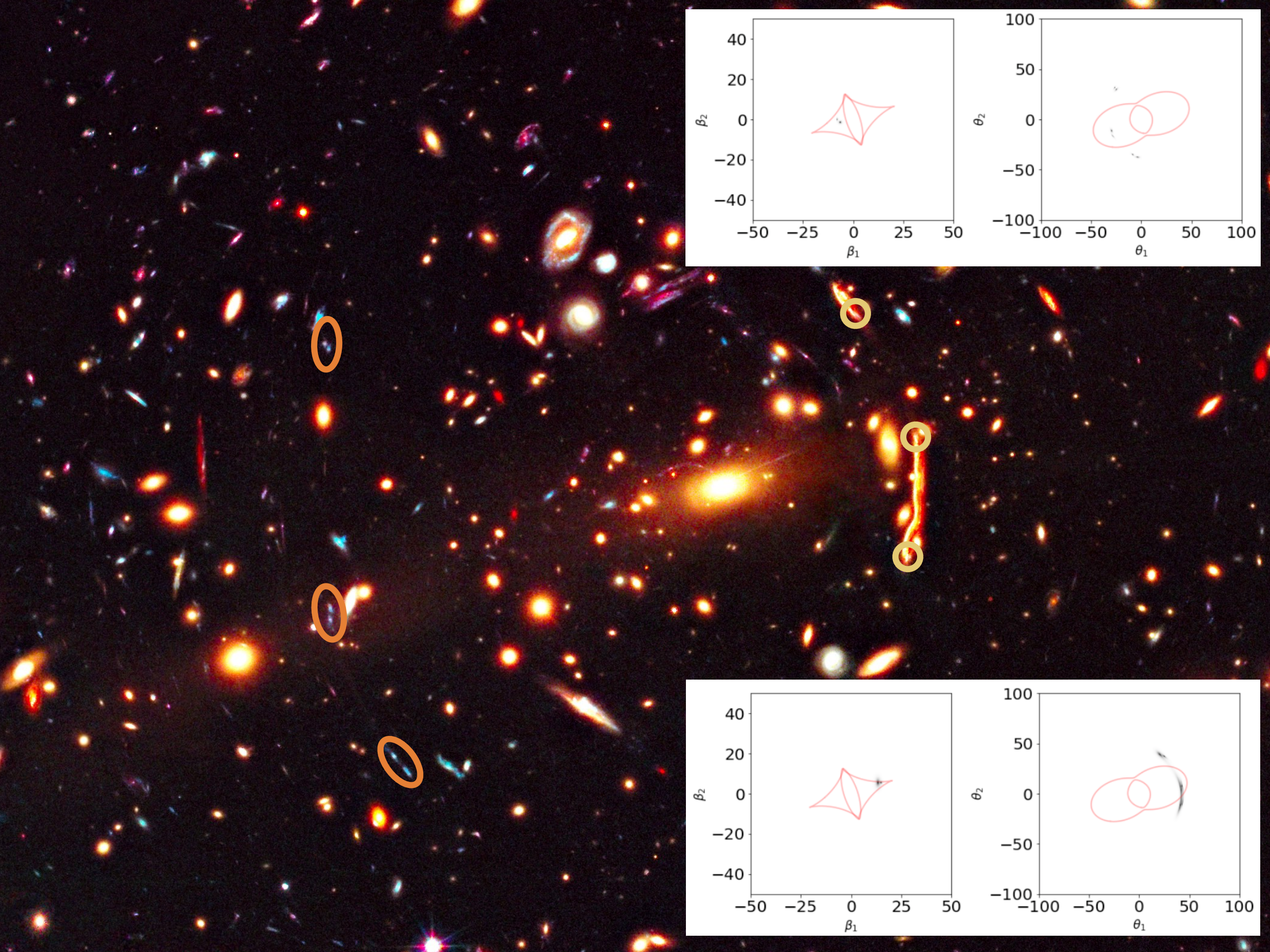


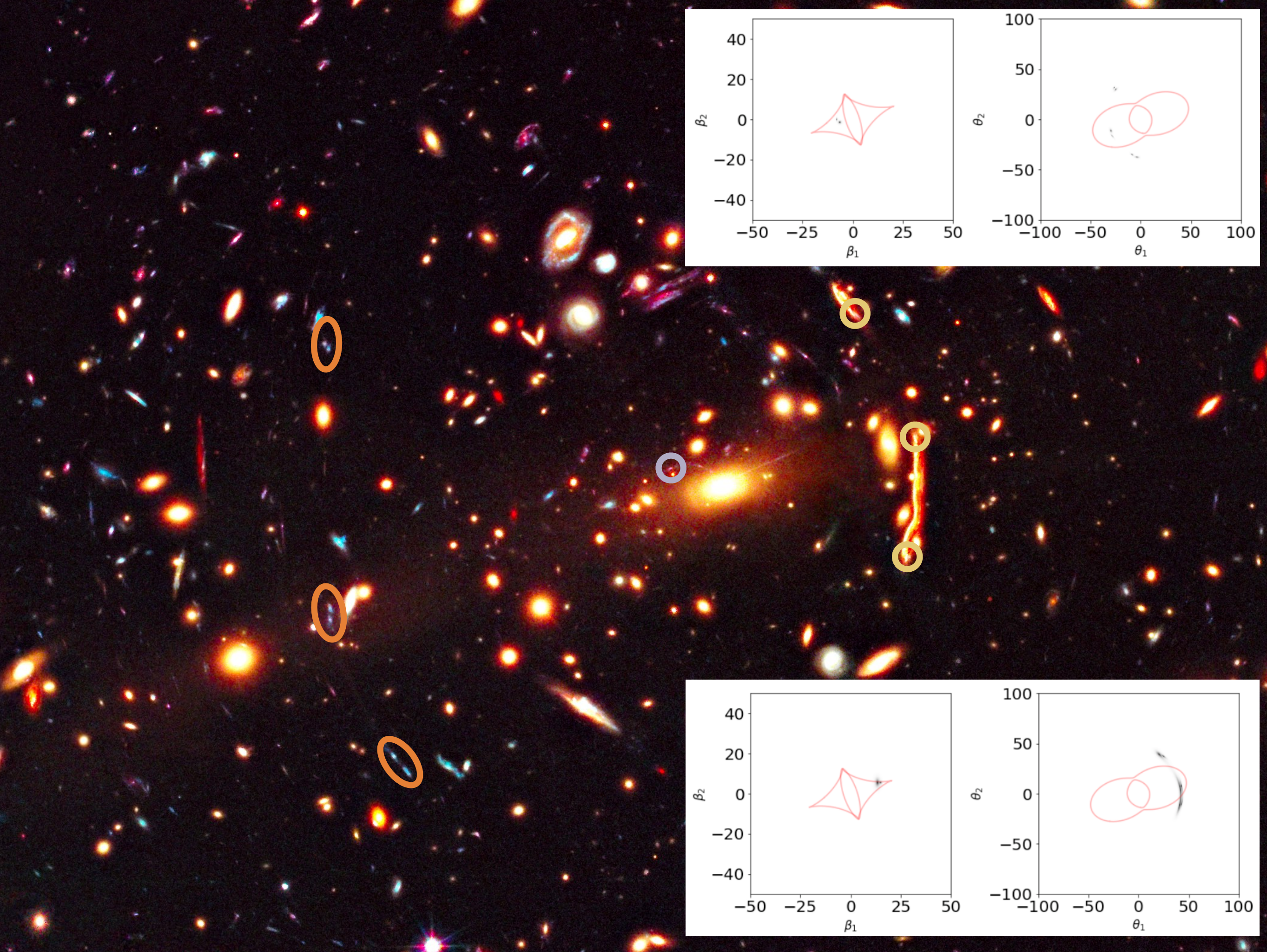


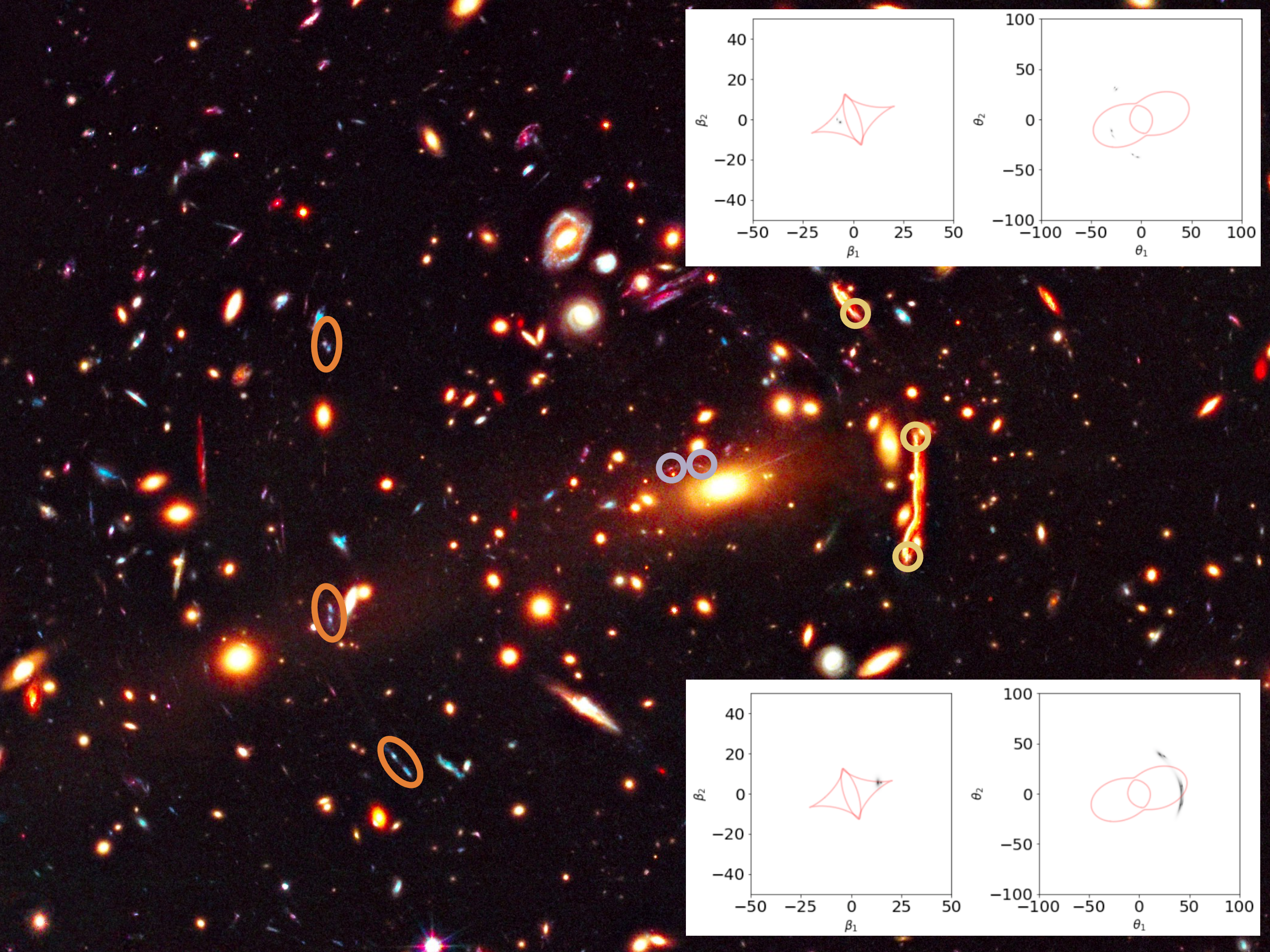


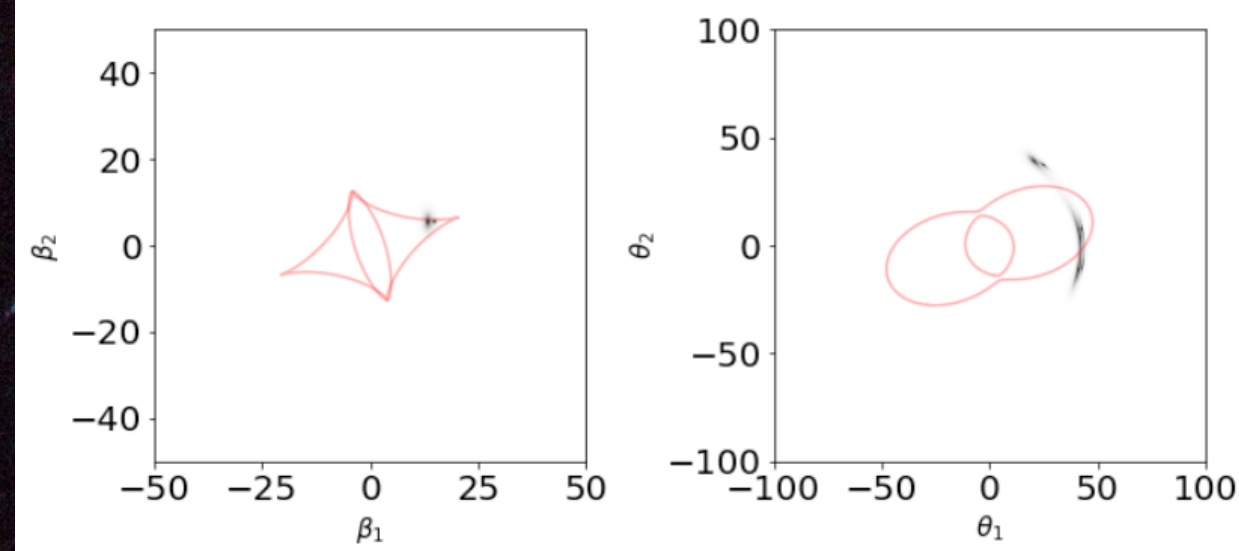
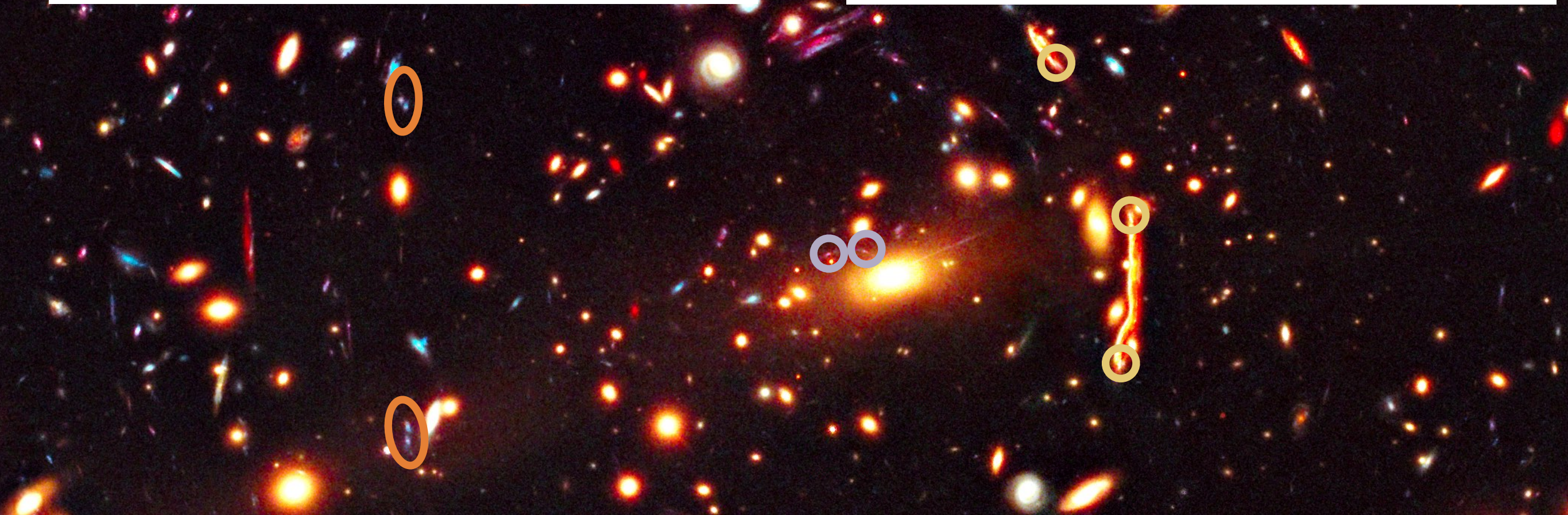
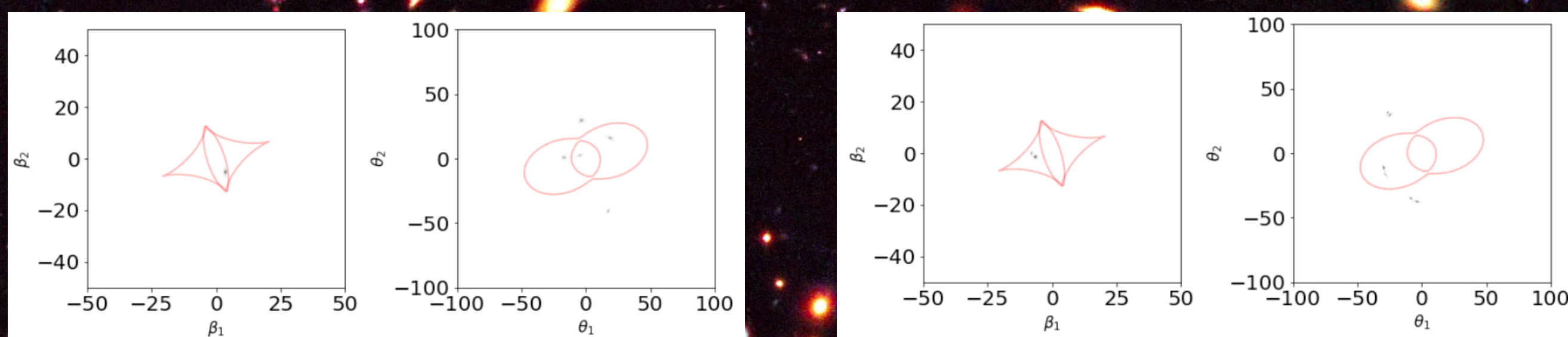


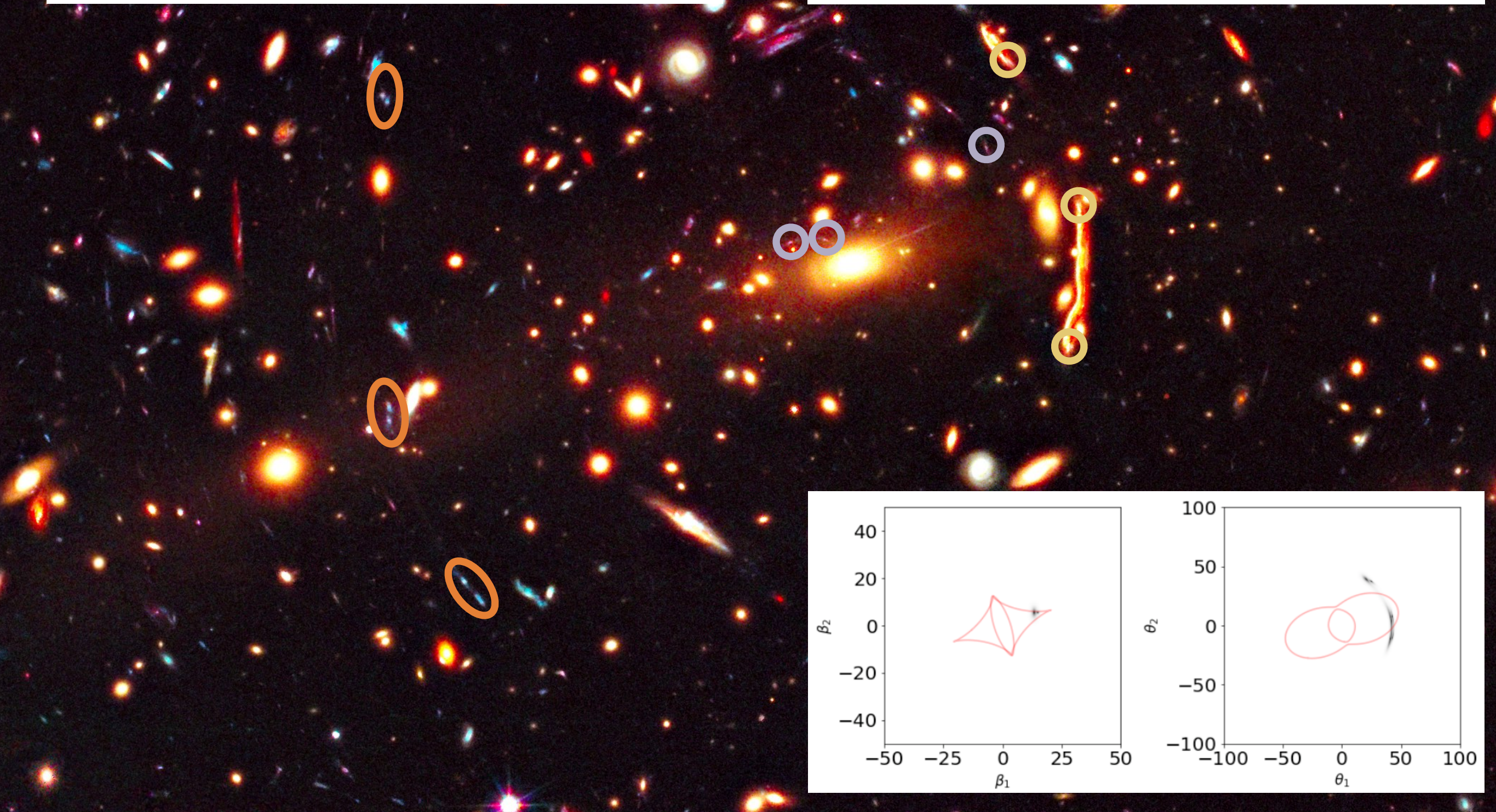
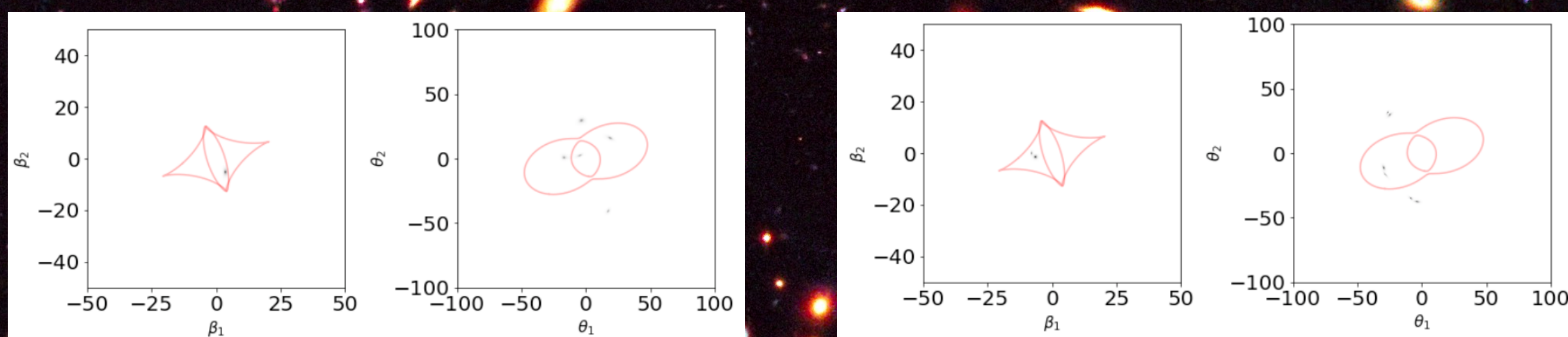


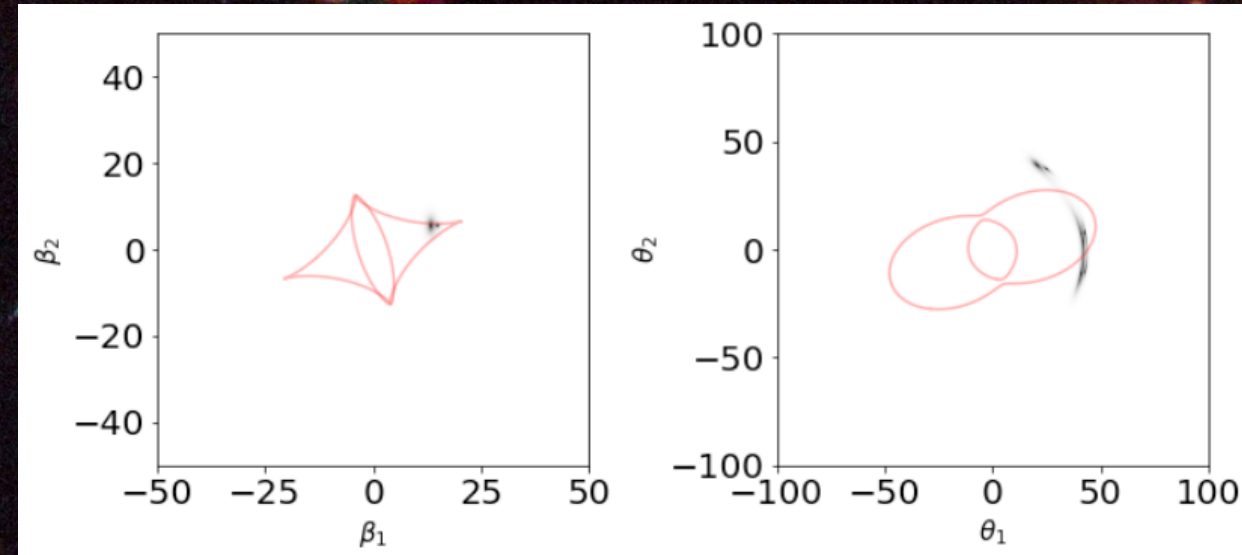
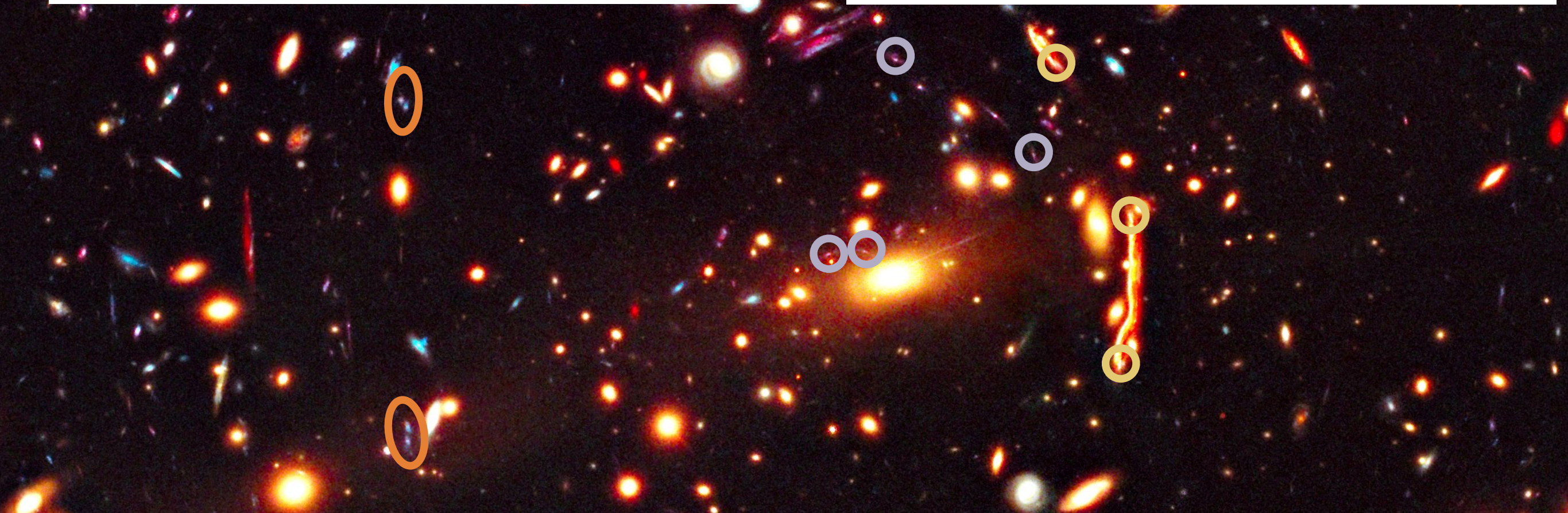
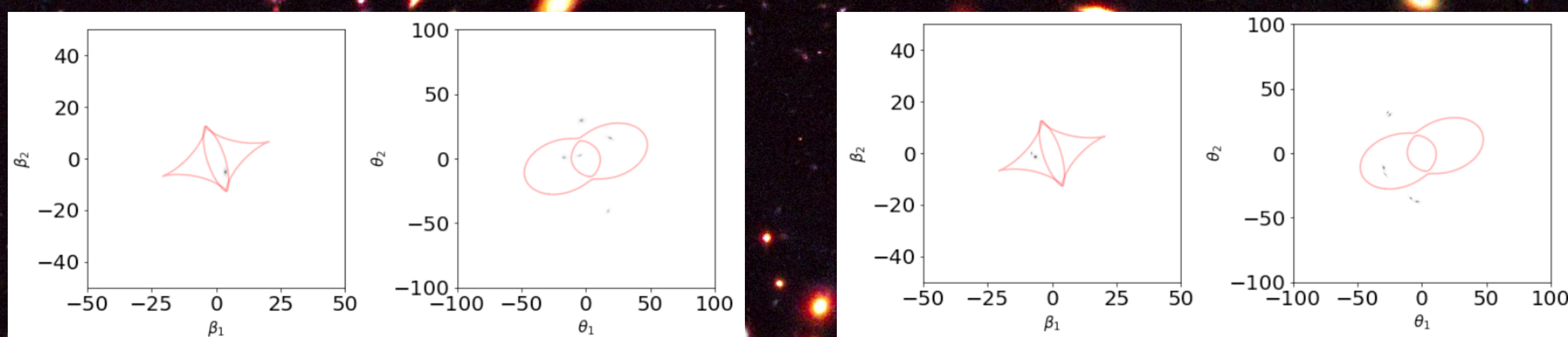


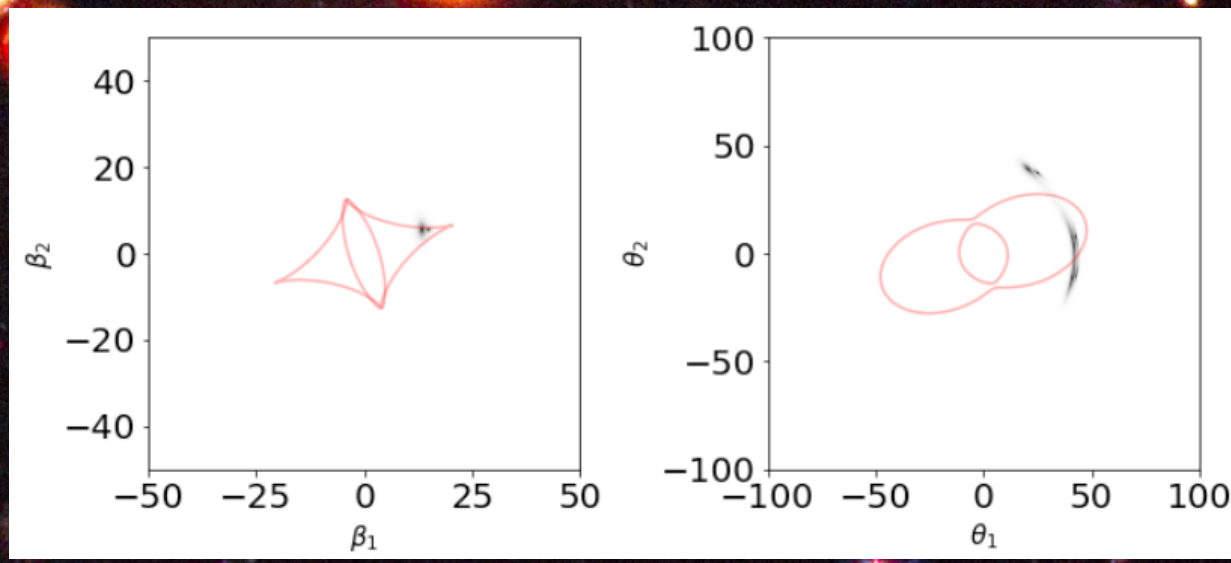
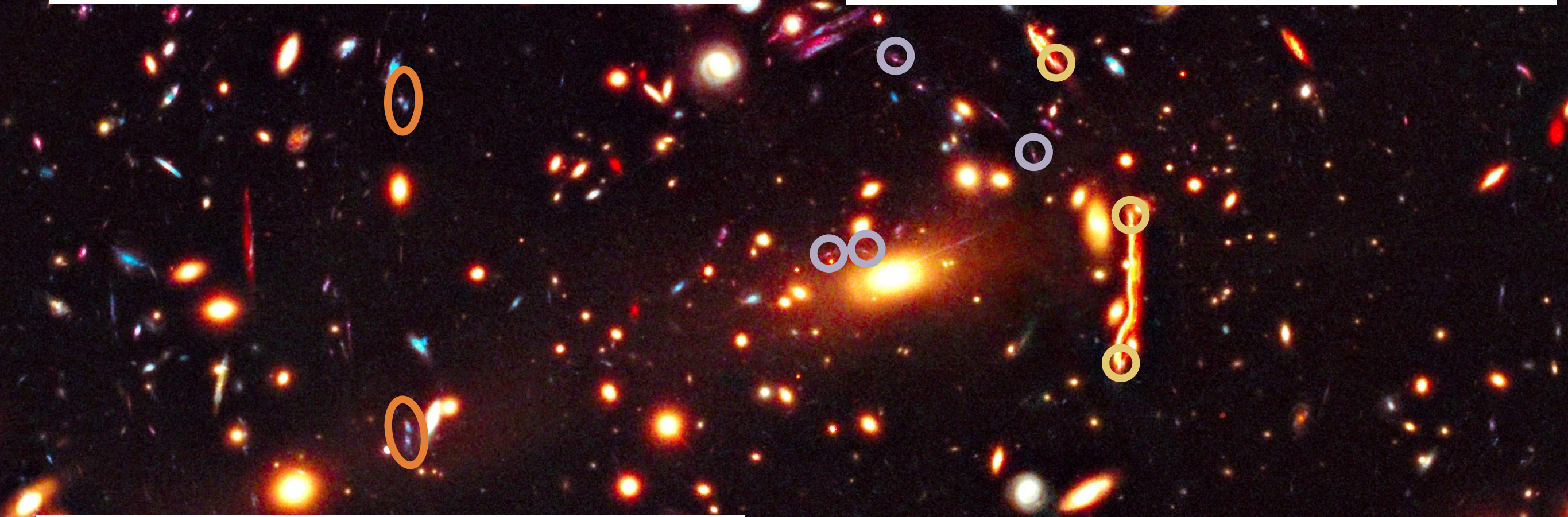
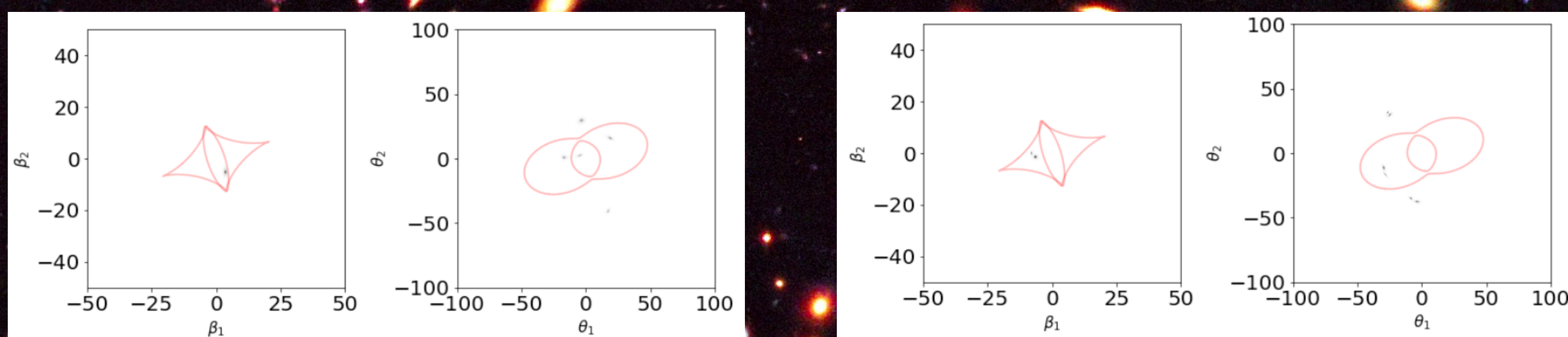


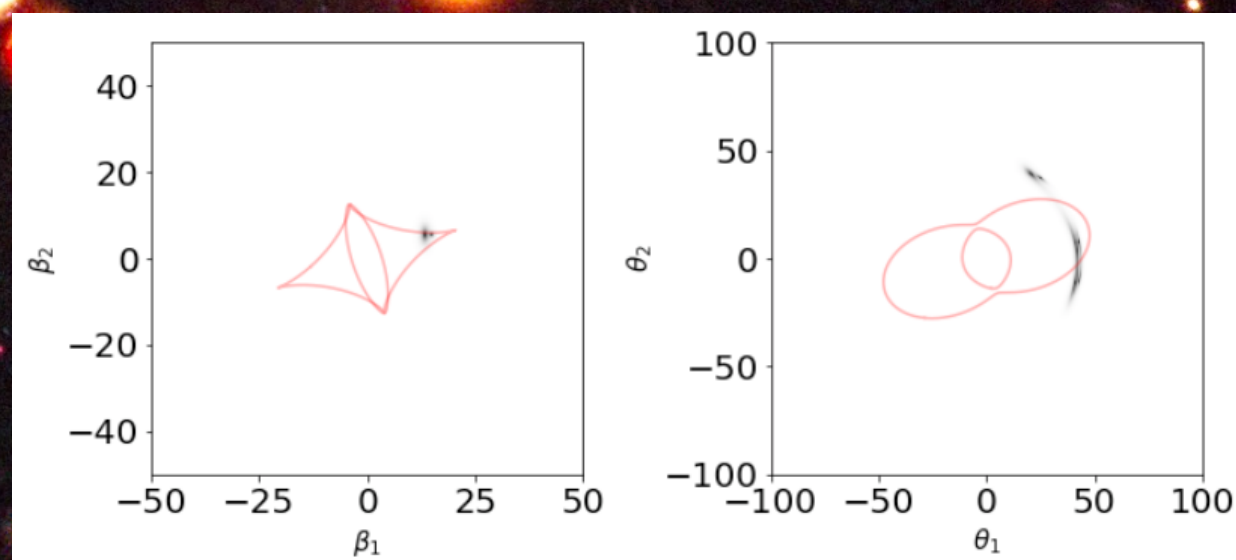
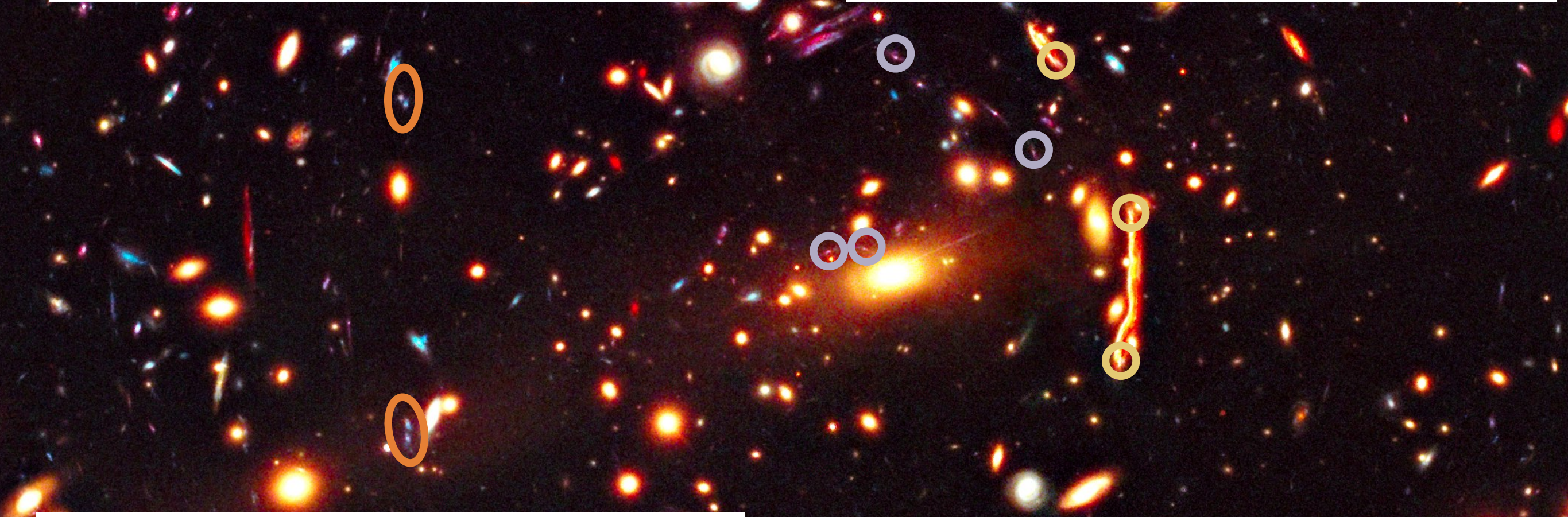
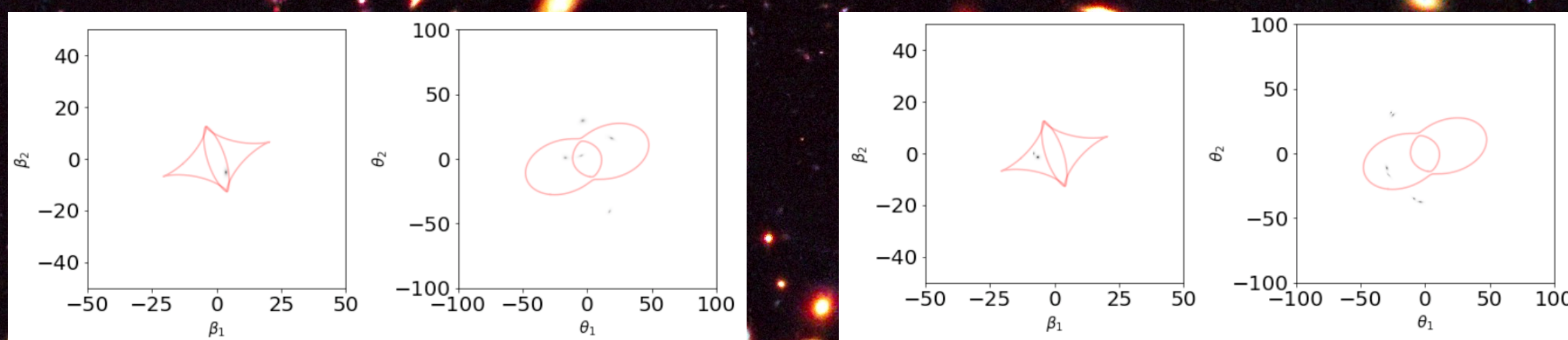






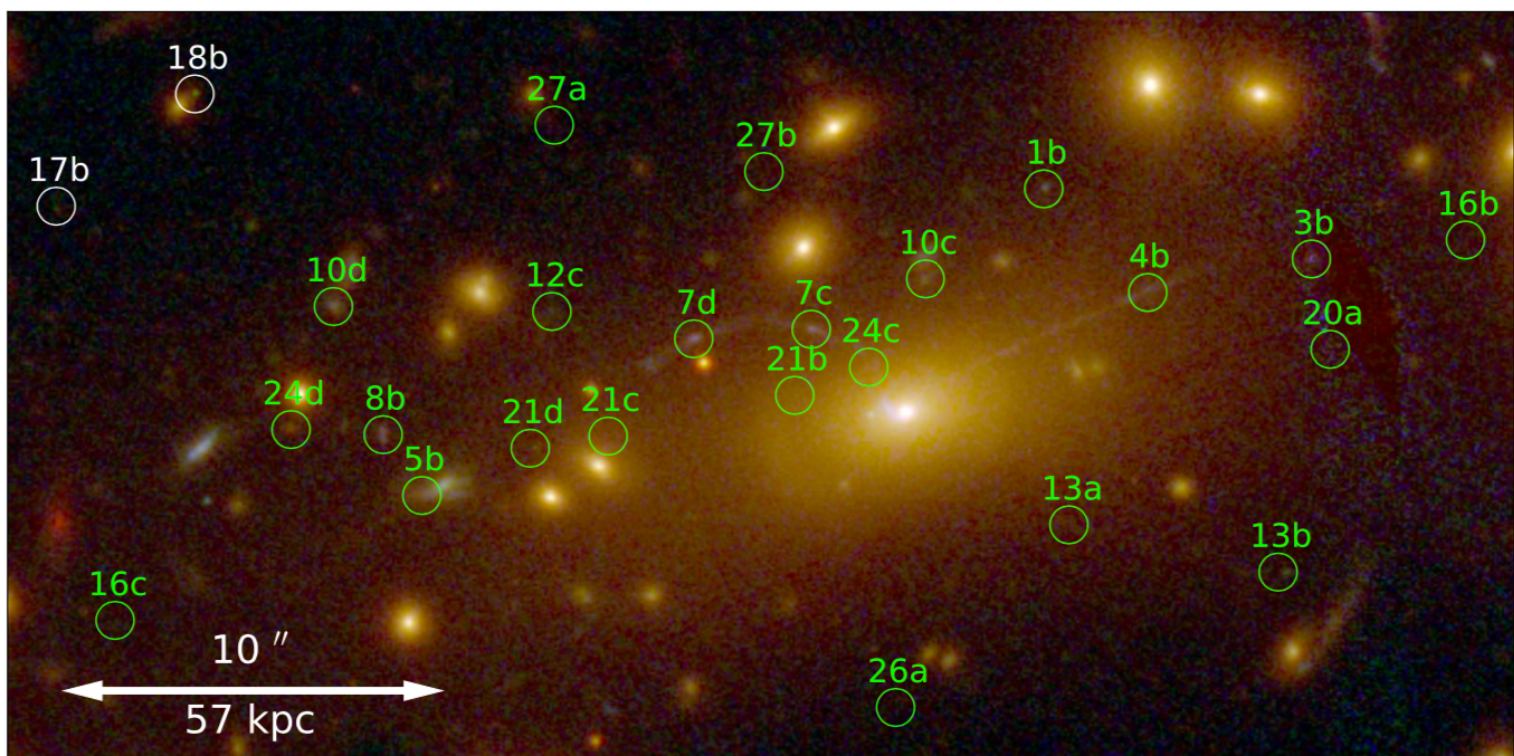
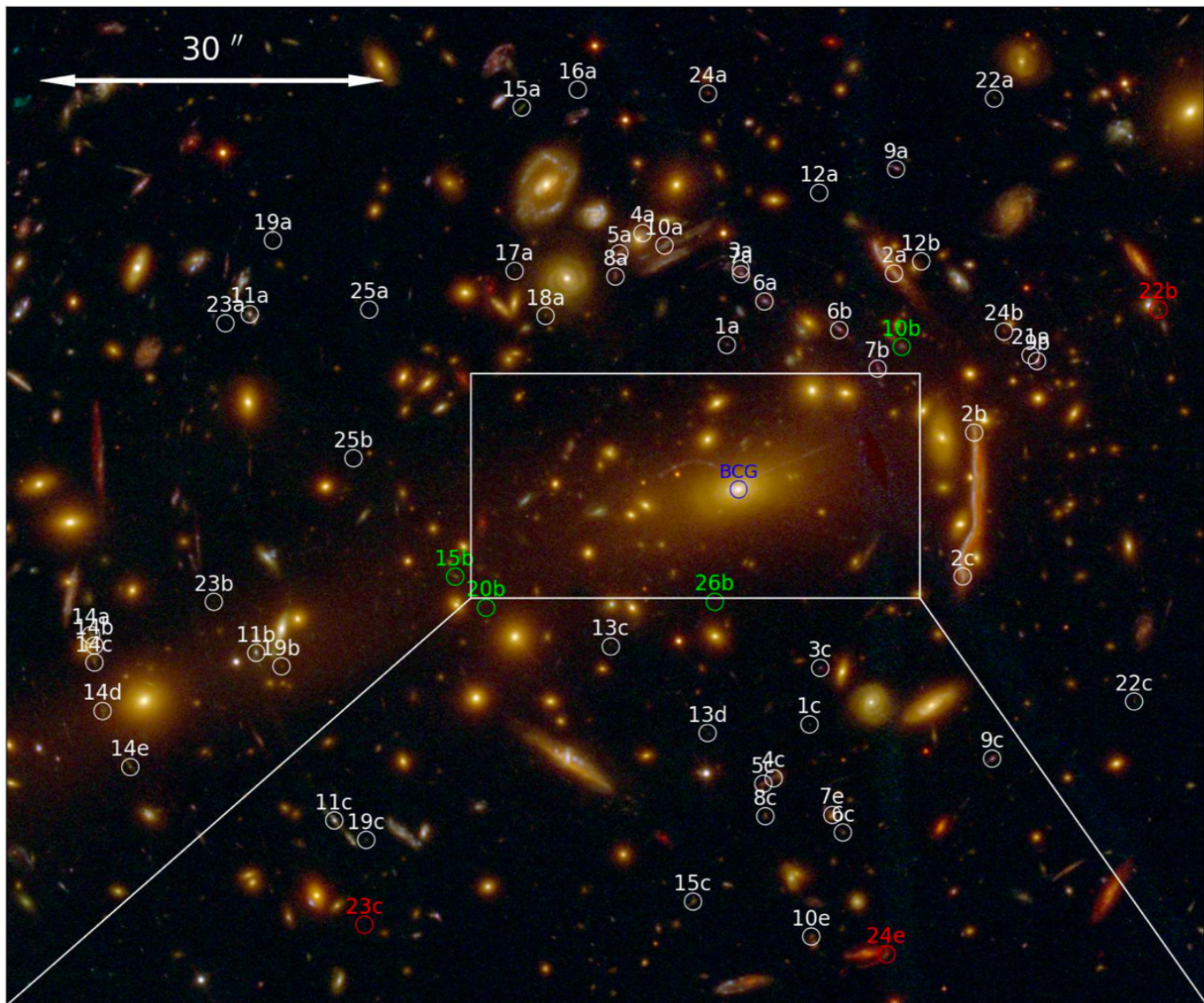






MACSJ1206

- 27 families of multiple images; 82 multiple images in total
- $z=[1.0-6.1]$
- Cluster redshift: $z=0.44$



MODEL OF MACSJ1206 (CAMINHA ET AL. 2017)

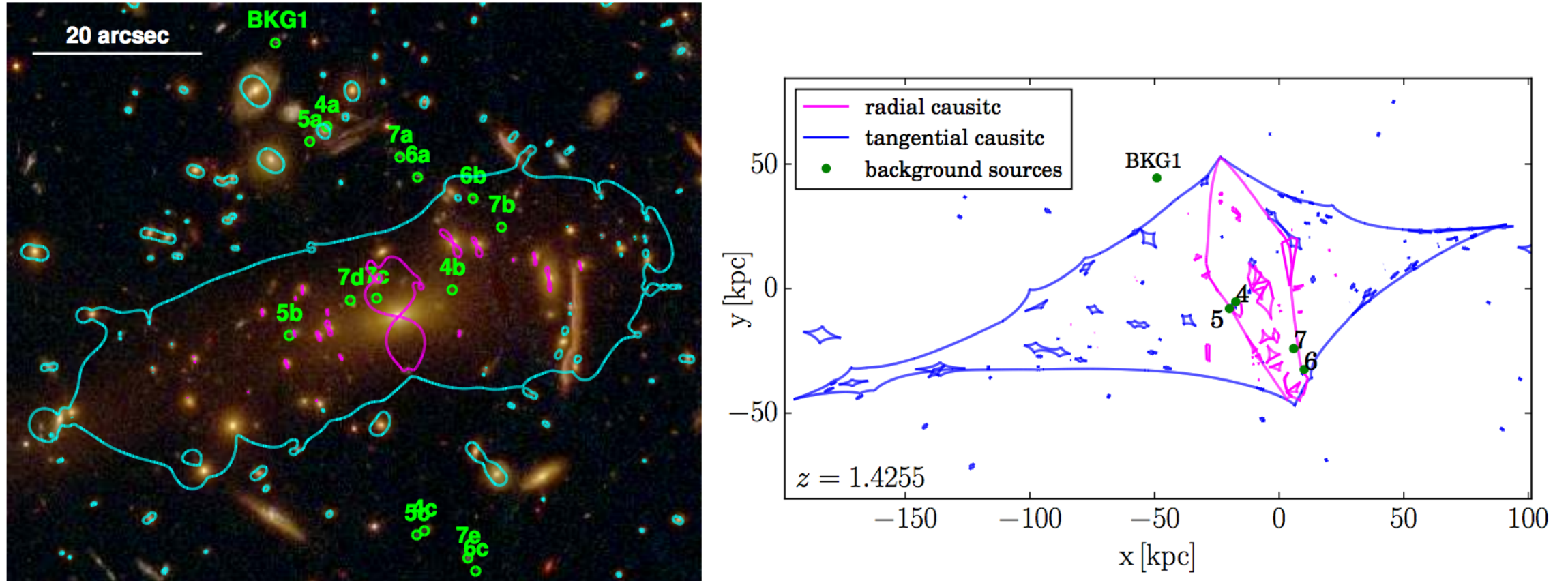
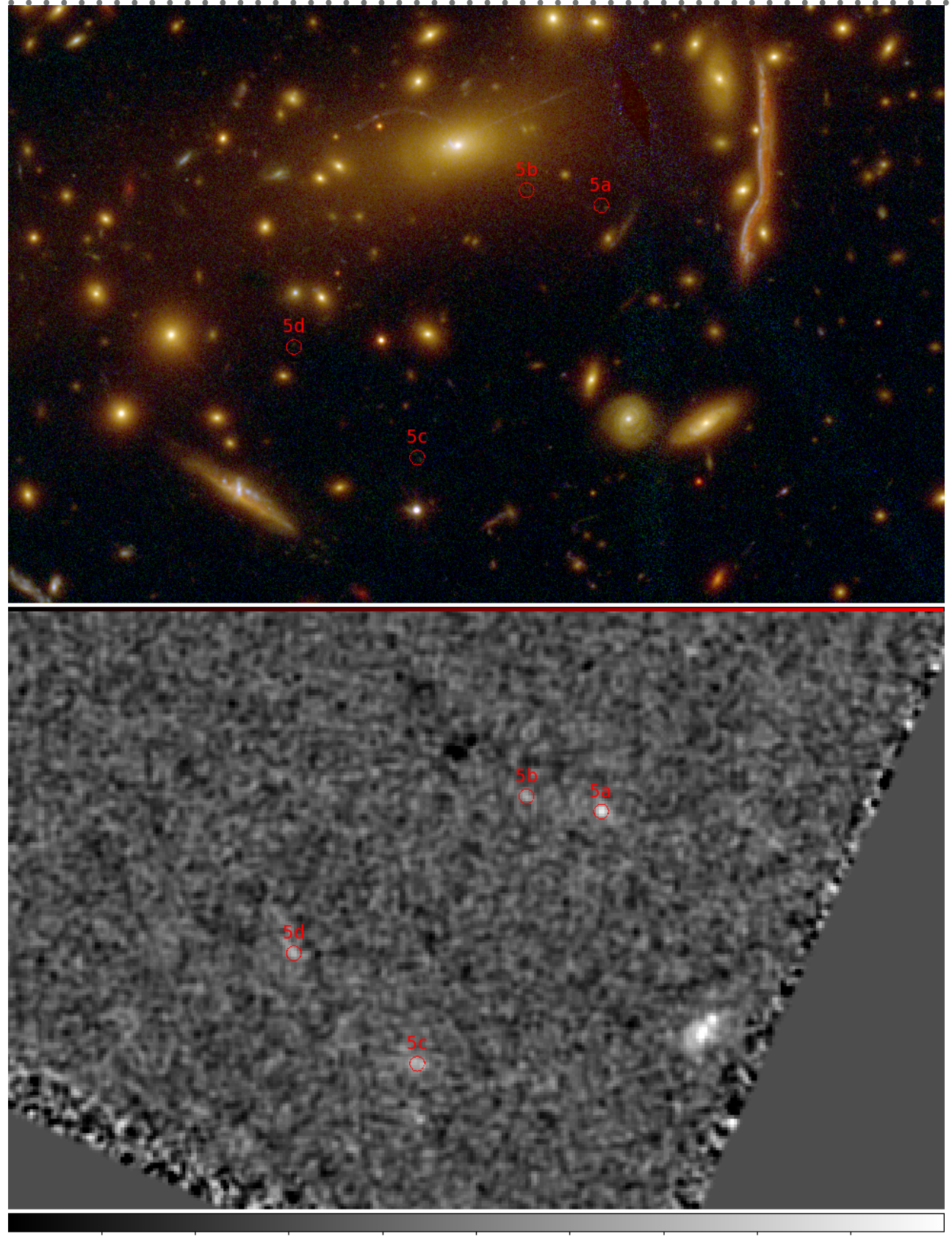
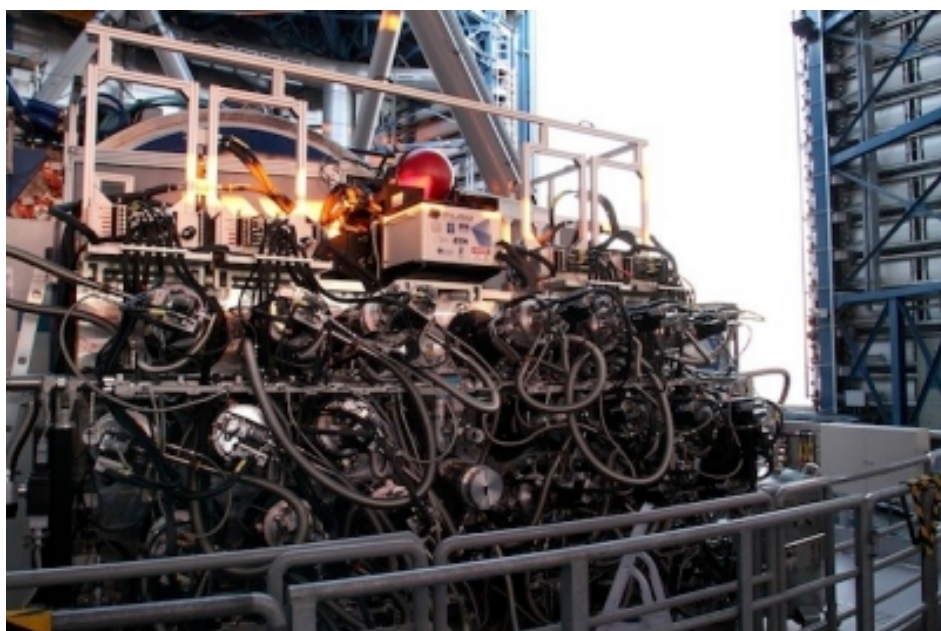


Fig. 6: Critical curves and caustics of the reference model P3 ε for a source at $z_{src} = 1.4255$ (the mean redshift values of the sources). Left panel: Tangential (cyan) and radial (magenta) critical lines on the image plane. The green circles show the observed positions of the multiple images belonging to the four families within $\Delta z \leq 0.0011$. BKG1 is a background galaxy not multiply lensed by MACS 1206. Right panel: Tangential (cyan) and radial (magenta) caustics on the source plane, and the reconstructed positions of the background sources.

RECENT ADVANCEMENTS: MUSE (THE MULTI-UNIT SPECTROSCOPIC EXPLORER) @VLT

- an Integral Field Spectrograph located at the Nasmyth B focus of Yepun, the VLT UT4 telescope.
- It has a modular structure composed of 24 identical IFU modules that together sample, in Wide Field Mode (WFM), a near-contiguous 1 squared arcmin field of view.
- Spectrally the instrument samples almost the full optical domain with a mean resolution of 3000.
- Spatially, the instrument samples the sky with 0.2 arcseconds spatial pixels in the currently offered Wide Field Mode with natural seeing (WFM-noAO).
- E.g. Ly-a emission up to $z=6.5$

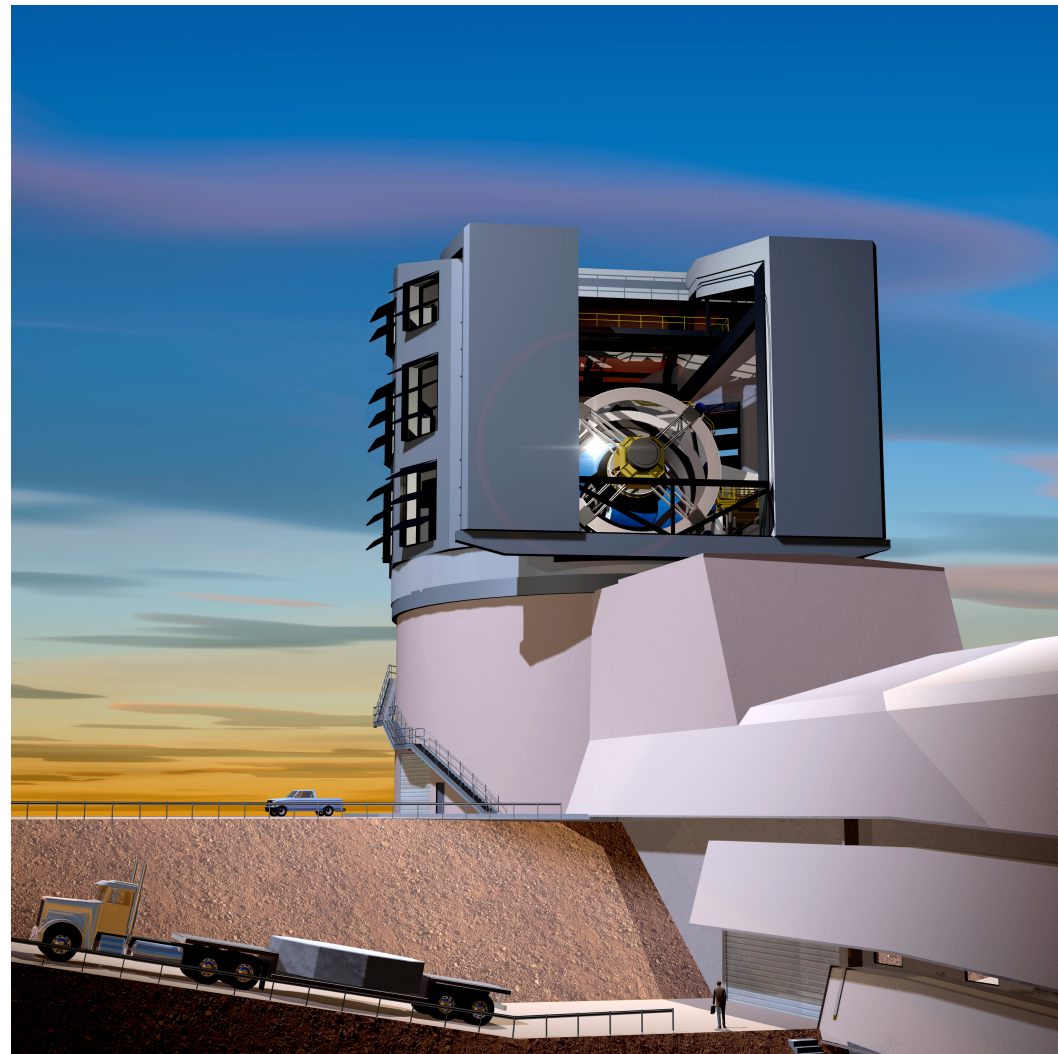


THE NEXT GENERATION OF LENSING SURVEYS

- Soon (2021-2025), some imaging surveys will begin covering large areas of the sky to depth and with high spatial resolution
- These surveys were proposed mainly as cosmological experiments employing weak lensing
- However, the data will be of good quality also to exploit strong lensing
- Large-Synoptic-Survey-Telescope (LSST)
- Euclid

Table 1. The LSST Baseline Design and Survey Parameters

Quantity	Baseline Design Specification
Optical Config.	3-mirror modified Paul-Baker
Mount Config.	Alt-azimuth
Final f-ratio, aperture	f/1.234, 8.4 m
Field of view, étendue	9.6 deg ² , 319 m ² deg ²
Plate Scale	50.9 μm/arcsec (0.2" pix)
Pixel count	3.2 Gigapix
Wavelength Coverage	320 – 1050 nm, <i>ugrizy</i>
Single visit depths, design ^a	23.9, 25.0, 24.7, 24.0, 23.3, 22.1
Single visit depths, min. ^b	23.4, 24.6, 24.3, 23.6, 22.9, 21.7
Mean number of visits ^c	56, 80, 184, 184, 160, 160
Final (coadded) depths ^d	26.1, 27.4, 27.5, 26.8, 26.1, 24.9

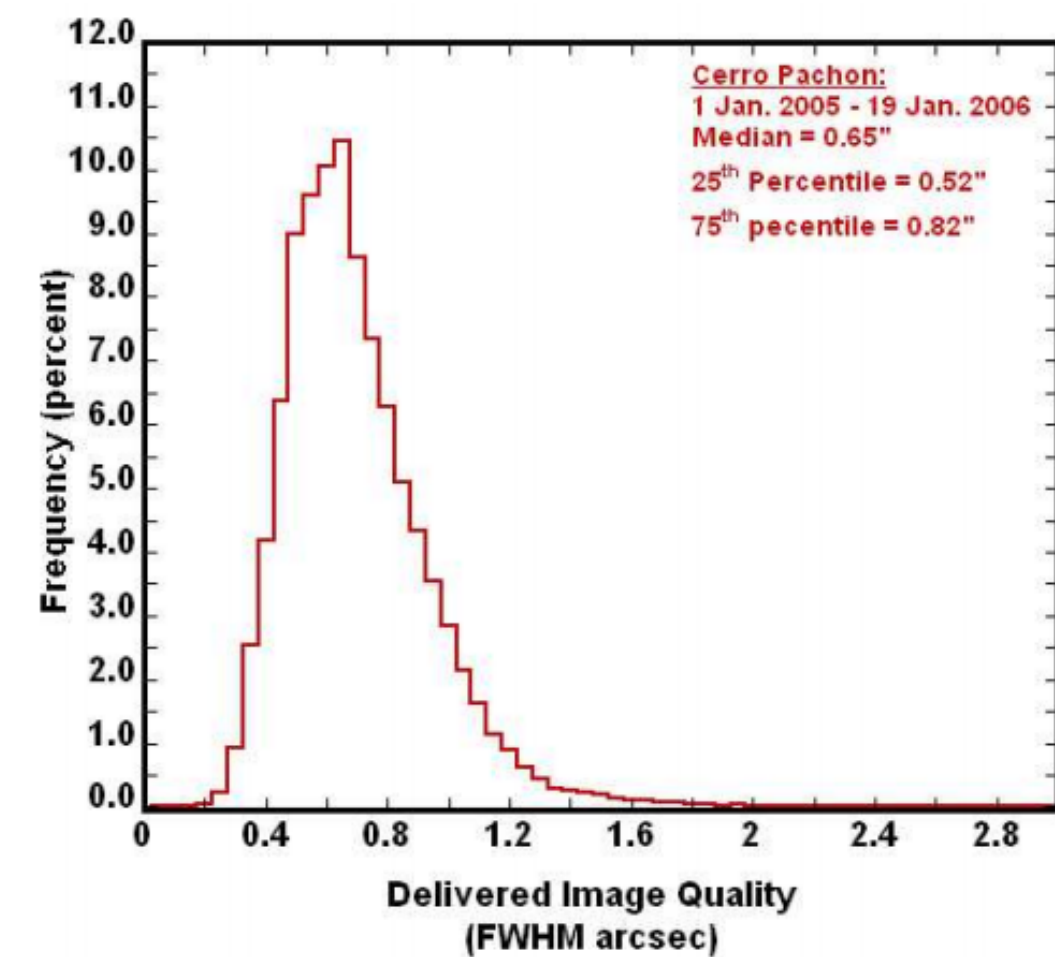


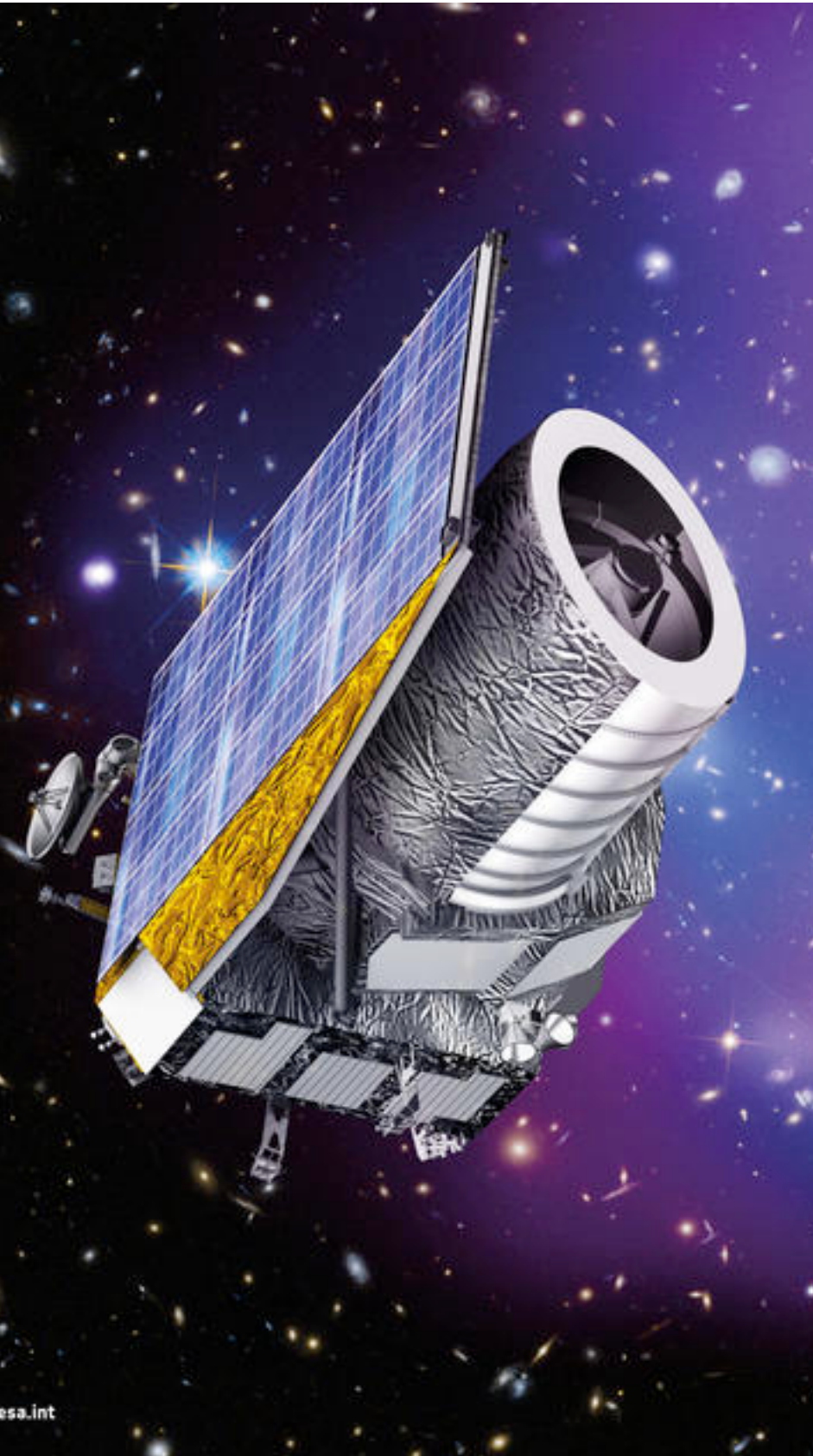
Imaging the entire sky in two days!

Many visits: lensed QSOs and SNe

In full operation from 2023.

LSST <https://www.lsst.org/>

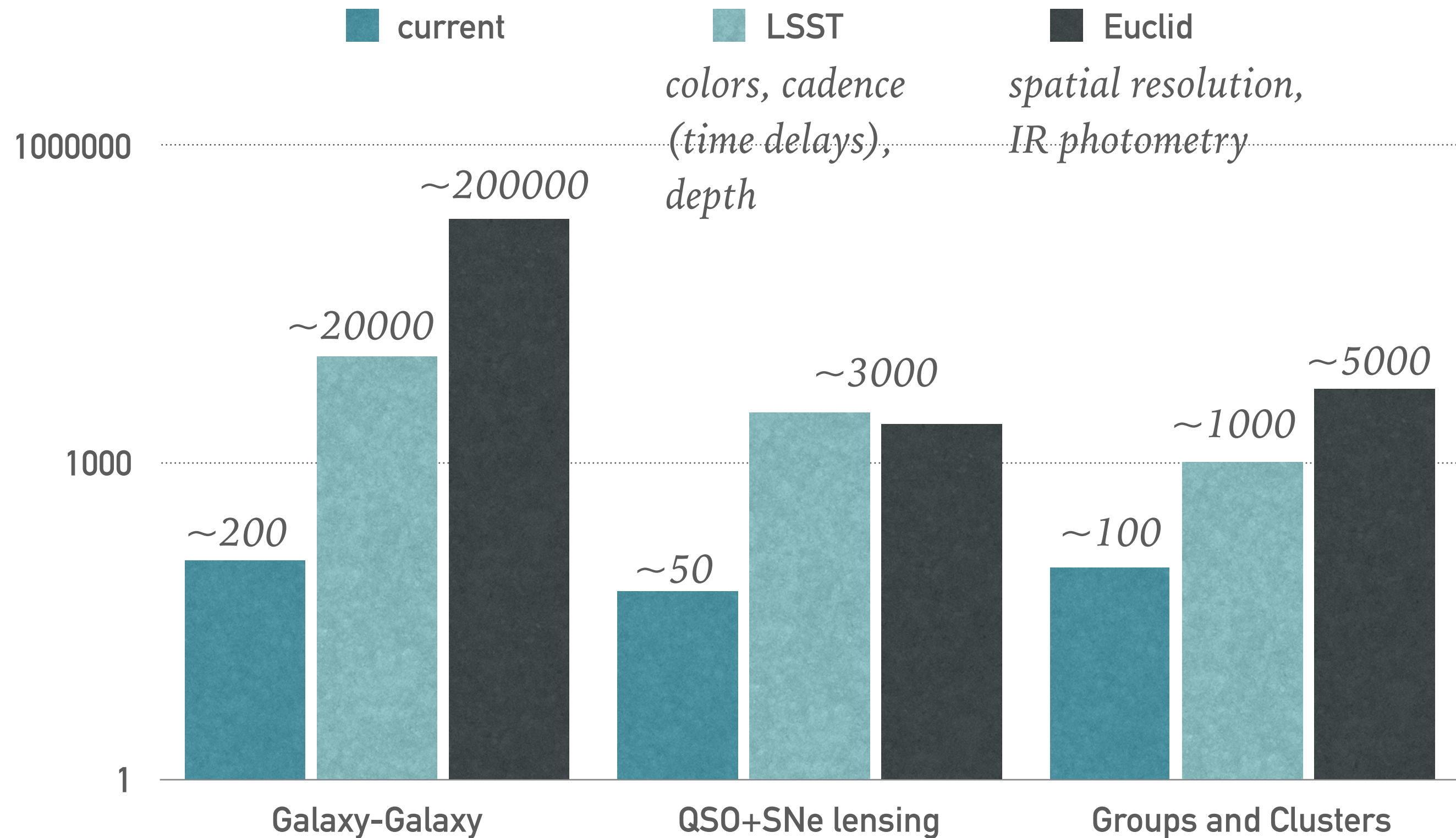




SURVEYS									
	Area (deg ²)	Description							
Wide Survey	15,000 (required) 20,000 (goal)	Step and stare with 4 dither pointings per step.							
Deep Survey	40	In at least 2 patches of > 10 deg ² 2 magnitudes deeper than wide survey							
PAYLOAD									
Telescope	1.2 m Korsch, 3 mirror anastigmat, f=24.5 m								
Instrument	VIS	NISP							
Field-of-View	0.787×0.709 deg ²	0.763×0.722 deg ²							
Capability	Visual Imaging	NIR Imaging Photometry			NIR Spectroscopy				
Wavelength range	550–900 nm	Y (920-1146nm),	J (1146-1372 nm)	H (1372-2000nm)	1100-2000 nm				
Sensitivity	24.5 mag 10σ extended source	24 mag 5σ point source	24 mag 5σ point source	24 mag 5σ point source	3 10 ⁻¹⁶ erg cm ⁻² s ⁻¹ 3.5σ unresolved line flux				
Detector Technology	36 arrays 4k×4k CCD	16 arrays 2k×2k NIR sensitive HgCdTe detectors							
Pixel Size	0.1 arcsec	0.3 arcsec			0.3 arcsec				
Spectral resolution	R=250								
SPACECRAFT									
Launcher	Soyuz ST-2.1 B from Kourou								
Orbit	Large Sun-Earth Lagrange point 2 (SEL2), free insertion orbit								
Pointing	25 mas relative pointing error over one dither duration 30 arcsec absolute pointing error								
Observation mode	Step and stare, 4 dither frames per field, VIS and NISP common FoV = 0.54 deg ²								
Lifetime	7 years								
Operations	4 hours per day contact, more than one ground station to cope with seasonal visibility variations;								
Communications	maximum science data rate of 850 Gbit/day downlink in K band (26GHz), steerable HGA								

Laurejis et al. 2012

STRONG LENSING IN THE ERA OF EUCLID AND LSST



Source: LSST science book; Euclid SL white paper (in progress)

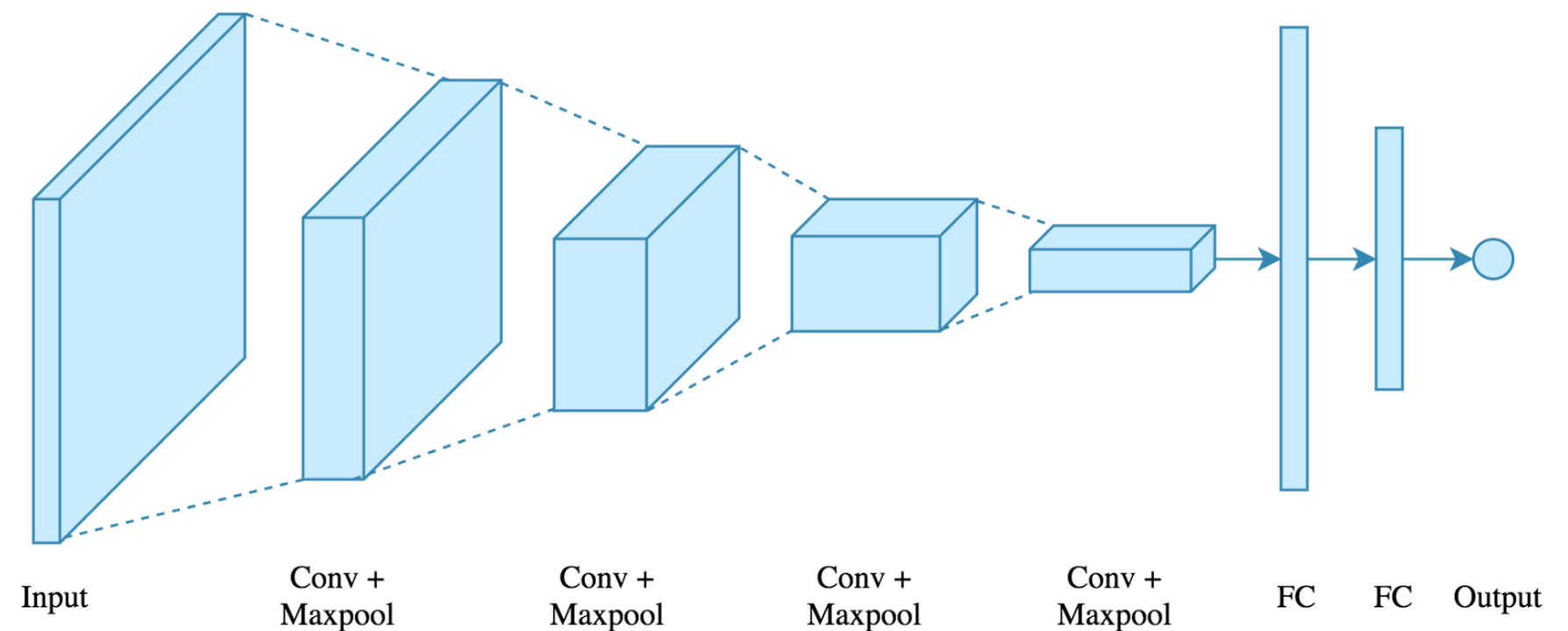
WE ENTERED A NEW ERA: AUTOMATED SEARCHES FOR LENSES

- The strategy had to be changed: large areas, big depth, large number of potential lenses, making difficult the lens identification in the usual way
- The idea of “automated detection” has taken place
- Machine learning! Deep learning with CNNs...

CONVOLUTIONAL NEURAL NETWORKS (AND THEIR VARIANTS)

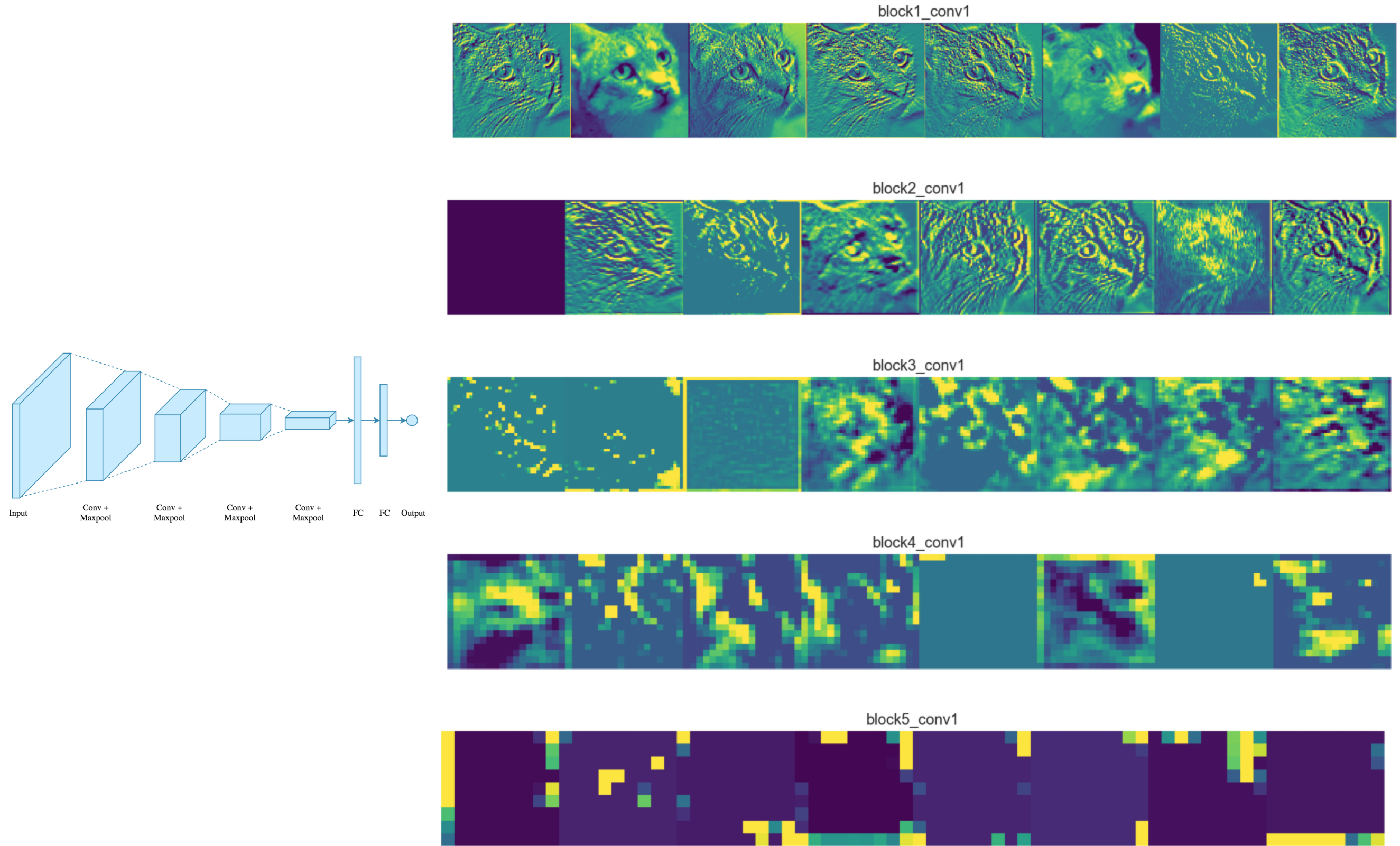
- Input images are processed with 2D “filters” via convolutions
- Filters and weights are “learned” by the networks, using a process called “supervised learning”
- The network is initialized with random numbers and fed with examples (images with known classification)
- During the training phase, the weights and the filters adjust their value/shapes to obtain the correct classification of the given examples
- In a subsequent phase, one has to verify that the method works on a test sample
- Finally, the method can be applied to any image with unknown classification

CONVOLUTIONAL NEURAL NETWORKS (AND THEIR VARIANTS)

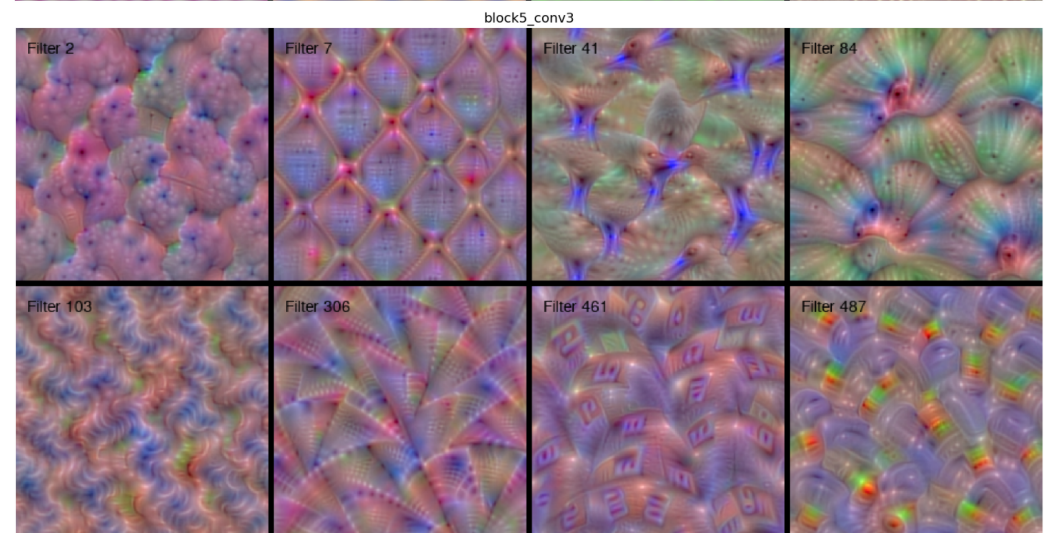
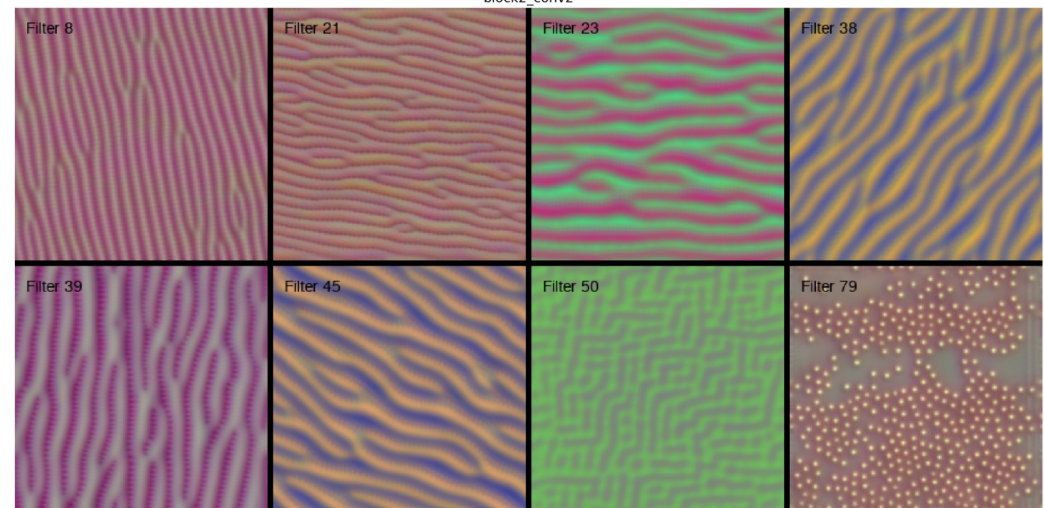
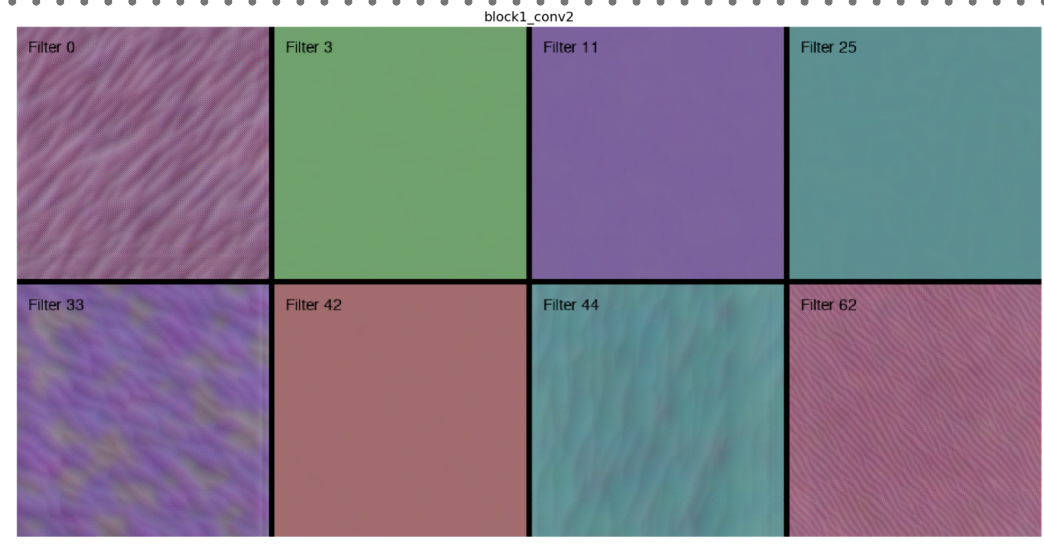
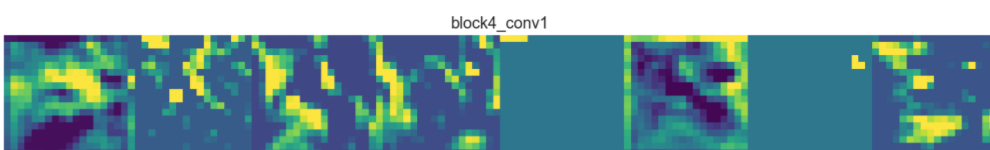
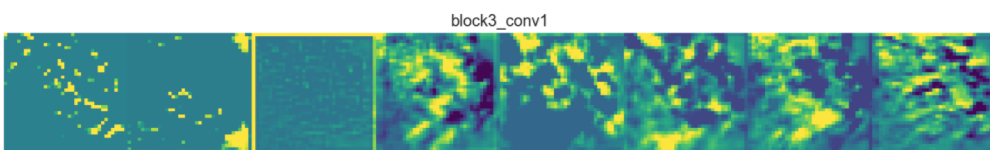
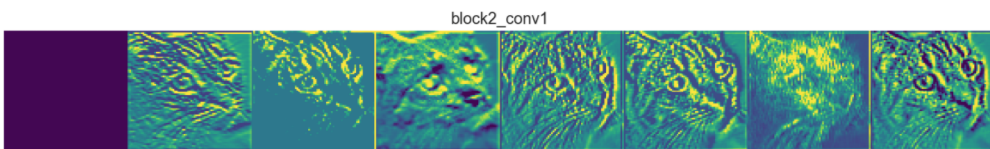
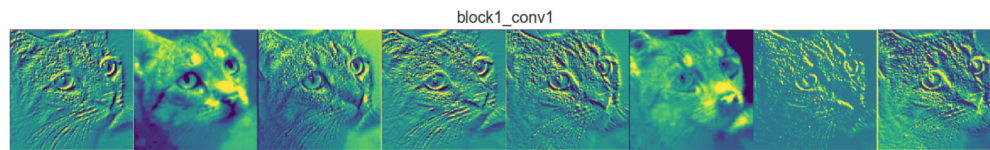


<https://towardsdatascience.com/applied-deep-learning-part-4-convolutional-neural-networks-584bc134c1e2>

CONVOLUTIONAL NEURAL NETWORKS (AND THEIR VARIANTS)



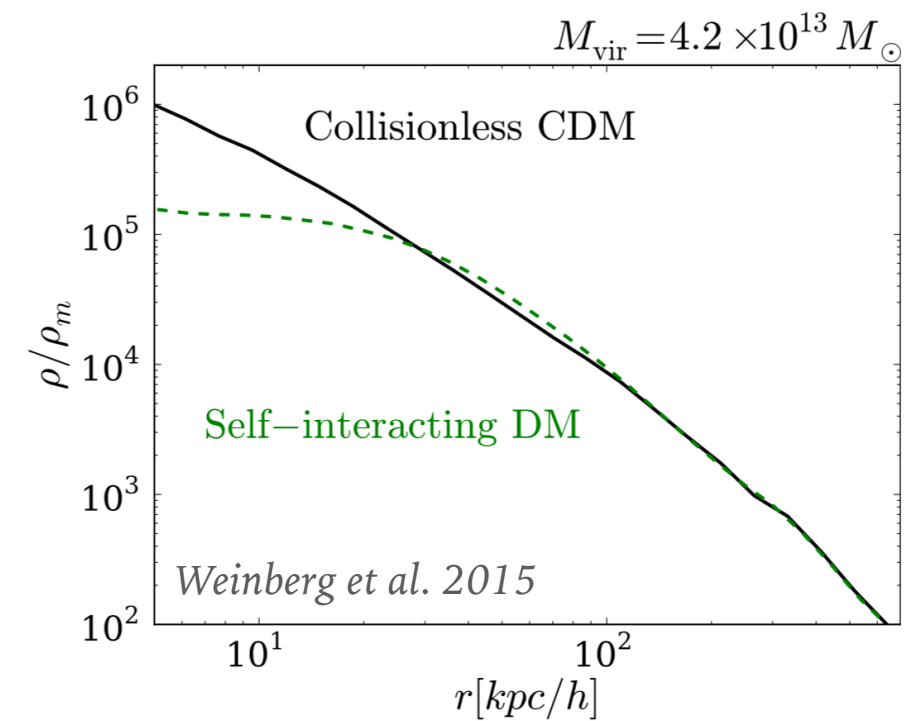
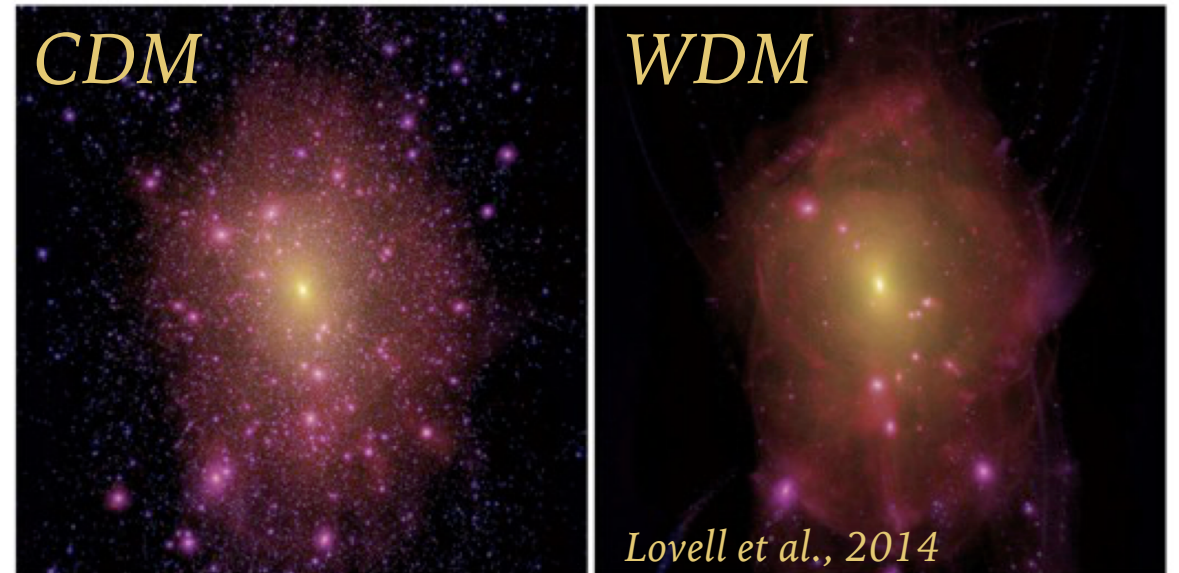
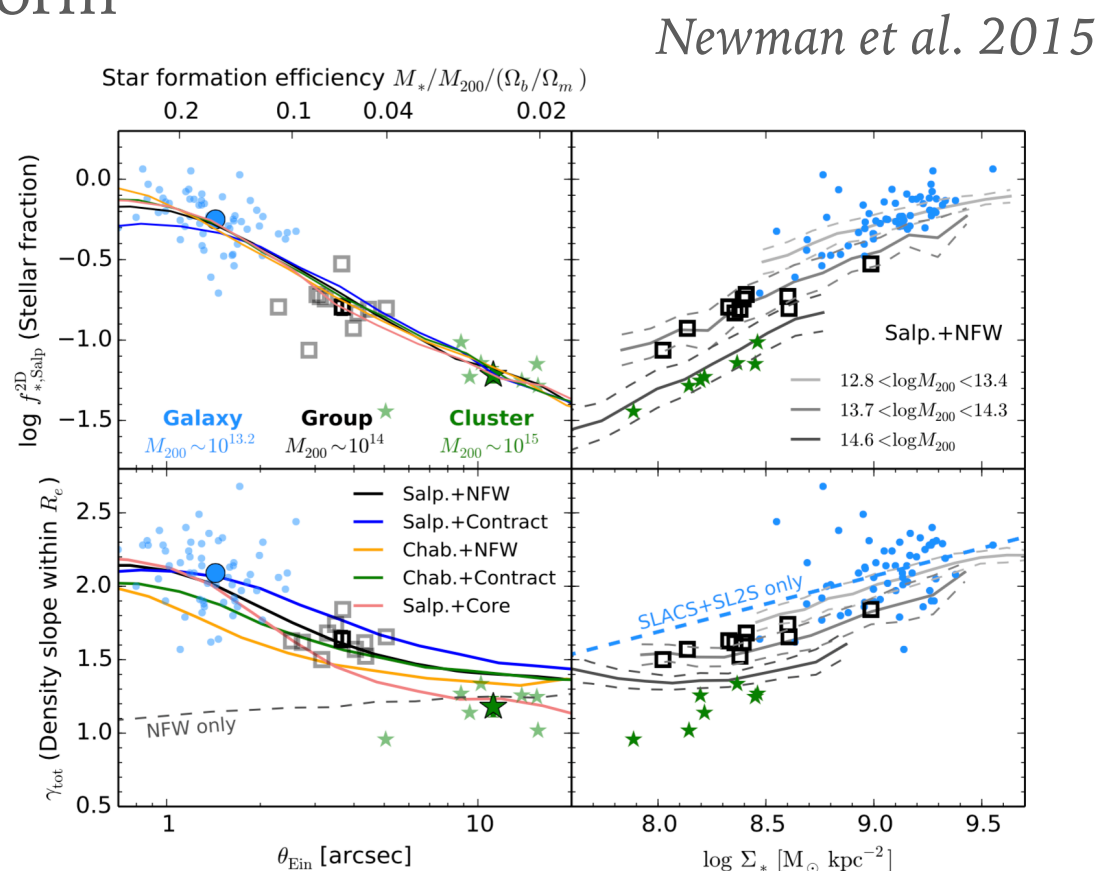
CONVOLUTIONAL NEURAL NETWORKS (AND THEIR VARIANTS)



**WHY TO LOOK AT THE
CORES OF GALAXIES AND
CLUSTERS?**

1) STUDY THE MATTER DISTRIBUTION IN THE COSMIC STRUCTURES

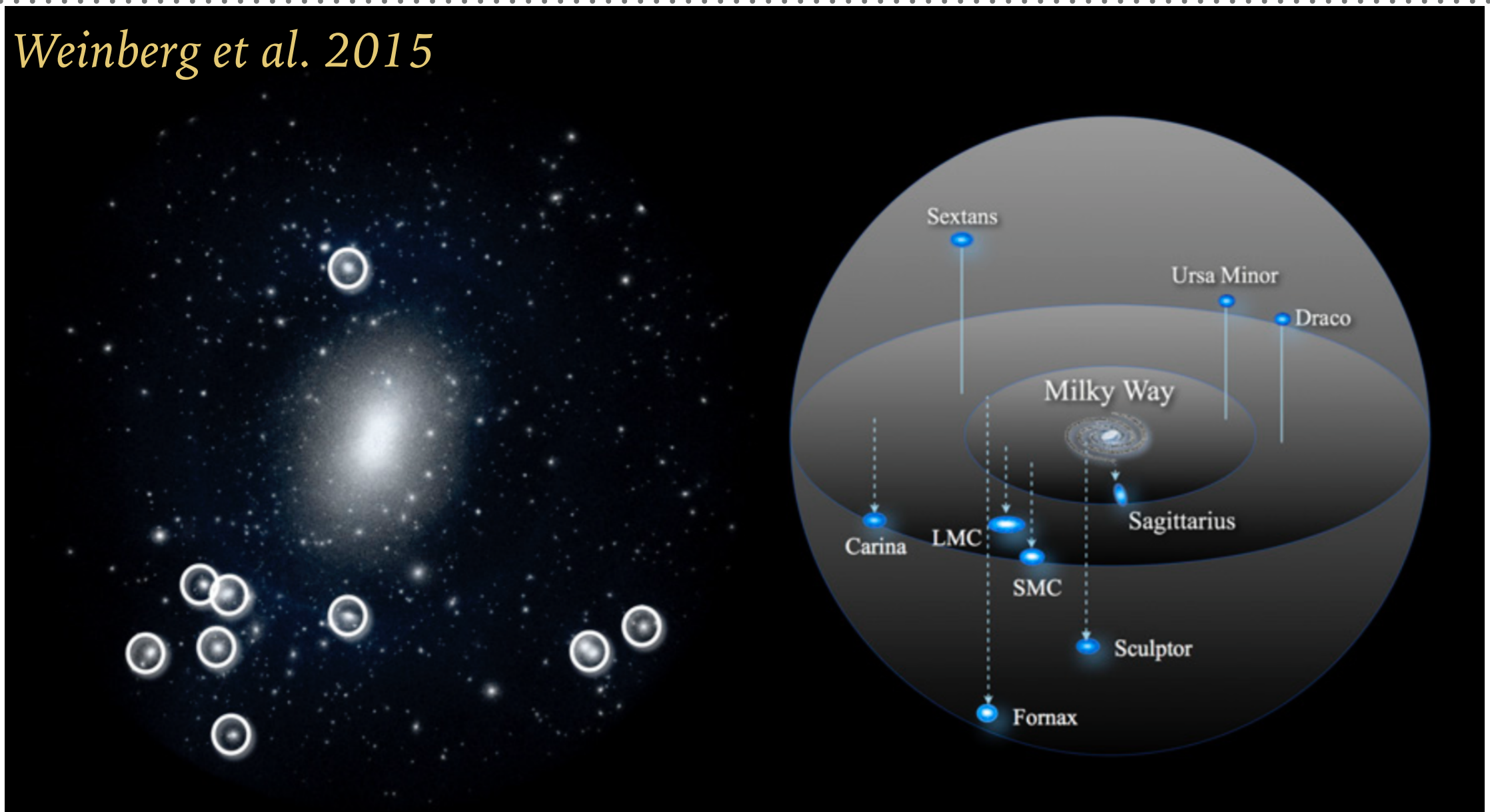
- **Nature of DM:** inner-slope of the density profiles, substructures, core shapes (CDM vs WDM, SIDM, etc)
- **Interplay between baryons and dark matter:** relative spatial distribution of DM and baryons; how baryons affect DM; how do galaxies form



$$\text{NFW} \quad \rho(r) = \frac{\rho_s}{(r/r_s)(1+r/r_s)^2}$$

SUBSTRUCTURES: THE MISSING SATELLITE AND “THE TOO BIG TO FAIL” PROBLEMS

Weinberg et al. 2015

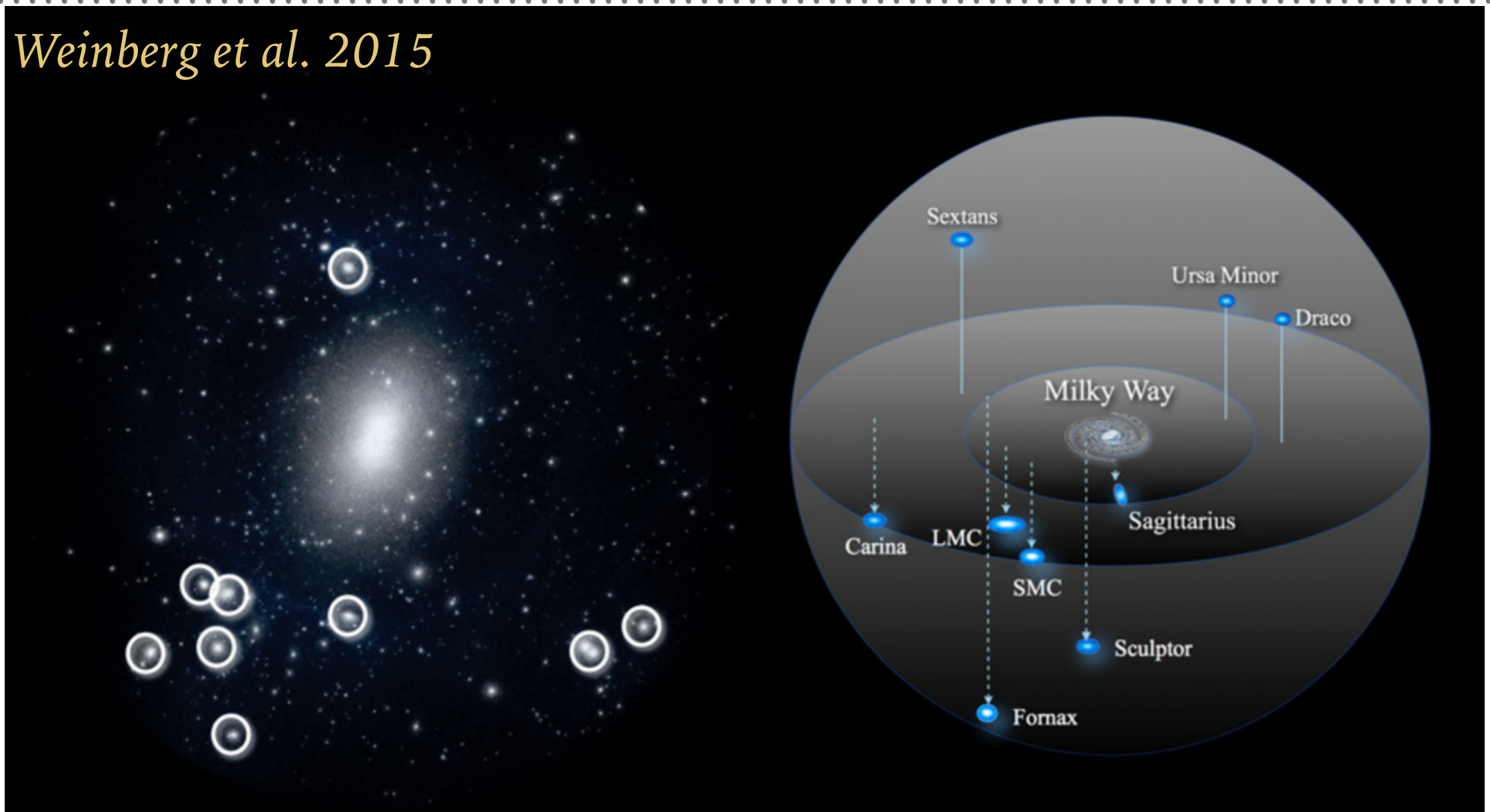


The missing-satellite problem: simulations show that CDM forms many more sub-halos than observed around the Milky-Way

The too-big-to-fail problem: the biggest sub-halos in simulations are too massive and dense to host the observed dwarf-satellites (x5 in mass)!

SUBSTRUCTURES: THE MISSING SATELLITE AND “THE TOO BIG TO FAIL” PROBLEMS

Weinberg et al. 2015



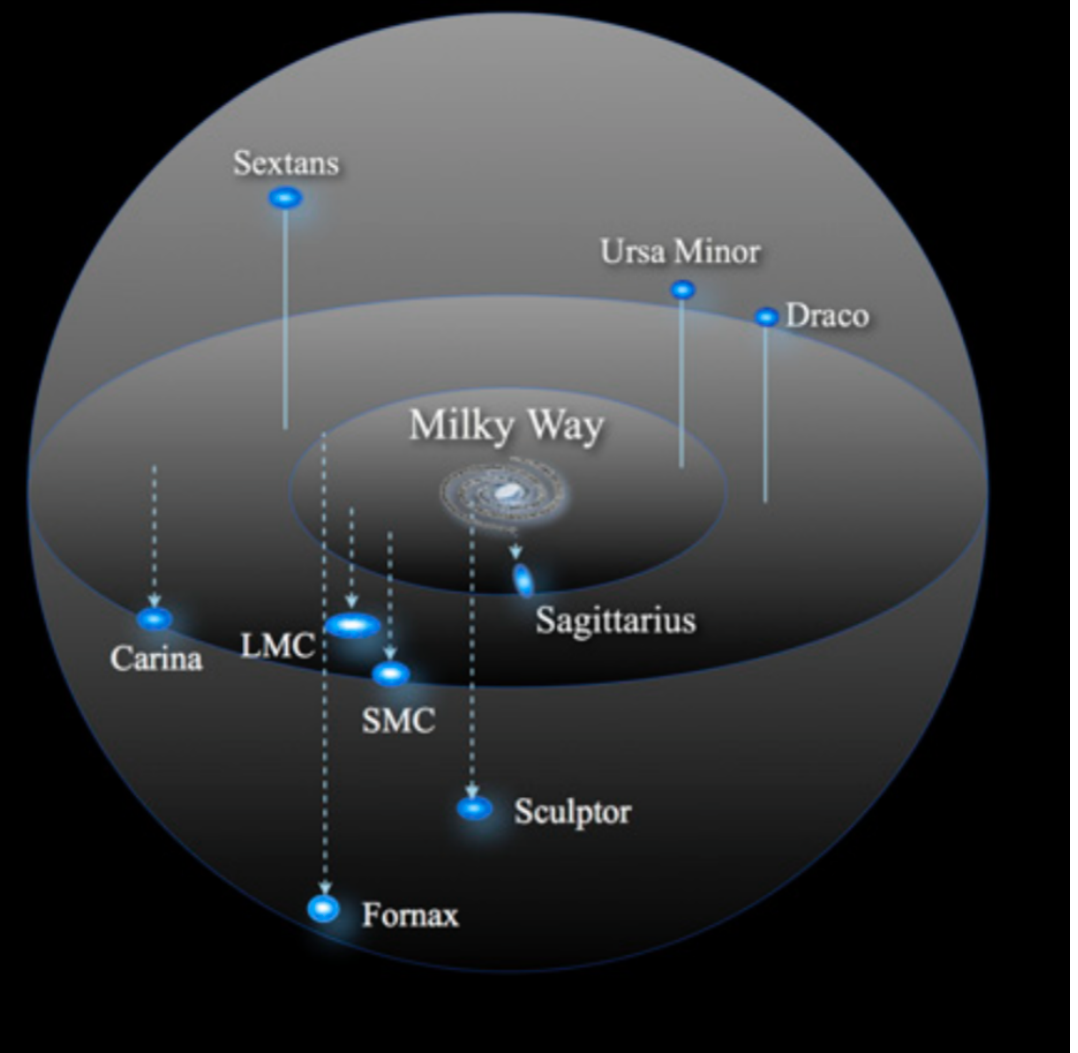
~~The missing satellite problem: simulations show that CDM forms many more sub halos than observed around the Milky Way~~

~~The too-big-to-fail problem: the biggest sub-halos in simulations are too massive and dense to host the observed dwarf-satellites ($x5$ in mass)!~~

SUBSTRUCTURES: THE MISSING SATELLITE AND “THE TOO BIG TO FAIL” PROBLEMS

Weinberg et al. 2015

UV photo-ionizing
radiation, SN
explosions, galactic
winds + new
satellites from SDSS:
small halos are no
longer a problem.



~~The missing satellite problem: simulations show that CDM forms many more sub-halos than observed around the Milky Way~~

~~The too-big-to-fail problem: the biggest sub-halos in simulations are too massive and dense to host the observed dwarf-satellites ($x5$ in mass)!~~

SL IS SENSITIVE TO SUBSTRUCTURES!

- Substructures perturb lensed images!
- They can be revealed by comparing what is observed to the images that a smooth mass distribution would produce
- This technique is called “Gravitational imaging”
- It requires very high spatial resolution, achievable using radio interferometers (VLBI, ALMA)

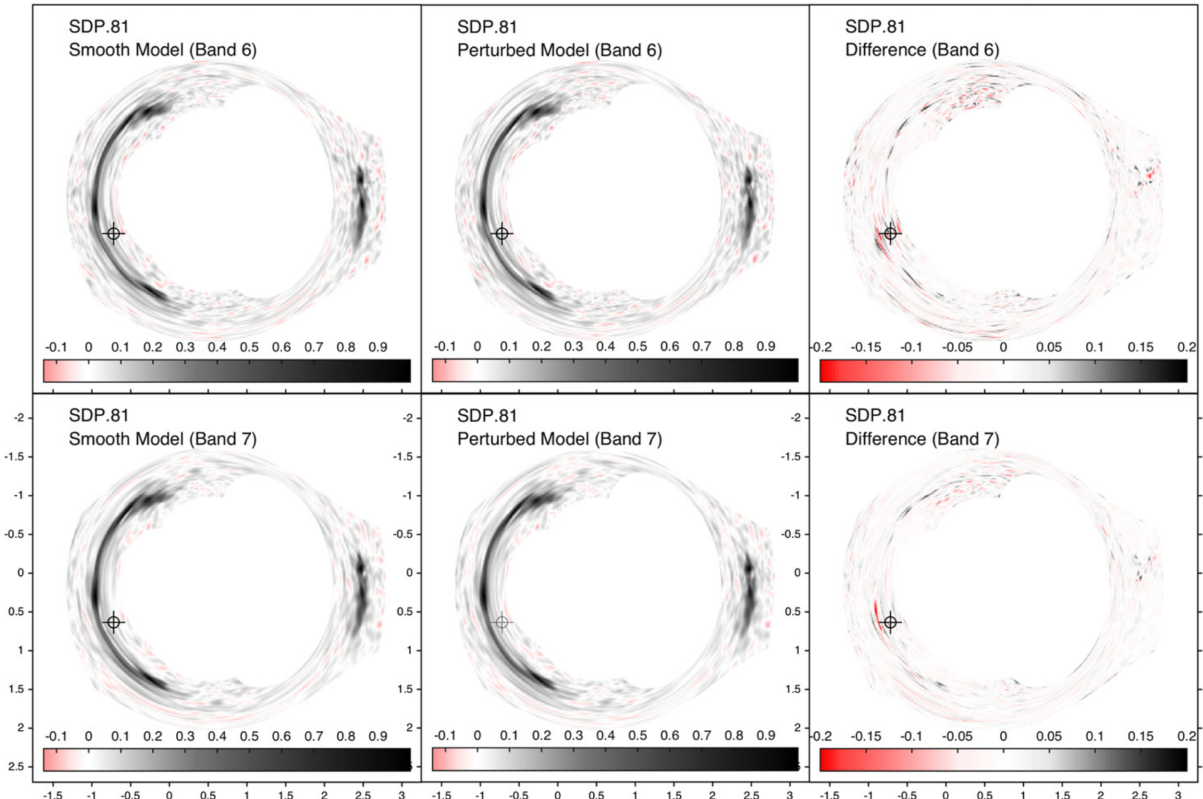
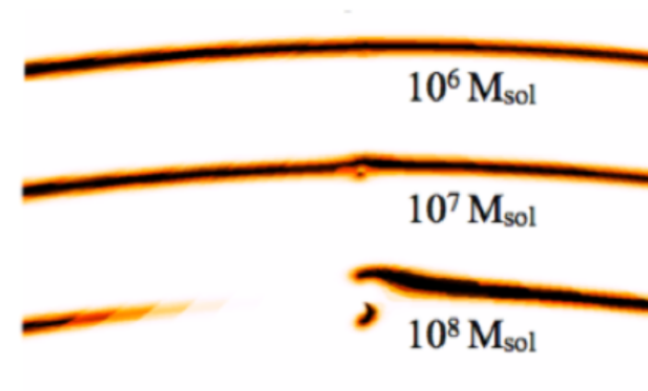
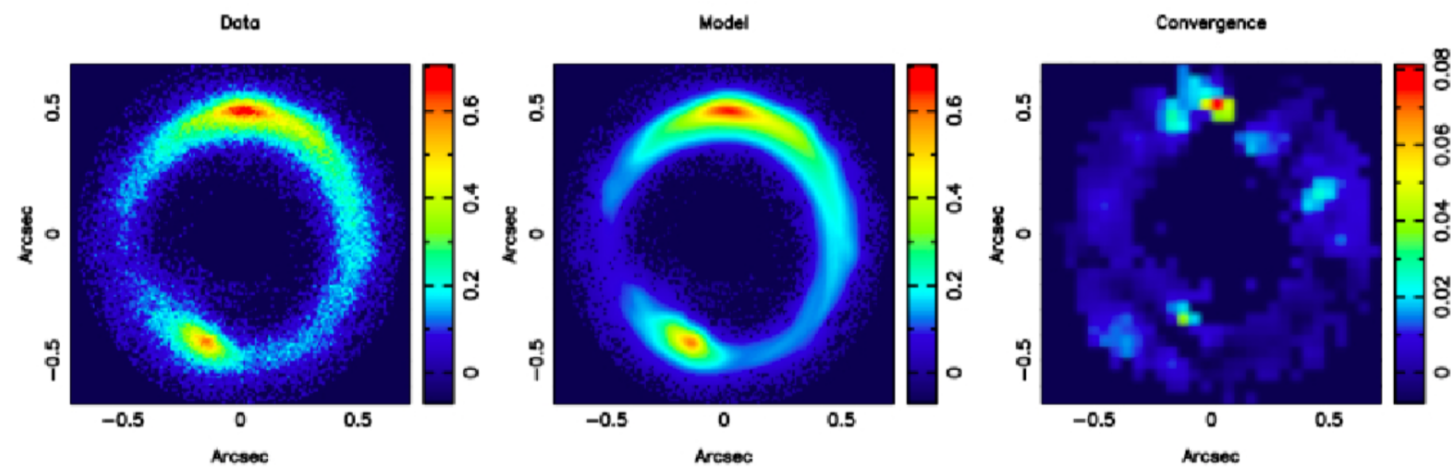


Figure 6. Top left: the sky emission model in band 6 for the best-fit smooth lens parameters for the SDP.81 data. Top middle: the same for the perturbed model. Top right: the difference between the two models. The bottom panels show the same for band 7. The bright feature in the difference plots is mainly caused by the astrometric anomaly of the arc. In each row, the images have been scaled to the peak flux of the smooth model.

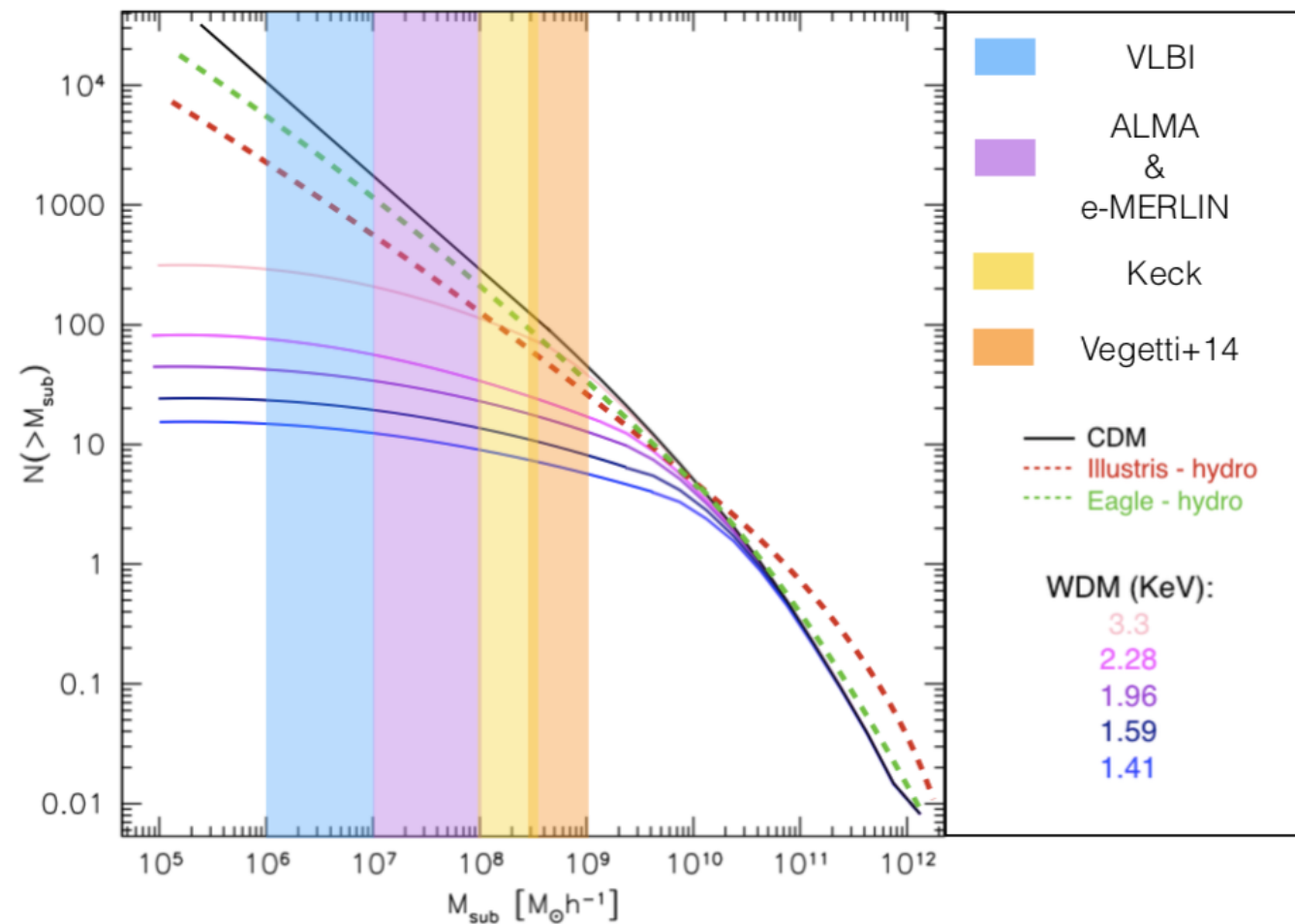
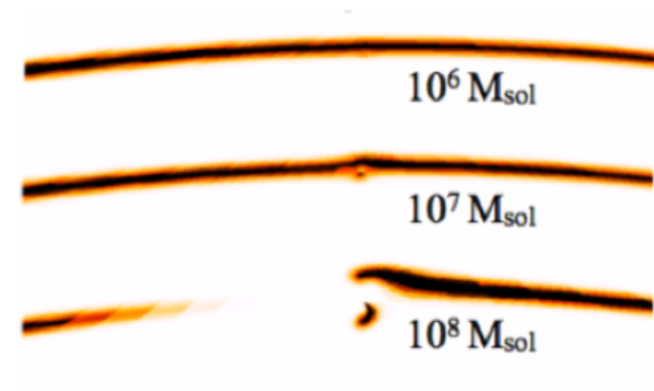
Hezaveh et al. 2016

Vegetti et al. 2012



SL IS SENSITIVE TO SUBSTRUCTURES!

- Substructures perturb lensed images!
- They can be revealed by comparing what is observed to the images that a smooth mass distribution would produce
- This technique is called “Gravitational imaging”
- It requires very high spatial resolution, achievable using radio interferometers (VLBI, ALMA)



Vegetti et al. 2012

